THE EFFECT OF COPPER SULPHATE ON FROTH STABILITY

Wadzanai Nyabeze

BSc(Eng) in Chemical Engineering, University of Cape Town

A dissertation submitted to the University of Cape Town in fulfilment of the requirements for the degree of Master of Science in Chemical Engineering.

November 2015

DECLARATION

I declare that this dissertation, submitted for the degree of Master of Science in Chemical Engineering at the University of Cape Town is my own work, and has not been submitted prior to this for any degree at this university or any other institution. I know the meaning of plagiarism and declare that all work in this document, save for that which is properly acknowledged is my own.

Wadzanai Nyabeze

ACKNOWLEDGEMENTS

I would like to express my gratitude to my supervisor, Dr Belinda McFadzean for her unparalleled supervision and support. I would also like to thank Mr Martin Harris, Professor Andrea Gerson and Professor Sandy Lambert for their guidance and suggestions for the research work.

I would also like to thank my sponsors, the National Research Fund (NRF) and the Reagents Research Group (RRG) for their financial support. This project would not have been a success without them.

A special mention goes to the Flotation Research Group for technical advice throughout my studies and to the CMR laboratory staff for their assistance with my experimental work.

My utmost gratitude goes to my parents, siblings and family members for the continuous support and believing in me always. I would also like to thank my friends for their moral support and encouragement.

Above all I would like to thank God Almighty for making all things possible.

Tinotenda Mwari

SYNOPSIS

Froth flotation is a mineral beneficiation process implemented in the recovery of valuable minerals from unwanted gangue material. Copper sulphate is used as an activator in the flotation of base metal sulphides (BMS) as it promotes interaction of collector molecules with the mineral surfaces. It is also used in certain platinum group minerals (PGM) flotation operations in South Africa although the mechanism by which improvements in flotation performance are achieved is not well understood. Some investigations suggest that changes in flotation performance are affected by changes in the froth phase, rather than activation of minerals by true flotation in the pulp zone. The present study focussed on exploring the effect of using copper sulphate as an activator and sodium isobutyl xanthate (SIBX) as a collector on froth stability in Platinum Group Mineral (PGM) operations. This was done on two PGM containing ores namely Merensky and UG2 (Upper Group 2) ores from the Bushveld Complex of South Africa.

The dynamic froth stability factor (Σ) and froth half life time ($t_{1/2}$) were used as measures of froth stability. These were obtained using a froth stability column which is a non-overflowing system. The effect of activation on pure minerals in the pulp phase was also analysed using a microflotation cell which eliminates the froth phase and hydrodynamic interactions found in normal flotation cells. The microflotation cell was used as a measure of hydrophobicity which was directly linked to the flotation recovery. The adsorption of reagents onto the mineral surfaces was confirmed by the use of zeta potential and ethylenediaminetetraacetic acid (EDTA) extraction of surface products. The pulp phase effects were analysed through the floatability of pure minerals and analysis of surface products after copper sulphate activation and these were linked to the outcomes from the froth stability tests.

It was hypothesised that copper sulphate destabilised the froth for a Merensky ore and for a UG2 ore but due to different reasons because of the mineralogical compositions of the two ores. For the Merensky ore, the froth destabilisation was postulated to be due to the formation of Cu(I) on the base metal sulphide surfaces which promotes the formation of hydrophobic copper-xanthate species. This would result in an increase in contact angle which promotes bubble coalescence. For the UG2 ore which has far less base metal sulphides than Merensky ore, it was

hypothesised that the destabilisation of the froth would be due to the non-selective precipitation of hydrophilic colloidal hydroxides on mineral surfaces which reduce the amount of hydrophobic froth stabilising particles reporting to the froth phase.

The froth stability measurements showed the froth was destabilised by copper sulphate for both ores as hypothesised. However, this was due to different reasons. For the Merensky ore, the formation of hydrophobic copper xanthate species was confirmed by the EDTA extraction tests as well as the microflotation tests. However, the EDTA tests also revealed the presence of copper hydroxide on the Merensky ore surfaces. These copper hydroxides could have contributed to the destabilisation of froth by reducing the amount of froth stabilising particles reporting to the froth phase. Microflotation tests supported this argument as the presence of ions in synthetic plant water reduced the floatability of talc and pyrrhotite. The zeta potential tests confirmed adsorption of copper sulphate onto the pure mineral surfaces and it was assumed the cations in synthetic plant water also adsorb onto the mineral surfaces in a similar manner.

For the UG2 ore, in addition to copper hydroxides forming on the mineral surfaces, chemically reacted copper was also found on the mineral surfaces using the EDTA extraction tests. This was unexpected since copper sulphate is known to activate sulphide minerals and UG2 ore has a very low sulphide mineral content. The activation of oxide minerals which are abundant in the UG2 ore could have contributed to the destabilisation of the froth also via the formation of hydrophobic copper xanthate species which promote bubble coalescence. In the absence of xanthate, the copper hydroxide coatings could have reduced the amount of froth stabilising particles reporting to the froth phase which destabilises the froth.

The findings of this study showed that both the pulp and the froth zones were affected by copper sulphate addition. Copper sulphate was found to change the particle hydrophobicity in the presence of xanthate which had a destabilising effect on the froth phase as the contact angle was increased beyond an optimum for stability to be conferred. Copper sulphate alone was found to render the particles hydrophilic reducing the amount of froth stabilising particles reporting to the froth phase. The decrease in froth stability could have an effect on the overall flotation performance as a result of possible activation of gangue minerals by copper sulphate

when xanthate is used as a collector subsequently. It is recommended to analyse the flotation performance in continuous systems using water recovery and solids recovery as well as quantitative assays for the PGMs or BMS. It is also recommended to assess the use of copper sulphate as an activator on PGM flotation operations in the light of these findings.

TABLE OF CONTENTS

LIST OF FIGURES

LIST OF TABLES

NOMENCLATURE

A	Cross sectional area of the froth stability column	(cm^2)
Cu	Chemical symbol for elemental copper	(-)
Fe	Chemical symbol for elemental iron	(-)
H_{max}	Maximum foam/froth height reached	(mm)
J_g	Superficial gas velocity	(cm/s)
K_{sp}	Solubility product constant	(-)
u_E	Electrophoretic mobility	($\mu mcmV^{-1}s^{-1}$)
$pH_{i.e.p}$	Isoelectric point pH	(-)
a	Particle radius	(μm)
M^{n+}	Cation of charge n	(-)
$t_{1/2}$	Froth half-life time	(s)
X^-	Xanthate ion	(-)

Greek Symbols

Σ	Dynamic froth stability factor	(s)
α	Empirical dimensionless constant	(-)
θ	Contact angle	(°)
μ	Ionic strength	($mol.kg^{-1}$)
τ	Average bubble lifetime	(s)
ε	Fluid dielectric constant	($F.m^{-1}$)
ζ	Zeta-potential	(mV)
η	Dynamic viscosity	(Pa.s)
κ	Debye-Huckel parameter	(cm^{-1})

Acronyms

AAS	Atomic Absorption Spectroscopy
BET	Brunauer Emmett Teller
BMS	Base Metal Sulphide
EDTA	Ethylenediaminetetraacetic acid
PGM	Platinum Group Mineral
PSD	Particle Size Distribution
PZC	Point of Zero Charge
SIBX	Sodium Isobutyl Xanthate
ToF-SIMS	Time-of-Flight Secondary Ion Mass Spectrometry
UG2	Upper Group 2
XPS	X-ray Photoelectron Spectroscopy

GLOSSARY

Electrical double layer	A region on the boundary between two different phases consisting of two oppositely charged layers.
Activator	A chemical reagent used to improve flotation efficiency by increasing the affinity of collectors for mineral surfaces.
Adsorption	The adhesion of a gas, liquid or dissolved substance to a solid surface.
Concentrate	A solid product of flotation separation which has the bulk of the gangue removed.
Collector	A chemical used to attach onto the valuable minerals to aid particle attachment to the gas-liquid interface.
Depressant	A chemical reagent used to reduce the recovery of unwanted particles to the concentrate.
Entrainment	The nonselective recovery of both hydrophobic and hydrophilic particles in the water recovered to the concentrate.
Flotation	A separation method used for separating particles based on their hydrophobic or hydrophilic properties.
Foam	A mass of small bubbles in liquid caused by agitation or bubbling of air through a two phase system.
Froth	A mass of small bubbles in liquid caused by agitation or bubbling of air through a three phase system.
Frother	A surface active agent used to stabilise the froth. Also referred to as a surfactant.
Gangue	Commercially worthless material within or surrounding valuable minerals in an ore.
Hydrophilicity	The physical property of being attracted to water.

Hydrophobicity	The physical property of being repelled by water.
Isoelectric point	The pH at which a mineral particle has a neutral net charge with both positive and negative charges present in equal amounts on the surface.
Ore	A rock containing valuable minerals which can be extracted from and gangue.
Point of zero charge	The pH at which a mineral particle carries no net electrical charge in the absence of positive and negative charges on the surface.
Slurry	A semi-liquid mixture of consisting of finely ground ore and water.
Three-phase	A system consisting of three phases – solid, liquid and gas.
Two-phase	A system consisting of two phases – liquid and gas.
Zeta Potential	The potential difference that exists between the surfaces of a mineral particle immersed in a conducting liquid and the bulk liquid.

1 INTRODUCTION

1.1 Background

Flotation is a particle separation method used in the beneficiation of valuable minerals from gangue based on the difference in wettability of different mineral surfaces. There are two distinct phases in a flotation system, namely the pulp phase and the froth phase. The pulp phase is the region where the adsorption of mineral to air bubbles occurs and the froth phase is the region which ensures transportation of the valuable minerals from the pulp phase to the concentrate (Wiese et al., 2011). Foam or froth is a colloidal system comprising a gas, which is the dispersed phase and the liquid, which is the continuous phase (Malysa, 1992). In their studies, Woodburn et al. (1994) developed a semi-empirical model combining froth surface features with froth dynamics using image analysis techniques. Analysis of both the pulp phase and the froth phase was necessary to characterise the flotation system however as the recovery of gangue was related to the grade of the froth (Woodburn et al., 1994).

The Bushveld Complex in South Africa hosts the largest concentration of Platinum Group Elements (also referred to as PGEs) namely: Platinum, Palladium, Ruthenium, Rhodium, Osmium and Iridium, the three main PGE-bearing ores being Merensky, Upper Group 2 (UG2) and Platreef (Schouwstra et al., 2000). These ores are quite different from each other and require different approaches to metallurgical processing. An example being UG2 ore which has a much lower content of nickel and copper sulphides but a higher PGM and chromite content than Merensky ore (Jones, 1999). Platreef can be considered as metallurgically similar to Merensky ore but it is enriched in palladium (Jones, 1999). In this study, Merensky and UG2 ores were used in the analysis of the effect of copper sulphate on froth stability.

In the Merensky reef, the platinum group minerals (PGMs) are strongly associated with base metal sulphides (BMS). The reef contains approximately 1% sulphide minerals which are made up of approximately 45-55% pyrrhotite, 30-35% pentlandite, 15-20% chalcopyrite, and trace amounts of pyrite (Wiese et al., 2007).The majority of the PGMs in the Merensky ore occur either in pentlandite grains or at the pentlandite-gangue grain boundaries (Jones, 1999). The UG2 reef

contains less than 0.1% of BMS and chromite is a main gangue constituent of the ore (Ekmekçi et al., 2003).

Collectors are used to separate the unwanted gangue material from the BMS by making the mineral surfaces hydrophobic (aerophilic) which then attach to rising air bubbles in a water-ore pulp to achieve the separation (Chandra & Gerson, 2009). Xanthates are a class of collectors used in the flotation of sulphide minerals. Activators are chemical compounds (usually inorganic electrolytes) which interact at the mineral surface thus altering its chemical nature to promote its interaction with the collector (Rao, 2003). The most common activator used in the flotation industry is copper sulphate. For copper sulphate to be successful as an activator, the multi-phase conditions need to be favourable for the formation of the xanthate-metal salt on the surface of the particle (Grobler et al., 2005). Frothers or surfactants are surface-active compounds used to stabilise bubble formation in the pulp phase and to form a stable froth layer that can be removed before the bubbles burst (Kawatra, 2002; Farrokhpay & Zanin, 2011).

In order to maximize PGE recovery in Merensky ore, the recovery of the BMS needs to be optimized, particularly pentlandite which has a higher solid solution content of PGMs (Wiese et al., 2006). Copper sulphate was traditionally used as an activator for sphalerite (zinc sulphide). It has since been used on PGM operations to improve the recovery of BMS and consequently PGMs but some losses in the concentrate grade and recovery have been reported. Many mining operations are required to recycle water within their operations due to restrictions on water usage becoming more stringent (Manono et al., 2012). Some studies have analysed the effect of process/plant water on the grade and recovery of minerals i.e. flotation efficiency (Corin et al., 2011; Muzenda, 2010). The interactions of the ions in process water with the froth phase are still not fully understood.

Although there have been some recent papers focussing on the effect of copper sulphate in the froth phase (Ekmekçi et al., 2006), the majority focus on the pulp phase (Nicol, 1984; Prestidge et al., 1994; Trahar et al., 1997; Chen & Yoon, 2000; Fornasiero & Ralston, 2005; Shackleton et al., 2007; Chandra & Gerson, 2009).

There is no clarity whether copper sulphate acts as a pulp phase activator in PGM application and its froth modifying effects are poorly understood.

1.2 Research Objectives

This research is aimed at assessing the froth modifying effects of copper sulphate when it is used as a pulp phase activator in PGM operations in South Africa. This will be done through froth stability measurements techniques using a laboratory froth stability column. The research aims to establish a link between copper sulphate activation in the pulp phase to the froth phase through microflotation studies, zeta potential measurements and surface analysis of the activation products.

1.3 Key Questions

The following key questions were developed from the objectives:

- Is there a difference in the effect of copper sulphate on the froth stability of a Merensky ore and a UG2 ore?
- How does the addition of copper sulphate change the surface charge of pure minerals?
- How does the addition of copper sulphate change the floatability of pure minerals?
- What activation products were formed on mineral surfaces when copper sulphate was added?

1.4 Thesis Scope

The scope of this thesis included the evaluation of the use of copper sulphate as a pulp phase activator on the froth stabilities of Merensky and UG2 ores. Microflotation tests were used to investigate the pulp phase effects in the absence of the froth phase. It also involved investigations of the surface charge using zeta potential measurements. The surface products of activation were analysed using Ethylenediaminetetraacetic acid (EDTA) extraction techniques. An attempt was made to link the products of activation in the pulp phase to the effects in the froth phase.

This thesis does not include the analysis of the effects of different reagents used in flotation operations (such as collectors and frothers) on the froth phase. The

operating factors affecting froth stability such as the air flow rate were not investigated. These parameters were maintained constant. The same milling time was used to achieve similar particle size distributions to avoid variations in froth stability due to particle size.

1.5 Thesis Structure

This thesis is structured into 6 chapters followed by references and appendices. A synopsis of each chapter is presented in this section.

Chapter One: Introduction

An introduction is made to the froth flotation process in this chapter. A brief background on the mineralogy of the ores analysed in this study is also given as well as the use of copper sulphate as a pulp phase activator in PGM flotation operations. The research objectives are outlined in this chapter followed by the key questions. The scope of the study is also given in this chapter.

Chapter Two: Literature Review

The second chapter gives a review of the literature pertinent to this study. The importance of the froth phase and froth stability in flotation processes is reviewed. Factors affecting froth stability and methods used to quantify froth stability are also explored. A brief review on the mineralogy of the minerals used in this study is given based on earlier research as well as the use of activators in flotation operations. At the end of this chapter, the key findings of the literature review are summarised and the proposed hypotheses are presented.

Chapter Three: Experimental Methods

The experimental methodology used to test the validity of the proposed hypotheses is given in the third chapter. A description of the equipment, materials and reagents used in the study is also given. The conditions and operating procedures are also outlined in this chapter.

Chapter Four: Results

Chapter four presents the results of the experimental work. The results showing the effect of copper sulphate on the froth phase from the froth stability column are presented. This is followed by the microflotation results showing the effect of copper sulphate on the pulp phase of the flotation system. Lastly, the results showing surface analysis of copper sulphate activation is presented.

Chapter Five: Discussion

Chapter five is a discussion of the results presented in chapter four.

Chapter Six: Conclusions

This chapter presents a summary of the key findings of this research as well as the recommendations for future studies. The key questions and objectives of the study presented in chapter one are revisited as well as the hypotheses proposed in chapter two to determine if they were addressed.

2 LITERATURE REVIEW

Extensive research has been done on the effect of copper sulphate on the flotation process with a focus on activation of sulphide minerals in the pulp phase. The effects of using copper sulphate as a pulp phase activator on the froth phase are not fully understood.

This review begins with a background of activation in the beneficiation of sulphide minerals and the significance of froth stability on the flotation process. A review of factors affecting froth stability pertinent to this study will be made as well as the methods used to quantify froth stability. A mineralogical review of the ores and pure minerals used in the study is also given. The mechanisms of copper sulphate activation in the pulp phase are reviewed as well as some of the literature relating to froth behaviour observed in preceding studies where copper sulphate was used as an activator.

2.1 Background

Activation is a process whereby the surface of a mineral particle is modified so as to make it react more readily or strongly with a collector (Chen & Yoon, 2000).The role of the activator, copper sulphate, is to enhance the adsorption of thiol collectors onto the sulphide mineral surface, thereby enhancing sulphide mineral floatability and separation from the oxide gangue minerals (Wesseldijk et al., 1999). Copper sulphate has been widely used as an activator for sphalerite, pyrite, pyrrhotite and other sulphides during the processing of base metal sulphide ores and as a depressant in the flotation of some silicate minerals (Bulatovic, 2007).

The individual base metal sulphide minerals in Merensky ores (chalcopyrite, pentlandite and pyrrhotite) respond differently to different reagents and operating conditions (Wiese et al., 2007). These different reagents and operating conditions were also found to affect the froth stability. The surface chemistry and hydrophobicity of the mineral surface are also affected by changes in pH (Cilliers & Bradshaw, 1996). In alkaline conditions, the copper sulphate added to the system may precipitate non-selectively as a hydrophilic copper hydroxide species which can potentially react with the collector causing inadvertent activation of gangue minerals (Nagaraj & Brinen, 1995; Malysiak, 2003; Fornasiero & Ralston, 2005). Martinovic et al. (2005) in their studies on surface properties of gangue minerals in platinum

bearing ores, reported that copper sulphate addition increased the floatability of orthopyroxene and plagioclase but reduced that of talc.

Copper activation of mineral surfaces is also backed up by studies by Acar & Somasundaran (1992) who through ToF-SIMS (Time-of-Flight Secondary Ion Mass Spectrometry), XPS (X-ray Photoelectron Spectroscopy) and zeta potential measurements found that pyroxene surfaces are activated by Cu(II) ions as well as various positively charged copper hydroxide species such as $CuOH^+$ and $Cu_2(OH)_2^{2+}$ However, with respect to pyroxene, it was observed that hydrophobicity is not significantly enhanced in the presence of xanthate and absence of copper (Malysiak, 2003). It follows that pyroxene will only become hydrophobic when xanthate is added to a copper activated pyroxene mineral system (Shackleton et al., 2003) and this is what was observed by Malysiak (2003).

Electrochemical conditions also play a very important role in the flotation of real sulphide ores and single mineral tests conducted in many cases may be different from those carried out with an ore (Castro & Laskowski, 2011). Hydrophobic surfaces usually carry a negative electrical charge which creates an energy barrier to attachment. When they collide with bubbles the electrical double layer is compressed, which facilitates the attachment (Laskowski & Castro, 2014).

Coalescence has been described as a process involving the irreversible binding of two or more foam bubbles resulting in drainage of the interfacial film which eventually ruptures to form a single larger bubble (Hunter et al., 2008). The three main mechanisms contributing to the instability of foams according to Pugh (2005) are thin film drainage, bubble coalescence and bubble rupture.

2.2 Froth Stability

In the existing literature, the words “foam” and “froth” have been used interchangeably to convey the same meaning. In the context of this dissertation, foam will be used to refer to a two phase system composed of air bubbles and water only whereas froth is a three phase system consisting of air bubbles, particles and water.

Froth stability has been described in different ways by different authors. According to Aktas et al. (2008), froth stability is the time of persistence of a froth which is related

to froth structure and bubble size distribution. Zanin et al. (2009) argues that froth stability is a critical factor in determining froth recovery but it has no unique measure or precise definition. The structural features and dynamics of flotation froth are influenced by the mechanisms of attachment, entrainment, drainage and bursting (Barbian et al., 2007).

2.2.1 The importance of froth stability

The froth phase provides a zone where hydrophobic material is upgraded (Ekmekçi et al., 2006). The froth layer must be stable enough to flow over the discharge lip of the cell by gravity or to be removed mechanically by froth scrapers (Kawatra, 2002). It should also provide selective drainage of entrained particles back into the pulp. Thus it is a major contributor to the overall selectivity of the process (Kawatra, 2002). The stability of liquid lamellae between gas bubbles determines the stability of the froth phase and this affects the froth water content (Banford et al., 1998; Neethling & Cilliers, 2002). Water recovery in the concentrate is thus an important parameter in the analysis of froth stability (Ekmekçi et al. 2006).

Froth structure plays an important role in the overall flotation performance but its behaviour is still ill understood (Neethling & Cilliers, 2002). There are consequences that arise when the froth is too stable or when it is highly unstable. A too stable froth is difficult to pump and convey through the plant and if too much is produced, it will overflow from the flotation cell (Kawatra, 2002). In addition to this, if the froth is too stable, it could entrain a large amount of gangue resulting in poor grade of concentrate (Moolman et al., 1995). If the froth is unstable, the bubbles break and the hydrophobic particles prematurely return to the slurry (Kawatra, 2002). It is thus evident froth stability has a critical importance in the selectivity and flotation rate (Kawatra, 2002).

2.2.2 Factors affecting froth stability

Different factors contribute to the stability of the froth phase as a whole. These can be divided into internal and external factors. An external factor affecting froth stability is relative humidity. Industrial flotation cells are exposed to the atmosphere and relative humidity of less than 60% has been found to decrease froth stability drastically due to evaporation (Hartland, 2004; Li et al., 2010). Humidity effects were

not investigated in this study and it was assumed that these did not have a significant effect on the froth stability under the laboratory conditions.

The internal factors affecting froth stability can be categorized into operating factors, chemistry factors and particle factors. These are summarised in the schematic in Figure 2.1. This study involves the effect of copper sulphate (an activator) on the froth stability and therefore falls under chemistry factors. However, activators affect particle properties – in particular, the hydrophobicity of particles. The electrochemical potential (Eh) and pH of the system is also known to affect the froth stability, but this was beyond the scope of this study and were maintained constant. Operating factors were also not investigated as the same operating conditions were used for the studies.

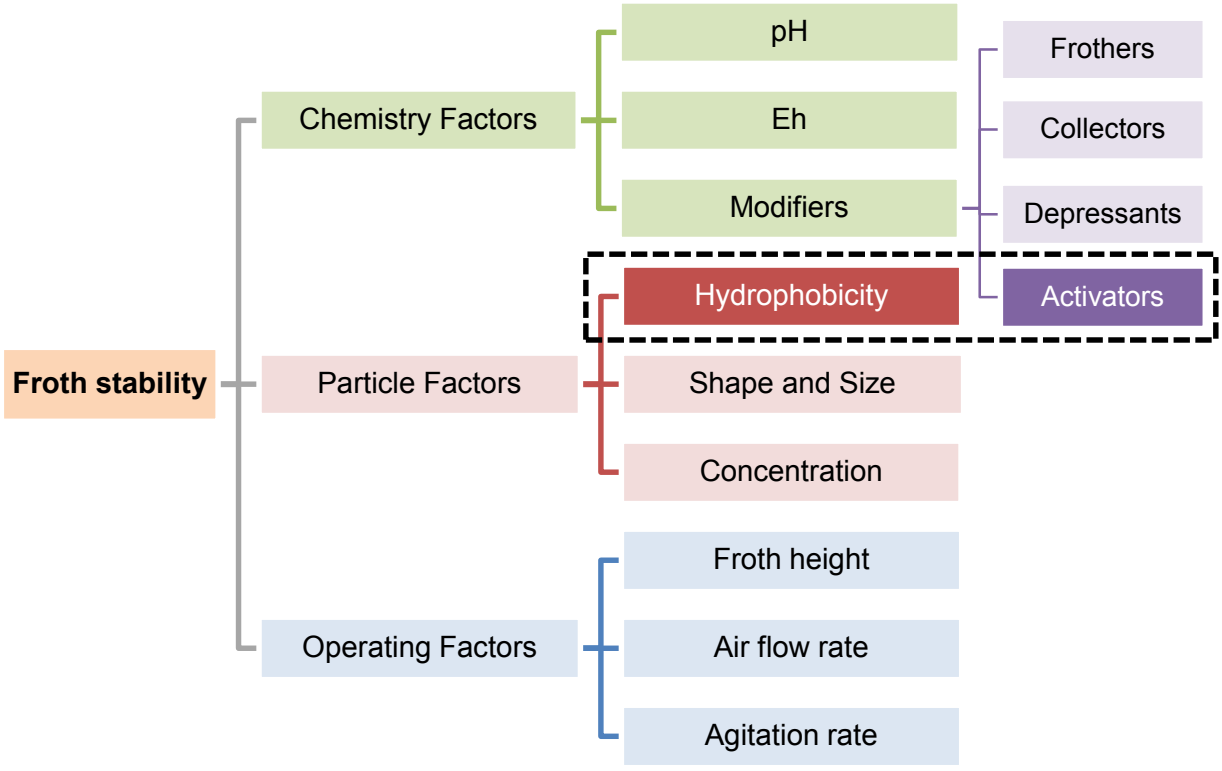

Figure 2.1: Schematic of the factors affecting froth stability

The factors affecting froth stability pertinent to this study are discussed in more detail in paragraphs (a) and (b).

a) Particle Properties

Several studies have been done on emulsion films stabilised by particles. Horozov (2008) suggested that the behaviour of solid particles in aqueous emulsion films (oil-

water-oil (o-w-o) is similar to that in foam films (gas-water-gas) therefore the stabilising mechanism in aqueous emulsion films could be relevant to aqueous foam films. Particle properties such as particle size, shape, concentration and hydrophobicity have been found to be the main factors affecting froth stability (Horozov, 2008).

Binks (2002) suggested that colloidal particles act in many ways like surfactant molecules, particularly if adsorbed to a fluid-fluid interface. A wide variety of solid particles have been used as stabilisers in emulsions and these include hydroxides, metal sulphates and silica only to mention a few (Binks, 2002). The author also added that the effectiveness of the solid in stabilising emulsions depends on several particle factors such as size, shape, concentration, wettability and inter-particle interactions.

In the studies by Ip et al. (1999) on the effect of particle properties on the stability of molten and aqueous aluminium foams, partially wetted particles were shown to accumulate at bubble surfaces providing a barrier preventing rupture and coalescence. Hunter et al. (2008) described this phenomena as particles creating a steric barrier to coalescence which increases the froth stability.

Naturally floatable gangue has been found to stabilise froth, whereas the sulphide minerals may destabilise froth depending on the hydrophobicity of the sulphide minerals (Wiese et al., 2011).The overall stability for any given system is a delicate balance of particle-interface, surfactant-interface and particle-surfactant interactions (Hunter et al., 2008). Particle shape, size and concentration effects are beyond the scope of this dissertation hence they will not be addressed further.

i. Particle charge

In the flotation system, it is important to consider surface forces at the interface of the particle and the liquid. A colloidal system can be described as a fine dispersion of one of the three states of matter (solid, liquid or gas) in another. Colloidal particles carry an electrical charge which produces a force of mutual electrostatic repulsion between adjacent particles (Verwey & Overbeek, 1948).The particles will remain discrete and disperse if the charge is high enough and they will agglomerate and settle out of suspension if the charge is removed.

The surface particle charge can be altered by the addition of electrolytes (changing ionic species in solution), by altering the pH of the system or by the addition of surface active agents or cationic surfactants which adsorb onto the mineral/colloid surface and change its characteristics (Verwey & Overbeek, 1948). The electrostatic interactions that exist between particles or between particle and bubble interfaces could have an effect on the lamella of the bubbles and hence the stability of the froth phase.

ii. Particle hydrophobicity

Flotation depends on the probability of attachment of particles to the bubbles and this probability is a function of the hydrophobicity of the particles (Chen, 2012). The model developed by Ross (1997) on particle-bubble attachment in flotation froths showed that in order for particles to attach to bubbles, they must be sufficiently hydrophobic. The process of film thinning and liquid drainage is critical in the formation of stable bubble-particle attachments and this is affected by the particle shape and surface hydrophobicity (Koh et al., 2009).

Contact angle can be used as a measure of hydrophobicity (Koh et al., 2009). When a solid particle is attached to a gas bubble in a liquid, the resulting contact angle is given by Young/Dupre's equation in terms of interfacial energies as:

$$\gamma_{sv} - \gamma_{sl} = \gamma_{lv}cos\theta \quad \text{.....2.1}$$

Where γ_{sv}, γ_{sl} and γ_{lv} are solid-vapour, solid-liquid and liquid-vapour interfacial tensions respectively and θ is the contact angle (Kawatra, 2002).

This is illustrated in Figure 2.1.

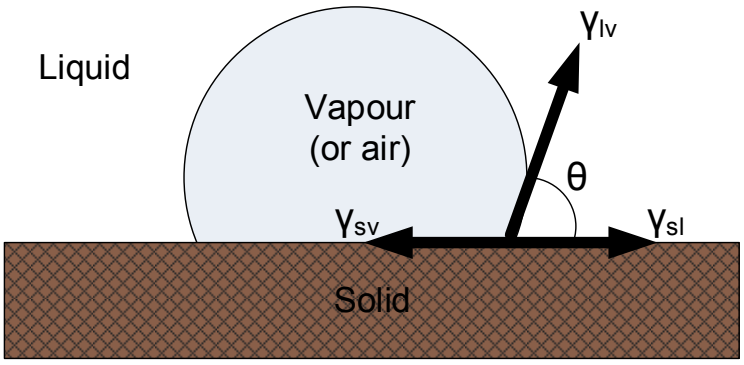

Figure 2.2: Contact angle (θ) between air bubble and a particle immersed in a liquid (Kawatra, 2002)

Models of film stabilisation predict an increase in the film stability as the contact angle decreases which suggests the very hydrophilic particles should stabilise films better than hydrophobic ones (Farrokhpay, 2011). However, in practise, this is not found to be the case. In studies on the effects of particle size, shape and hydrophobicity on the stability of three phase films, Dippenaar (1982) proposed that weakly hydrophobic particles can stabilise froths by attaching to both interfaces of the draining lamella and prevent the films from coming together. On the other hand, strongly hydrophobic particles were found to destabilise the froth by bridging the froth films and allowing rapid movement of the interface across the particle surface resulting in collapse of the bubble (Dippenaar, 1982).

Johansson and Pugh (1992) showed particles of intermediate hydrophobicity with a contact angle of 65° promoted maximum froth stability, whereas more hydrophobic particles with contact angle greater than 90° destabilised the froth. Hydrophilic particles were found not to have an effect on the froth properties in the same study. However, the contact angle at which film rupture occurs can be as low as 75° depending on particle size, shape and the number of particles as well as the separation distance between the particles in the film (Ata, 2012). Dudenkov (1967) found well dispersed hydrophobic particles to break froths presumably by the acceleration of coalescence of bubbles in the froth phase.

Johansson and Pugh (1992) in their investigation on the stability of froths using quartz particles with varying degrees of hydrophobicity found that fine hydrophobic particles destabilised the froth while those with intermediate hydrophobicity maximised froth stability. Cilliers and Bradshaw (1996) conducted experiments varying the hydrophobicity of artificial minerals and found out that the addition of fine quartz yielded an extremely stable froth whereas the presence of pyrite in the system caused coalescence of bubbles and the ultimate collapse of the froth. This is also consistent with what has been found in conventional flotation operations (Cilliers & Bradshaw, 1996).

iii. Particle hydrophilicity

Fairly hydrophilic particles have also been found to enhance froth stability since they collect in the plateau borders slowing down film drainage (Binks, 2002). On the other hand, (Bartsch, 1924) found partially hydrophobic particles stabilised foams

whereas, completely wetted (hydrophilic) particles had no effect on the stability. Hydrophilic particles (of contact angle less than 65°) were found not to have an impact on froth stability (Johansson & Pugh, 1992). The hydrophobic particles had an effect on the structure of the froth, allowing increased drainage rates of water in the froth resulting in drier froths in which the hydrophilic particles became more entrapped (Ata et al., 2004)

Murray and Ettelaie (2004) found that hydrophilic particles got trapped in thinning films and structured themselves in layers that could not be easily removed from the film and this was found to be true for particles well below the initial thickness of the thinning film.

b) Presence of inorganic electrolytes

Inorganic electrolytes are found in process water and they fall under chemical factors affecting froth stability on industrial plants. Process water is recirculated in flotation operations in order to reduce fresh water consumption. The process water has a high concentration of ions from the ore and from reagents. While there has been much work done on ions in two-phase systems, very little literature exists on the effects of ions in three-phase systems.

The two phase column flotation tests conducted by Quinn et al. (2007) using plant water with high inorganic salt content showed there was lower frother consumption due to reduction in bubble size caused by the salt solutions.

Several surface chemical mechanisms have been proposed for the action of electrolytes in flotation processes namely:

i. Disruption of hydration layers surrounding the particles and enhancing bubble-particle capture.
ii. Reducing the electrostatic interactions.
iii. Increasing charge on the surface of the bubbles to prevent primary bubble coalescence. (Pugh et al., 1997).

Gas bubbles are negatively charged in pure water and in solutions of simple inorganic electrolytes and in the presence of surfactants, the charge of the bubbles is governed by the charge of the head group (Li & Somasundaran, 1993). In their

studies on reversal of bubble charge in multivalent inorganic salt solutions, Li and Somasundaran (1993) found out that bubbles can be positively charged in electrolyte solutions of multivalent ions depending on the salt concentration and solution pH.

Two-phase studies showed multivalent ions have a greater effect on coalescence than monovalent ions (Zieminski & Whittemore, 1971; Deschenes et al., 1998). The change in bubble size produced by the addition of electrolytes was ascribed partly to the electric repulsive forces generated by the surface potentials which hinder bubble coalescence. This could also have been due to the effects of ion-water interactions such as the ionic entropy of hydration (Zieminski & Whittemore, 1971).

The ionic strength of an electrolyte solution, μ is a measure of the average electrostatic interactions of the ions in solution which may be determined by the following equation.

$$\mu = \frac{1}{2}\sum_i^n C_i Z_i^2 \quad \text{.....2.2}$$

where C_i and Z_i are the molar concentration and the charge of the ith ion in solution respectively and the summation sign is taken over all ionic species in solution (Quinn et al., 2007).

Manono et al. (2013) found that a change in ionic strength could affect the flotation process by affecting the surface reactions occurring at the mineral surface and also the stability of the froth. Their study showed increasing ionic strength resulted in an increase in water recovery and reduction in bubble size which is consistent with earlier findings in literature (Muzenda, 2010; Farrokhpay & Zanin, 2011). In addition, the foam height and collapse time of a two-phase system increased with increasing ionic strength, showing that ionic strength of plant water plays an important role in froth stability.

In separate studies by Manono et al. (2012), the impact of ionic strength was attributed to the fact that inorganic ions in water slowed the inter-bubble drainage and when inorganic ions were present at high ionic strength, they inhibited bubble coalescence resulting in more stable froths. Candidate causes for inhibition by electrolytes include decreased gas solubility, double-layer effects, changes in

viscosity, the Gibbs-Marangoni effect, and other surface tension effects (Weissenborn & Pugh, 1996; Deschenes et al., 1998; Craig, 2004).

The findings of Pugh et al. (1997) show that there is a correlation between the flotation performance and the thickness of the electrostatic double layer, which suggests that the electrostatic interaction played a role in the process. Moreover, electrolytes with small, strongly charged and hydrated cations (divalent and trivalent) were found to give good flotation response (Pugh et al., 1997).

2.2.3 Quantitative analysis of froth stability

Many measures of froth stability have been employed including air recovery, water recovery, bubble size on top of the froth, bubble burst rate, bubble growth rate, froth rise velocity and froth decay (Barbian et al., 2003; Zanin et al., 2009).

The methods to quantify froth stability can be classified into non-overflowing and overflowing systems. Non-overflowing systems are batch operations while overflowing systems are continuous operations. Measuring froth stability quantitatively in a consistent manner is still a significant challenge especially at industrial scale (Barbian et al., 2006).

In this dissertation, non-overflowing systems will be discussed which can further be classified into (a) dynamic and (b) static methods. In the dynamic test, the foam is allowed to reach a state of dynamic equilibrium between the rates of formation and decay. A static test on the other hand has a rate of foam formation of zero and once the foam is formed, it is allowed to collapse without regeneration by input of gas or further agitation (Barbian et al., 2003).

a) Dynamic Test

A dynamic method of measuring froth stability was developed by Bikerman (1973) in which gas was passed (at different flow rates, Q) through a column containing a solution with known concentration of frother. In the Bikerman test, the height of the froth in the column increases with time and the froth height, H is measured as a function of time t, using the pulp-froth interface as the reference. The foam column reaches a maximum height where it becomes constant and equilibrium is achieved.

Bikerman (1973) proposed the ratio of steady state foam volume to gas flow rate as a unit of foaminess for dynamic foams, which is denoted as $\sum$. This is a measure of the average time that the gas remains entrained in the foam.

Dynamic froth stability can be defined as:

$$\sum = \frac{V_f}{Q} = \frac{A.H_{max}}{Q} \quad \text{.....2.3}$$

where $\sum$ is the dynamic froth stability factor, V_f is the volume of foam at equilibrium, Q is the gas volumetric flow rate, H_{max} is the equilibrium foam height and A is the cross-sectional area of the column (Bikerman, 1973).

The values of froth height as a function of time $H(t)$ can be fitted by an exponential model of the form below to determine the value of H_{max}:

$$H(t) = H_{max}(1 - e^{-\frac{t}{\tau}}) \quad \text{.....2.4}$$

where τ is the characteristic average bubble lifetime. Figure 2.3 shows the exponential model fitted to the experimental data.

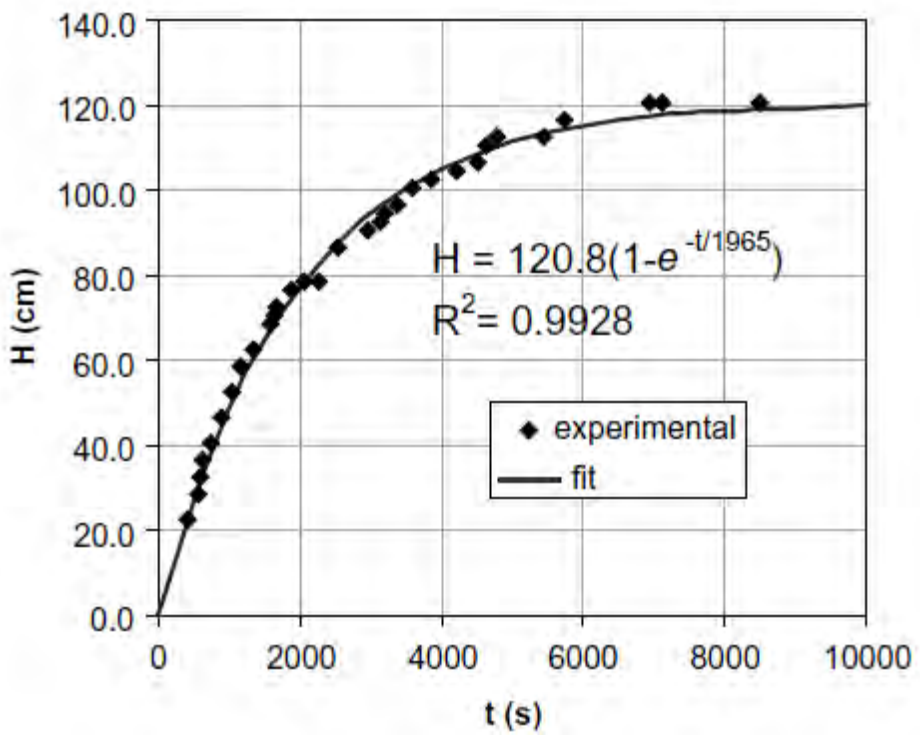

Figure 2.3: Variation of froth height with time in an industrial flotation cell (Barbian et al., 2005).

From this model, H_{max} and τ can be used to quantify froth stability.

b) Static Test

In their studies, Zanin et al. (2009) used bubble half-life, $t_{1/2}$ and bubble size on top of the froth as indicators of froth stability on flotation concentrators treating porphyry copper ore. $t_{1/2}$ is the time taken for the foam to drop to one half of its initial height, $H_{max,}$ when the air flow is discontinued. The data from the froth decay process can be fitted to an equation of the form (Zanin et al., 2009):

$$\frac{H_f}{H_{f\,max}} = \frac{1}{2} - \alpha ln\left(\frac{t}{t_{\frac{1}{2}}}\right) \quad \text{.....2.5}$$

In the equation, α is an empirical dimensionless constant. The froth half-time was used to characterize the stability of mineral flotation froths at both laboratory and industrial scales and there was good agreement between the results (Zanin et al., 2009). Figure 2.4 shows the fit of industrial scale data from the tests conducted by Zanin et al. (2009) to equation 2.5.

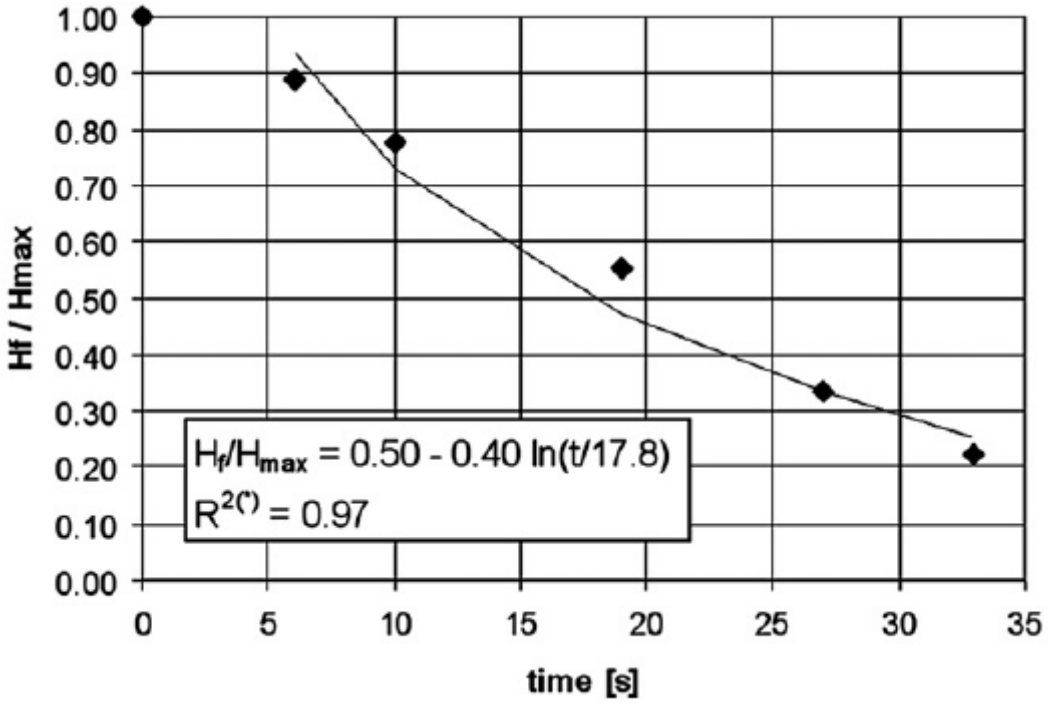

Figure 2.4: Froth decay profile used in the analysis of froth decay (Zanin et al., 2009)

The froth stability column used in this study is discussed in the experimental methodology chapter of this dissertation.

2.3 Electrical characteristics at interfaces

The electrical characteristics of mineral surfaces are important in understanding most of the pulp phase chemistry. These properties are determined by two potentials namely electrochemical and electrokinetic (Bulatovic, 2007). Collins and Jameson (1976) in their studies on the influence of particle size and charge on flotation of fine particles concluded double layer effects on the surfaces of particles and bubbles have a significant role on the overall process.

2.3.1 Electrical Double Layer

The electrical double layer exists around each colloid particle. A negatively charged colloid and some positive ions (counter-ions) form a firm layer around its surface known as the Stern layer. Additional positive ions are repelled by the Stern layer as well as other positive ions trying to approach the colloid resulting in the formation of the diffuse layer of counter ions. The distribution of ions around each colloid is shown in Figure 2.5 (a) below. The Stern layer and the diffuse layer form the electrical double layer. The thickness of the electrical double layer depends on the type and concentration of the ions in solution (Verwey & Overbeek, 1948).

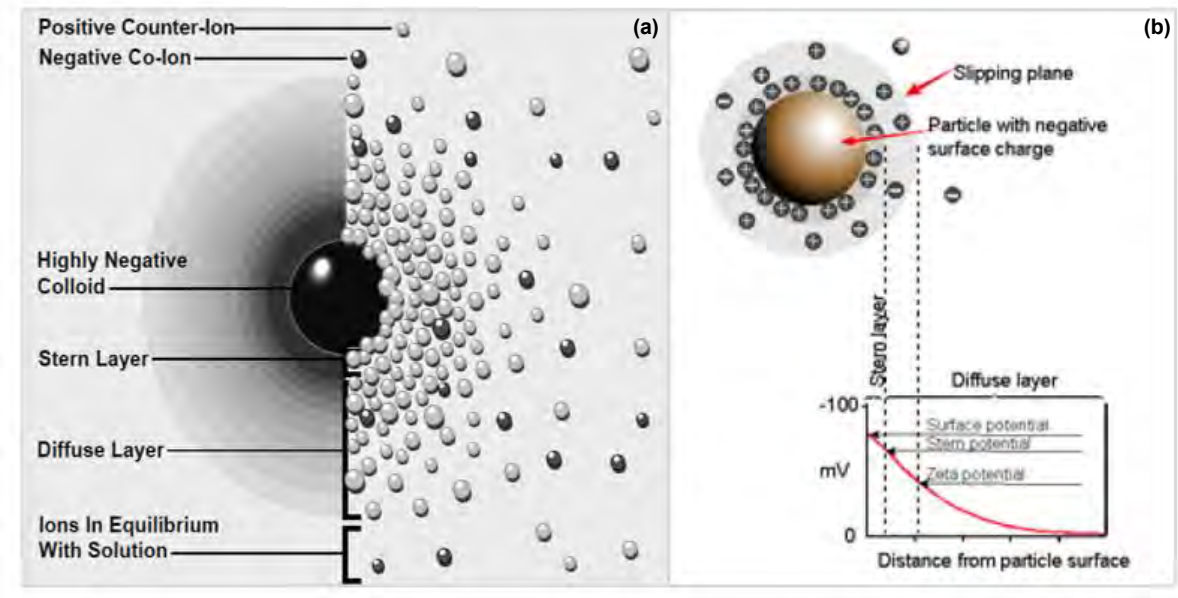

Figure 2.5: The distribution of ions around a colloid (a) and a schematic representation of zeta potential (b). (Zeta-Meter, (1997) (a), Zetasizer, (2011) (b)).

Figure 2.5 (b) illustrates the electrical double layer. When electrical double layers overlap, the result is attraction or repulsion depending on the charge i.e. when the charges have the same sign, the resulting force is repulsive which results in film

stabilisation by electrostatic repulsion (Hartland, 2004). The double layer repulsive forces provide a disjoining pressure that slows or prevents film drainage (Craig, 2004).

On the other hand, if the layers are of opposite charge, the resulting force is attractive resulting in thinning and rupturing of the film between the particle and the bubble (Mao et al., 1998). The electrical double layer theory plays an important role in the adsorption of reagents onto the mineral surface (Bulatovic, 2007). Hydrophobic particles are known to create an energy barrier which compresses the electrical double layer which facilitates attachment.

2.3.2 Zeta Potential

Zeta potential is the electrical potential at the junction between the Stern layer and the diffuse layer - illustrated in Figure 2.5 (b). The electrophoretic mobility (u_E) which is the velocity of a charged particle per unit electric field can be measured to obtain the net charge on the particle and this depends on the suspending fluid properties such as the viscosity and the dielectric constant (Hunter,1993). The ionic concentration of an electrolyte affects the thickness of the electrical double layer (Pugh et al., 1997). If all the particles in suspension have a large positive or negative zeta potential, they repel each other. The tendency for particles to come together is high when the zeta potential is low.

On the zeta potential versus pH curve, a zeta potential of zero indicates the isoelectric point pH ($pH_{i.e.p}$) which is normally the point where the colloidal system is least stable. $pH_{i.e.p}$ is the pH at which a colloid particle has a neutral net electrical charge and both positive and negative charges are present in equal amounts on the colloid surface. The point of zero charge (PZC) on the other hand is the pH at which a colloid particle carries no net electrical charge in the absence of positive and negative charges at the colloid surface (Adamson & Gast, 1967) . In literature, the two terms have been taken to have the same meaning. The PZC is determined by titration in various concentrations of electrolyte solution. The zeta potential versus pH graphs will intersect at a common pH with zero net electrical charge and this is the point of zero charge (Adamson & Gast, 1967). The PZC and $pH_{i.e.p}$ are shown in Figure 2.6.

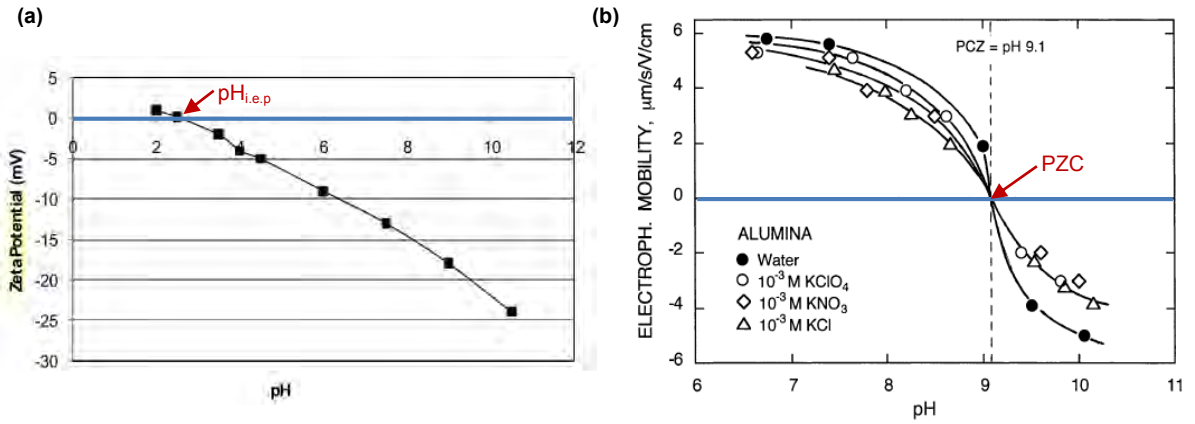

Figure 2.6: The difference between the pH$_{i.e.p}$ (a) and PZC (b) of a particle (Farrokhpay & Zanin, (2011) (a); Fuerstenau & Pradip, (2005) (b)).

The zeta potential and isoelectric point of a mineral are influenced by the surface speciation resulting from the variations in pH, conditioning time, temperature, reagent type and reagent concentration (Chandra & Gerson, 2009). Zeta potential can be used to control the degree of adsorption between the collector and the mineral.

2.4 Mineralogy

2.4.1 Ore mineralogy

The Bushveld complex in South Africa is the world's largest source of platinum group minerals (PGMs). The three reserves of platinum-group metals are concentrated on three narrow but extensive layers in the Bushveld Complex namely the Merensky Reef, the Platreef and the UG2 chromitite layer. Each of these three has distinctive associated mineralogy and they require different approaches in metallurgical processing (Jones, 1999).

The two ores used in this study were Merensky and UG2. Table 2.1 summarizes some of the key mineralogical differences between the two ores.

Table 2.1: Comparison between UG2 and Merensky ores (Jones, 1999).

Merensky	UG2
Dominated by orthopyroxene (~60%) and plagioclase (~20%).	Dominated by chromite (~60-90%), with less silicate minerals orthopyroxene (~5-25%) and plagioclase (~1-10%).
Cr_2O_3 (chromium (III) oxide) content is about 0.1%	Cr_2O_3 content is about 30%.
BMS make up to 3% of the ore-chalcopyrite, pyrrhotite and pentlandite with pyrite in trace amounts (<0.1%).	BMS represent less than 0.1% of the mass of the reef, the most abundant being chalcopyrite, pentlandite and pyrrhotite.
Minerals found in a silicate substrate. Majority of the PGMs associated with pentlandite, in either the grains or along the pentlandite-gangue boundaries.	Sulphide grains are generally finer than those of the Merensky reef. PGMs found in a chromite matrix.
PGM content in the reef ranges between about 4 and 10 g/t.	PGM content in the reef between 4.4 and 10.6 g/t.
Average PGM mineral grain size about 45 µm, concentrate milled to about 55% passing 75 µm to liberate the PGM minerals.	Average PGM mineral grain size about 15 µm, concentrate finely milled to about 80% passing 75 µm to liberate the PGM minerals.

Lower concentrate grade because for a given quantity of ore, the mass of concentrate is higher than in UG2 ore. The smelting costs are thus higher than UG2.	The grades of UG2 concentrate are higher than Merensky concentrate (around 1.3% of the feed ore), hence the amount of concentrate to be smelted is smaller.

Sulphide mineral surfaces undergo significant changes in the surface layers due to structural and chemical rearrangements after immersion in solutions (Smart et al., 1998). Knowledge of the mineralogy of the ores is important so as to understand the reactions occurring in the pulp phase between the mineral surface and the activator - copper sulphate.

Four pure minerals were selected for further tests using zeta potential determinations and microflotation. These were chromite, plagioclase, pyrrhotite and talc. The mineralogy of these minerals is further discussed below:

2.4.2 Chromite mineralogy

The chemical composition of chromite is ($FeO.Cr_2O_3$). Chromite is an oxide mineral and it is generally regarded as naturally hydrophilic hence it is almost entirely recovered to the concentrate by entrainment. The chromite content in UG2 is significantly higher than for Merensky and its recovery to the final concentrate has detrimental effects in downstream smelting (Hay & Roy, 2010).

2.4.3 Plagioclase mineralogy

Plagioclase is a silicate gangue mineral found in both Merensky and UG2 ores which belongs to the feldspar group of minerals. The two variations are albite ($NaAlSi_3O_8$) and anorthite ($CaAl_2Si_2O_8$) both found mixed in the mineral's crystal lattice structure (Martinovic et al., 2005). Plagioclase is considered to be a hydrophilic mineral.

2.4.4 Pyrrhotite mineralogy

Pyrrhotite is a non-stoichiometric mineral with a variable chemical composition ($Fe_{1-x}S$). The ratio of sulphur atoms to iron atoms varies i.e. the value of x varies from 0 to 0.2 (Miller et al., 2005). It exists as magnetic and non-magnetic forms also

dependent on the x value. Pentlandite, the best known PGE carrier often occurs within pyrrhotite hence the recovery of PGMs is strongly related to the flotation characteristics of pyrrhotite (Vermaak, 2005).

2.4.5 Talc mineralogy

Talc is a naturally hydrophobic magnesium silicate gangue mineral which is friable and hydrous with a chemical composition of $Mg_3Si_4O_{10}(OH)_2$ (Nashwa, 2008). Minor amounts of talc are found in UG2 ore when compared to Merensky ore which requires the use of a talc depressant making the cost of treatment of UG2 ore lower than Merensky ore (Jones, 1999).

According to Morris et al. (2002), 90% of the talc surface is hydrophobic making it easily recoverable in the flotation concentrate. Talc is problematic in flotation of these ores because it is naturally hydrophobic and although present in small amounts, it has a disproportionate effect as it has a strong froth stabilising effect which results in an increase in the recovery of other minerals by entrainment (Martinovic et al., 2005).

2.5 The role of copper sulphate in the pulp phase

The effect of addition of copper sulphate in the PGM industry is still controversial and causes a wide range of responses (Wiese et al., 2007; Moolman et al., 1995). In addition, the PGM's in Platreef and UG2 ore are not associated with BMS, yet copper sulphate is still added on some concentrators. In this case, it is not known whether there is a beneficial effect on true flotation of the PGM's or whether there are froth effects.

The subject of activation of sulphides is still subject to debate due to the varying conditions used in the different studies that have been done. The following sections will discuss copper speciation, classical sphalerite activation, activation of other sulphides and gangue mineral activation.

2.5.1 Copper speciation

Speciation diagrams for metal ion systems show the concentration of different species as a function of pH. They can thus be used to estimate the metal hydroxyl species occurring at a given pH.

Heavy metal ions undergo a series of pH-controlled hydrolysis reactions in a binary water-cation system (Wang et al., 1989). The following reactions occur spontaneously for Cu(II):

$$Cu^{2+} + OH^- \leftrightarrow Cu(OH)^+ \quad \text{2.6}$$

$$2Cu^{2+} + 2OH^- \leftrightarrow Cu_2(OH)_2^{2+} \quad \text{2.7}$$

$$Cu^{2+} + 2OH^- \leftrightarrow Cu(OH)_2\,(aq) \quad \text{2.8}$$

$$Cu^{2+} + 2OH^- \leftrightarrow Cu(OH)_2\,(s) \quad \text{2.9}$$

$$Cu^{2+} + 3OH^- \leftrightarrow Cu(OH)_3^- \quad \text{2.10}$$

$$Cu^{2+} + 4OH^- \leftrightarrow Cu(OH)_4^{2-} \quad \text{2.11}$$

The initial hydrolysis occurs in equation 2.6. Equations 2.7 and 2.9 show dimer formation and precipitation reactions respectively.

Figure 2.7 is a copper speciation diagram showing the hydrolysis of cupric ions at 25°C. At pH lower than 6, Cu^{2+} ions are predominant. $Cu(OH)_2$ (solid) is produced as the pH is raised, while the concentration of Cu^{2+} ions progressively decreases (Rao, 2003). The type of species present influences the adsorption mechanism as well as the flotation efficiency (Ralston & Healy, 1980).

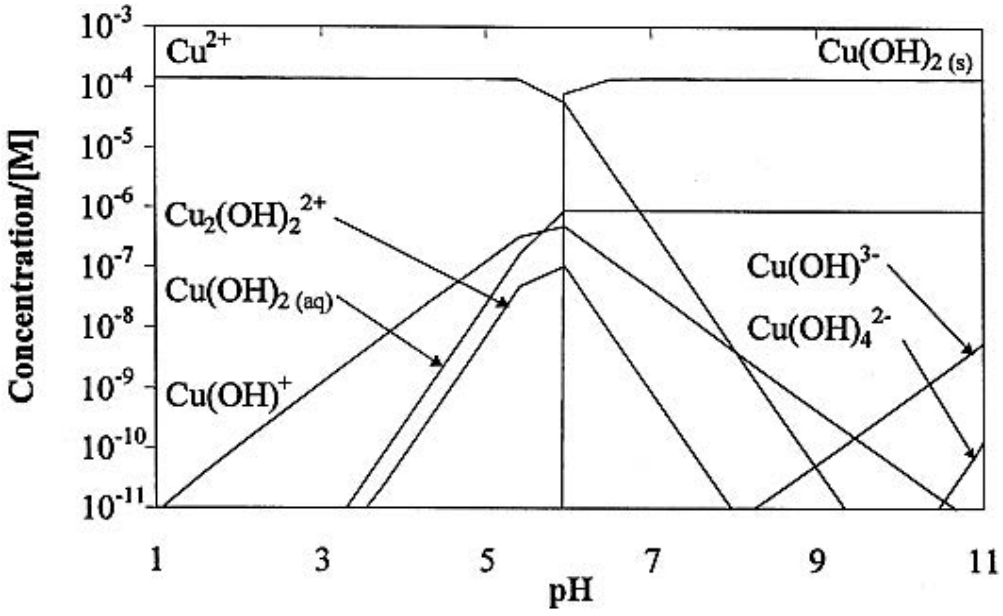

Figure 2.7: Speciation diagram for 1*10^{-4} M Cu^{2+} (Fuerstenau, 1982)

Poor bubble-particle contact near neutral pH region has been attributed to the precipitation of copper xanthate in the presence of excess copper ions which depleted the solution of xanthate ions (Chen & Yoon, 2000). The depression of xanthate could also be due to the presence of $CuOH^+$ ions at the near neutral pH which do not form 'flotation active' activation products such as CuS suggesting a longer conditioning time is needed under these conditions (Chen & Yoon, 2000). The precipitation of $Cu(OH)_2$ is expected to lead to a marked decrease in zeta potential since $Cu(OH)_2$ does not carry any charge (Malysiak, 2003).

2.5.2 Sphalerite activation

Extensive studies have been done on the activation of metal sulphides. The exchange reaction between many heavy metal ions such as Cu^{2+} and Pb^{2+} and sphalerite is thermodynamically favourable and the reaction mechanism is well documented in literature (Ralston & Healy, 1980; Trahar et al., 1997; Finkelstein, 1997; Chen & Yoon, 2000).

The most widely accepted mechanism of copper activation of sphalerite is a two-step process including a fast initial step and a slower second step. The first step is a direct ion exchange between Cu^{2+} and Zn^{2+} ions. Two copper complexes have been found to form on mineral surfaces namely Cu(I) which is usually Cu_2S and Cu(II) in the form of CuS (Finkelstein, 1997). The second step involves the diffusion of copper ions into the protective Cu(I)S film and into the lattice of the mineral (Prestidge et al.,1994). The other mechanism suggested is an electrochemical redox reaction which involves oxidation of sulphur on the mineral and reduction of copper (Finkelstein,1997). It is expected that similar mechanisms occur for the activation of other base metal sulphides in the Merensky and UG2 ores investigated.

a) Activation mechanism in the absence of xanthate

Wiese et al. (2007) and Chandra and Gerson (2009) agree that the addition of copper sulphate to metal sulphide mineral containing systems results in a complex set of responses. The generic overall reaction between metal ion (M^{2+}) and sphalerite in the presence of a thiol collector in acidic conditions is well documented in literature (Wang et al., 1989; Trahar et al., 1997; Chandra & Gerson, 2009). There is very little literature for the activation of sulphide minerals in alkaline conditions. It is

important to understand the reactions occurring at these conditions because most flotation processes occur at alkaline conditions due to mineralization of the ores (Wiese et al., 2007).

The acidic activation model is supported by the reaction stoichiometry as the concentration of metal ions adsorbed onto the mineral surface is more or less the same as the concentration of metal ions released from the surface into the bulk solution. In addition to this, it is also thermodynamically favourable (Wang et al., 1989). The ion exchange reaction is shown below:

$$ZnS_{(s)} + M^{2+}_{(aq)} \leftrightarrow MS_{(s)} + Zn^{2+}_{(aq)} \quad \text{.....2.12}$$

whereas in alkaline conditions, the suggested reaction is (Trahar et al. 1997; Chandra & Gerson, 2009).

$$ZnS_{(s)} + M(OH)_{2(s)} \leftrightarrow MS_{(s)} + Zn(OH)_{2(s)} \quad \text{.....2.13}$$

b) Activation mechanism in the presence of xanthate

Chandra and Gerson (2009) showed that copper sulphate could lead to the activation of gangue minerals in the presence of dithiophosphate (DTP), a secondary collector, but not with xanthate alone. These authors also showed that Cu(I)-xanthate is the main surface product formed, especially at low pH (below 6). The following reactions occur at the mineral surface at low pH.

$$Cu^{2+}_{(aq)} + 2X^{-}_{(aq)} \rightarrow CuX_{2(surface)} \quad \text{.....2.14}$$

This is followed by rapid decomposition.

$$2CuX_{2(surface)} \rightarrow 2CuX_{(surface)} + X_{2(surface)} \quad \text{.....2.15}$$

where X^- represents a thiol anion (xanthate collector) and X_2 is dixanthogen.

The activation mechanism in alkaline conditions is more complicated because the activating Cu^{2+} ions are in the form of insoluble metal hydroxides (Wiese et al., 2007). The mechanism is thus dependent on the copper-containing hydroxide species which are precipitated onto the sphalerite surface. In addition, aqueous Cu^{2+} and/or $Cu(OH)_2$ also react with collector molecules leading to non-selective

adsorption of hydrophobic CuX or dixanthogen (X_2) on sphalerite surfaces (Chandra & Gerson, 2009).

In alkaline conditions, surface $Cu(OH)_2$ directly interacts with the xanthate where the OH^- ion is exchanged with the xanthate ion and the resulting product decomposes to form Cu(I)-xanthate and hydrophobic dixanthogen on the surface (Ralston & Healy, 1980; Martinovic et al., 2005; Chandra & Gerson, 2009). These mechanisms are explained by the following equations:

$$Cu(OH)_{2(surface)} + 2X^-_{(aq)} \rightarrow CuX_{2(surface)} + 2OH^-_{(aq)} \quad \text{.....2.16}$$

$$2CuX_{2(surface)} \rightarrow 2CuX_{(surface)} + X_{2(surface)} \quad \text{.....2.17}$$

2.5.3 Sulphide mineral activation

As stated earlier, PGMs are mainly associated with base metal sulphide minerals in the Merensky reef. Pentlandite, chalcopyrite and pyrrhotite form the primary BMS and, among these, pyrrhotite is the most difficult mineral to float from alkaline slurries (Buswell & Nicol, 2002; Miller et al., 2005). It has been termed a 'slow floating' mineral and it is a poor catalyst for oxygen reduction as compared to other sulphide minerals (Buswell & Nicol, 2002). It was thus postulated that losses in PGM recovery are associated with losses in pyrrhotite recovery.

According to Buswell and Nicol (2002), the beneficial effects of copper ions to flotation performance appear to be related to an enhancement of the oxidation of xanthate. Miller et al. (2005) suggest the reaction for the activation of pyrrhotite with cupric ions in acidic conditions (pH below 5) is a direct ion exchange with ferrous ions at the pyrrhotite surface. Under these conditions, copper sulphate significantly improves pyrrhotite recovery.

The role and effectiveness of copper ions in alkaline solutions is not fully understood and the conclusions are controversial (Miller et al., 2005). Some studies have shown that pyrrhotite flotation recovery is significantly improved with addition of copper sulphate in alkaline solutions (Miller et al., 2005). The addition of copper sulphate reduced the stability of the froth but increased the recovery of pyrrhotite and non-sulphide gangue (Ekmekçi et al., 2006). Pyrrhotite has been found to be successfully

activated to different extents by copper. Ekmekçi et al. (2010) used electrochemical impedance spectroscopy (EIS) and microflotation tests to investigate copper activation of four pyrrhotite samples with different crystallographic forms and compositions. The results showed a marked increase in pyrrhotite recovery for three of the samples in the presence of both copper and xanthate. The flotation response was correlated with the capacitance behaviour at the electrode surface which was related to the oxidation of xanthate to dixanthogen and the reduction of copper from Cu(II) to Cu(I) (Ekmekçi et al., 2010).

Buswell and Nicol (2002) proposed that copper(II) sulphide, CuS is only formed in acidic conditions and that no electrochemical reaction occurs at pH 9 between copper and pyrrhotite. Wang et al. (1989) suggested that copper(II) sulphide alone is unstable under normal conditions, therefore, it should not exist. The activation products rather could be copper(I) sulphide (Cu_2S) and elemental sulphur. This then renders the mineral surface hydrophobic and results in collectorless flotation in acidic conditions.

Other copper polysulphides which enhance surface hydrophobicity could also be formed such as CuS_2 and CuS_{1+x} (Luttrell & Yoon, 1984). Kartio et al. (1996) argue that polysulphides are not formed in the activation reaction, but rather as a result of subsequent oxidation of the activated metal sulphide.

In the case of pyrite, other authors argue that activation occurs via an electrochemical reaction as opposed to an ion exchange reaction. The following reaction was suggested by Allison (1972) as the initial step of the activation:

$$FeS_2 + 4Cu^{2+} + 6e \rightarrow Fe^{2+} + 2Cu_2S \quad \text{.....2.18}$$

Copper sulphate is sometimes used to improve the slow flotation of pentlandite. In their studies, Fornasiero & Ralston (2005) on the flotation of pentlandite found that chlorite, lizardite and quartz were activated with Cu(II) and Ni(II) in the presence of xanthate in the pH range 7 to 10.

2.5.4 Gangue mineral activation

The studies by Malysiak (2003) showed inadvertent activation of the silicate gangue minerals (pyroxene and feldspar) by heavy metal ions Cu(II) and Ni (II) which resulted in true flotation of these minerals.

Chromite is one of the main gangue constituents in UG2 ore and it is generally considered naturally hydrophilic and only reports to the concentrate by entrainment (Wesseldijk et al., 1999). However, these authors speculated that copper may activate chromite under certain conditions. They found that collectors alone have an insignificant effect on the flotation of chromite and they postulated that activation was due to the adsorption of copper hydroxide species at the chromite surface which act as sites for collector adsorption. They also observed recoveries of chromite above 60% in the presence of copper sulphate in mildly acidic solutions and this decreased to 20% at a pH value of 10.

The formation of copper hydroxide-xanthate at higher pH values is explained in the equation 2.19 below:

$$CuOH^{+} + X^{-} \rightarrow CuOHX \quad \text{.....2.19}$$

Mailula et al. (2003) showed an initial increase in chromite recovery with reduced water recovery which indicated the froth structure was affected and that there was a decrease in the froth stability. The higher chromite recoveries were related to high copper sulphate dosages which could have activated the chromite and increased its hydrophobicity. This tallied with earlier findings by Dippenaar (1982) showing inadvertent activation could be due to increased mineral hydrophobicity and destabilisation of the froth due to highly hydrophobic copper-xanthate species formed in excess copper conditions.

2.5.5 Summary of activation products

The solubility product (K_{sp}) can be used to predict if the formation of a chemical compound in solution is thermodynamically favourable. The lower the solubility product, the less soluble and more stable the complex formed. Table 2.1 summarises the solubility products of some of the components that could be present in the pulp phase. The literature available for metal xanthates was done on ethyl

xanthate. It is assumed that the solubility product values for isobutyl xanthates obtained in this study are similar to ethyl xanthate values because of the similarities in the molecular structures of the two compounds.

Table 2.2: Solubility products of possible activation compounds at 25°C (Goates et al., 1952; Somasundaran & Moudgil, 1987; Averill & Eldredge, 2012).

Compound		K_{sp}
Name	**Molecular Formula**	
Copper(I) Sulphide	Cu_2S	2.0×10^{-47}
Copper(II) Sulphide	CuS	8.0×10^{-37}
Iron(II) Sulphide	FeS	6.3×10^{-18}
Calcium Hydroxide	$Ca(OH)_2$	5.0×10^{-6}
Magnesium Hydroxide	$Mg(OH)_2$	5.6×10^{-12}
Copper(II) Hydroxide	$Cu(OH)_2$	4.8×10^{-20}
Iron(II) Hydroxide	$Fe(OH)_2$	4.9×10^{-17}
Iron(III) Hydroxide	$Fe(OH)_3$	2.8×10^{-39}
Copper Ethyl Xanthate	$Cu(EX)_2$	5.2×10^{-20}
Iron(II) Ethyl Xanthate	$Fe(EX)_2$	8.0×10^{-8}

A metal xanthate with a low solubility product will form a less soluble metal xanthate, hence the more metal xanthate present on the surface of the mineral. This can be linked to the hydrophobicity of the mineral. Shackleton (2007) speculated that the stability of Cu(OH)EX (s) would be expected to lie in between that of $Cu(EX)_2$ (s) and that of $Cu(OH)_2$ (s). Metal hydroxide xanthates were also found to be less hydrophobic than normal metal xanthates (Finkelstein, 1997). It should be noted however that the formation of these species is also dependent on the electrochemical potential (Eh) of the system amongst other factors.

There is still controversy on the nature of species formed as a result of heavy metal activation. The literature reviewed showed the possible formation of elemental sulphur, metal hydroxyl species, metal hydroxy-xanthate species, and metal(I) or (II) xanthate species. In addition, it is also not clear how these species are distributed on the mineral surface and how they interact with each other and their effect on the froth phase.

2.6 The role of copper sulphate in the froth phase

It is clear from the review of the pulp phase literature on copper activation that several products are formed which affect the particle properties. The link between these modified particles and their effects on the froth phase has not been established. Froth structure and stability affects its ability to transport particles into the concentrate launder (Chen, 2012). Processes occurring in the pulp leave their signature on the froth surface meaning the effect of chemical parameters such as reagent type, reagent concentration, ionic strength and fluctuations in pH are reflected in the characteristics of the surface froth (Moolman et al., 1995).

Ekmekçi et al. (2006) found that copper sulphate addition had a dual effect on the role of flotation of Merensky ore in that it caused the destabilization of the froth zone as well as activation of selected sulphide minerals. This was attributed to the coalescence of air bubbles in the froth phase due to the formation of strongly hydrophobic cuprous xanthate precipitates on the particle surface (Ekmekçi et al., 2006). The authors also found that excessive copper sulphate addition may have resulted in gangue activation by residual copper ions which increased the mass pull and decreased the grade of the concentrate (Ekmekçi et al., 2006).

In separate studies conducted on a UG2 concentrator, it was found that the addition of copper sulphate had a destabilizing effect on the froth zone. This is shown in Figure 2.8 through an entrainment function, using chromite as a non-floating tracer mineral. Entrainment is one of the ways in which gangue is recovered in the concentrate. Less chrome was recovered per unit water with the addition of copper, indicating that the froth was destabilized when copper was added. When the copper was not added, more chromite was entrained, indicating that the froth was more stable (McFadzean, 2014).

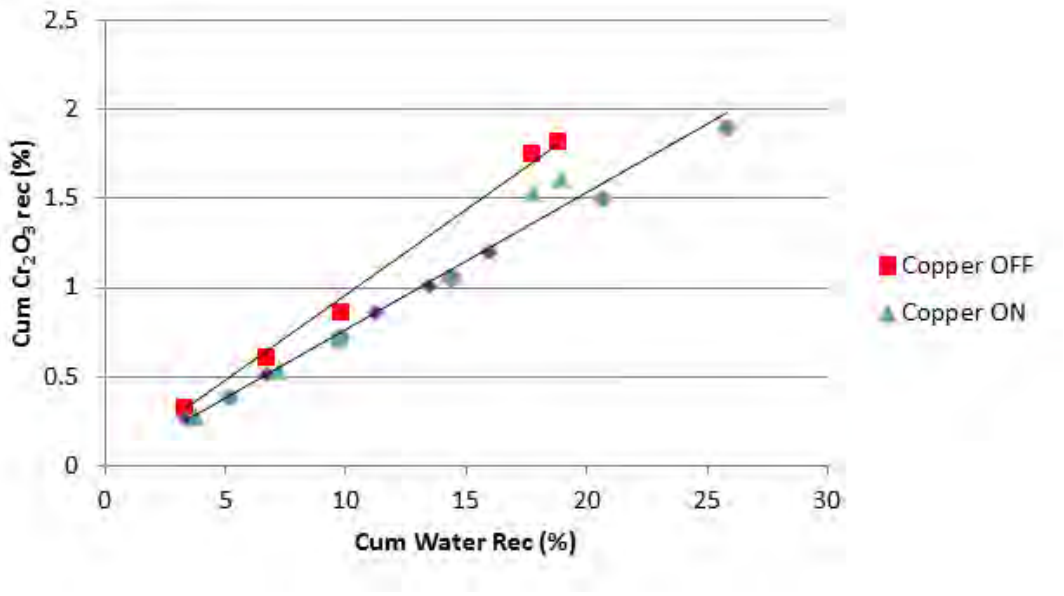

Figure 2.8: Entrainment function for chromite with and without copper as an activator (McFadzean, 2014).

The addition of copper sulphate resulted in a marked decrease in froth stability in the experimental work on batch flotation tests of Merensky ore conducted by Wiese et al. (2011). Since the experiments were conducted at pH 9, the majority of the copper present at these conditions was expected to be $Cu(OH)_2$ with small amounts of $CuOH^+$. These species react with xanthate to form copper (II) xanthate which decomposes to form copper (I) xanthate and dixanthogen (Chandra & Gerson, 2009) It was thought that these copper-xanthate precipitates destabilise the froth (Wiese et al., 2011).

The results from the experimental work done by Chan and Nyabeze (2013) on UG2 ore shows the addition of Cu^{2+}, Pb^{2+} and Mg^{2+} ions at alkaline pH destabilised the froth. They concluded that the sulphide minerals may have acquired a certain degree of hydrophobicity as a result of the precipitation of hydroxide species and the destabilising effect is shown in Figure 2.9. Plant water was used as the baseline.

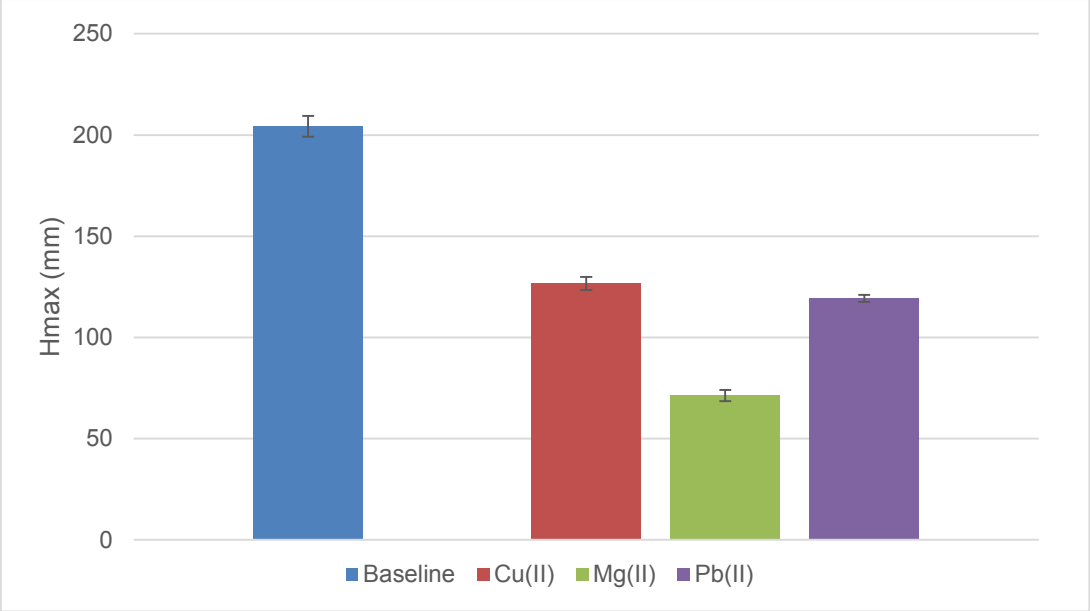

Figure 2.9: The effect of inorganic electrolytes on H_{max} of a UG2 ore at pH 9 (Chan & Nyabeze, 2013).

These authors also showed that there was little effect on froth stability with the addition of copper at lower pH values (pH 3 and 6) which suggested that the copper species present in solution at low pH's were incapable of destabilizing the froth phase. The presence of $Cu(OH)_2$ at pH 9 had a significant effect on froth stability as the value of H_{max} was greatly reduced (Chan & Nyabeze, 2013). This is shown in Figure 2.10.

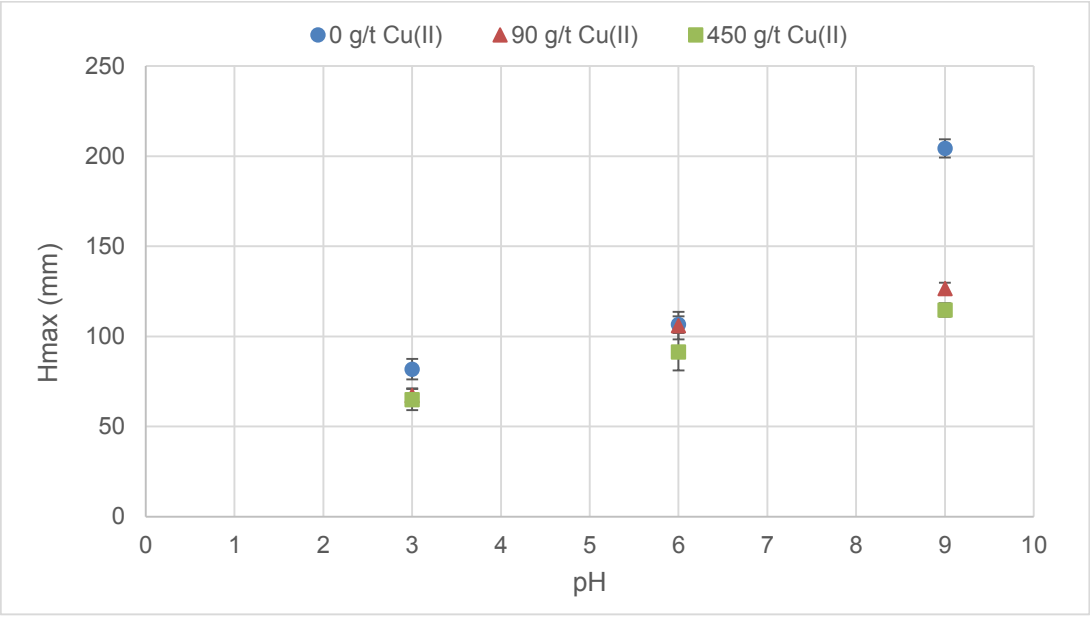

Figure 2.10: The effect of pH on H_{max} in three-phase at different copper dosages (Chan & Nyabeze, 2013).

The formation of insoluble precipitates in the pulp phase can influence the froth phase and reduce recoveries due to the increase in bubble coalescence, which

results in reduced froth height and froth stability. These insoluble precipitates could be a result of the interaction between the collector molecule and heavy metal ions.

2.7 Summary of literature and hypotheses

Overall, the reviewed literature shows there is lack in knowledge on the effect of solid/colloidal hydroxide species in the pulp phase in alkaline conditions on activation of mineral surfaces. The interactions of the activated minerals with xanthate under these conditions are not fully understood as well as the implications of this on the froth phase and recovery of valuable minerals.

Based on the literature reviewed, the following hypotheses are proposed:

1. The addition of copper sulphate to Merensky ore destabilizes the froth due to the formation of Cu(I) on the base metal sulphide surfaces resulting in the formation of a hydrophobic copper-xanthate species. This increases the contact angle and promotes bubble coalescence.

2. The addition of copper sulphate to UG2 ore destabilises the sparsely mineralised froth due to the non-selective formation of hydrophilic colloidal hydroxides on mineral surfaces. This reduces the amount of hydrophobic, froth stabilising particles reporting to the froth phase.

3 EXPERIMENTAL METHODS

This chapter describes the experimental approach used to test the hypotheses proposed. Since copper sulphate is used as an activator to enhance collector adsorption, tests were conducted to investigate the effect of the xanthate collector and copper separately. Tests were also conducted on the pure minerals and ores to test the effectiveness of copper sulphate as an activator when xanthate was added after copper activation.

The chapter begins with details of the sample preparation used as well as the materials and reagents used. The experimental apparatus used for the study are described and the detailed experimental procedures used are given. This is followed by an outline of the preliminary tests used to determine operating conditions. Lastly, an analysis of the reproducibility of the results and an outline of areas of uncertainty in this study is given.

3.1 Sample Preparation

3.1.1 Milling equipment

A 3 kg Sala stainless steel rod mill was used to grind the ores to achieve the required particle size distribution (PSD) for flotation. The mill has an internal diameter of 30 cm and it was charged with 22 stainless steel rods of length 28.5 cm and 25 mm diameter. Stainless steel rods were used to minimise the production of Fe^{3+} ions in the system. The mill is shown in Figure 3.1.

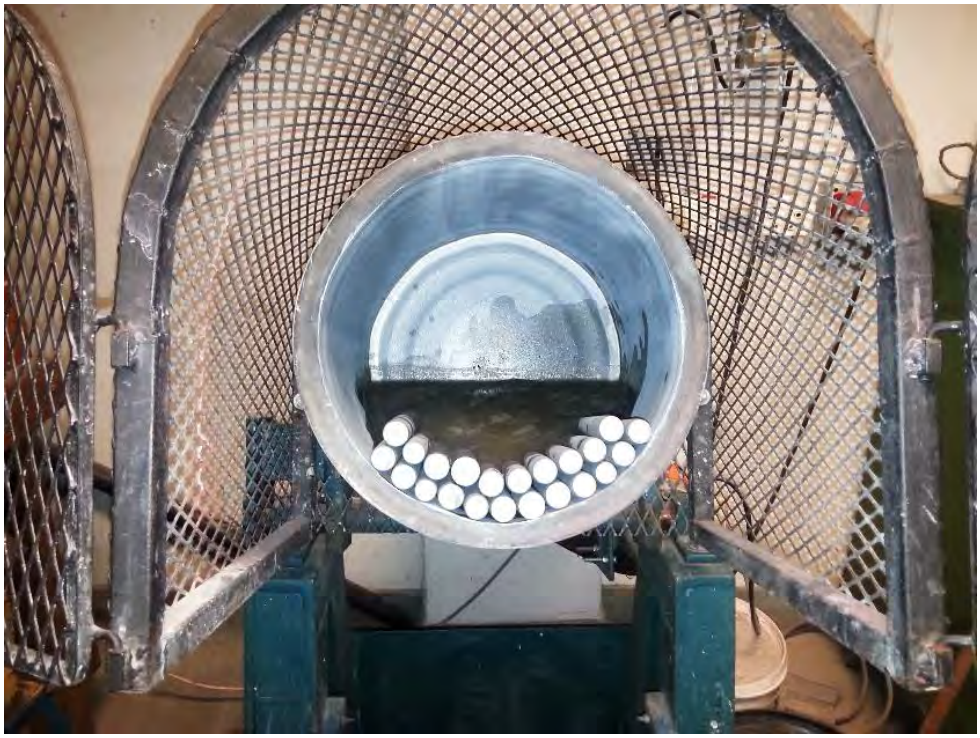

Figure 3.1: 3kg Sala rod mill loaded with wet ore.

3.1.2 Milling curves

The ores were pre-packaged in representative 1 kg packets with particle size less than 3 mm. Milling curves were conducted for both UG2 and Merensky ores and these were used to determine the milling time required to achieve a PSD of 60% passing 75 µm which is the grind that approximately matches the primary rougher feed used in the processing of these ores. 2 kg of ore was wet-milled at 66% solids density for different times. The mill speed was 77 rpm and copper sulphate was added to the mill prior to flotation. The milled slurry was wet screened using a 75 µm sieve, filtered and dried. The milling times required to achieve a grind of 60% passing 75 µm were 16 minutes 18 seconds and 15 minutes for UG2 and Merensky ores, respectively as shown in Figures 3.2 and 3.3.

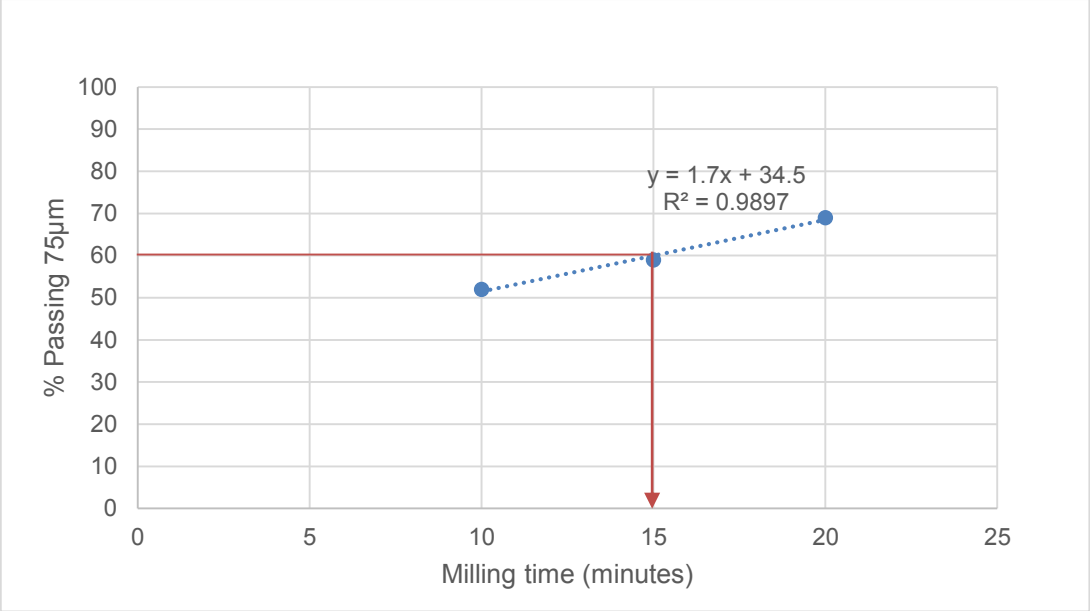

Figure 3.2: Milling curve for Merensky ore

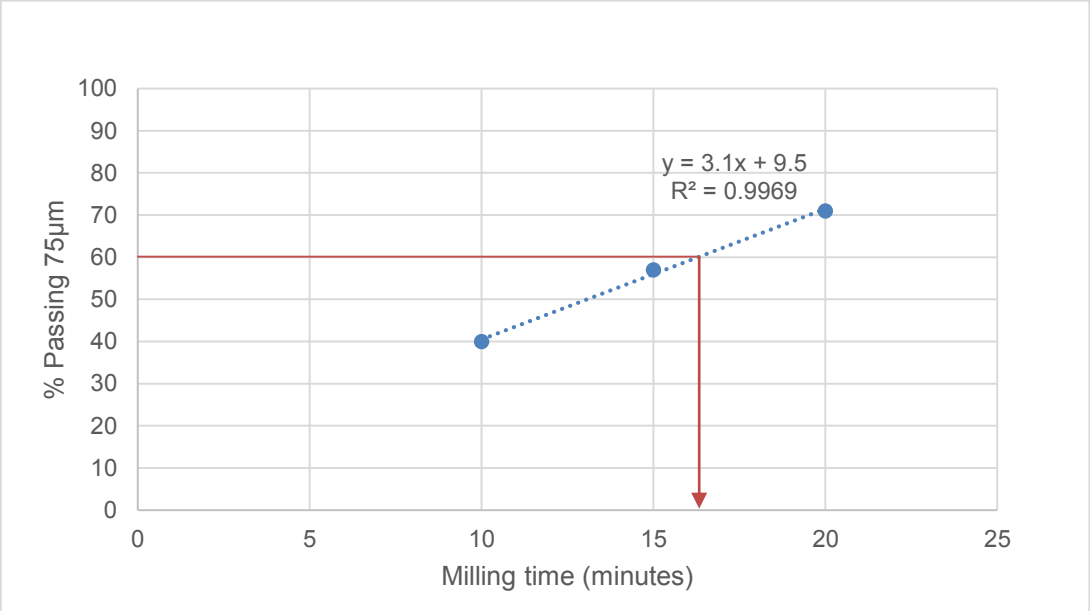

Figure 3.3: Milling curve for UG2 ore

3.2 Materials and Reagents

3.2.1 Ores and pure minerals

The ores used in this investigation were UG2 ore from Lonmin and Merensky ore from BRPM (Bafokeng Rasimone Platinum Mine) in the Bushveld Complex of South Africa.

The pure minerals used were pyrrhotite, plagioclase, chromite and talc. These were chosen carefully to ensure a representative range of gangue minerals and valuable minerals for the UG2 and Merensky ores. Pyrrhotite is the most abundant BMS in Merensky ore and it is closely associated with PGMs. Chromite is a gangue mineral in UG2 ore. Plagioclase and talc are hydrophilic and hydrophobic gangue minerals respectively, present in both ores and activation of these minerals by copper will reduce the grade of the concentrate and affect the froth characteristics.

Thermodynamically, pyrrhotite is not stable and reacts relatively quickly with its environment (Miller et al., 2005). As a result, in the preparation of pyrrhotite for the zeta potential and microflotation experiments special care was taken when handling the mineral. This included storing it under an inert nitrogen atmosphere and in a desiccator to prevent oxidation due to the presence of moisture in the air. Particles of the size fraction 100% passing 25 µm were used for the zeta potential tests and those in the -106 to 38 µm size fraction were used for the microflotation tests. The surface area was determined using the BET (Brunauer Emmett Teller) method for each of the minerals and ores. Table 3.1 shows the BET surface area for each mineral/ore size class investigated.

Table 3.1: BET surface area for each mineral/ore in each size class investigated

Mineral/Ore	BET surface area (m^2/g)		
	-25 µm	-106 +38 µm	60% passing 75 µm
	Zeta Potential	Microflotation	Frothing Column
Talc	5.9503	3.5679	-
Chromite	0.8722	-	-
Plagioclase	1.9473	-	-
Pyrrhotite	0.9486	0.1142	-

Merensky	-	-	0.3921
UG2	-	-	0.8217

The BET surface area was used to calculate the theoretical surface coverage of minerals by copper and xanthate collector. The theoretical surface area required per atom uptake of copper was taken to be 20.8 $Å^2$ as assumed by Gaudin et al. (1959). For xanthate, the theoretical surface area required per atom uptake for a thiol collector was taken to be 37 $Å^2$ as assumed by Bradshaw (1997). The detailed calculations of the surface coverages are given in Appendix A.

3.2.2 Synthetic Plant Water and Deionised Water

Flotation and froth stability tests were conducted in both deionised water and synthetic plant water. The deionised water had a specific conductance of 0.7 µS cm^{-1} and a surface tension of 72.8 mN m^{-1} at 20°C. It should be noted that dissolution of minerals present in the ores into the bulk solution resulted in a low level of ions present in the slurry. These were determined using Atomic Absorption Spectroscopy (AAS) and are shown in Table 3.2 and Table 3.3 for Merensky and UG2 ores, respectively.

Table 3.2: Deionised water cation composition with Merensky ore present

Cations Present	Ca^{2+}	Mg^{2+}	Cu^{2+}	$Fe^{2+/3+}$	Ni^{2+}
Concentration (ppm)	56.9	15.1	0.54	6.04	0.03

Table 3.3: Deionised water cation composition with UG2 ore present

Cations Present	Ca^{2+}	Mg^{2+}	Cu^{2+}	$Fe^{2+/3+}$	Ni^{2+}
Concentration (ppm)	25	6.9	0	1.36	0

It is evident from the data shown in the tables above that the Merensky ore has more dissolved cations in solution than UG2 ore. This is consistent with what has been observed on some PGM operations in South Africa (Lambert, personal communication 2015, January 28).

Synthetic plant water was made in the laboratory by modifying de-ionised water through the addition of chemical salts of analytical grade in Table 3.4. The synthetic plant water contains similar amounts of key ions typically found in flotation circuits on

industrial plants (Wiese et al., 2005). The ionic strength of the synthetic plant water was $2.4x10^{-2}$.

Table 3.4: Synthetic plant water composition

Chemical compound	Molecular Formula	Mass (g) in 20 L	Concentration (mol/l)
Magnesium sulphate heptahydrate	$MgSO_4.7H_2O$	24.60	0.00250
Magnesium nitrate hexahydrate	$Mg(NO_3)_2.6H_2O$	4.28	0.000417
Calcium nitrate tetrahydrate	$Ca(NO_3)_2.4H_2O$	9.44	0.000999
Calcium chloride dihydrate	$CaCl_2.2H_2O$	5.88	0.00100
Anhydrous sodium chloride	NaCl	14.24	0.00609
Anhydrous sodium carbonate	Na_2CO_3	1.20	0.000283

The composition of the synthetic plant water is summarised in Table 3.5.

Table 3.5: Total ions present in synthetic plant water recipe

Ions Present	Ca^{2+}	Mg^{2+}	Na^{+}	Cl^{-}	SO_4^{2-}	NO_3^{2-}	CO_3^{2-}	TDS
Concentration (ppm)	80	70	153	287	240	176	17	1023

3.2.3 Chemical Reagents

Hydrochloric acid (HCl) and sodium hydroxide (NaOH) solutions of concentration 0.1 M were used for pH adjustments. Di-sodium tetraborate from Sigma-Aldrich Co. was used as a buffer and as a background electrolyte for zeta potential determinations. Copper sulphate pentahydrate ($CuSO_4.5H_2O$) from Merck (Pty) Ltd was used as an activator. Purified sodium isobutyl xanthate (SIBX) obtained from Senmin (Pty) Ltd was used as a collector. EDTA (Ethylenediaminetetraacetic acid) was used to extract metal hydroxides from mineral surfaces in order to determine the nature of the copper species on the mineral surfaces.

DOW 200, a propylene glycol methyl ether was used as a frother and this was supplied by Betachem (Pty) Ltd. This is a polyglycol ether derivative which is soluble in water and produces compact, lasting and selective froth structures (Harris,1982). The frother concentration used in all the studies was above the critical coalescence concentration (CCC) for DOW 200 which is 18.4 ppm (Laskowski, 2004). This was to

reduce variations in froth stability caused by changes in bubble size due to frother properties.

The reagent solutions (copper sulphate, di-sodium tetraborate, EDTA and xanthate) were prepared using de-ionised water. All the chemicals used were of analytical grade quality.

3.3 Froth Stability Measurements

3.3.1 The Froth Stability Column

The froth stability column was used to analyse the effect of copper sulphate on the froth phase of the flotation system. The suitability of the froth stability column as equipment for measuring froth stability is discussed in section 2.2.3 (Quantitative analysis of froth stability) of this dissertation. The froth stability column is made of Perspex with a diameter of 10 cm and height of 100 cm. It is fitted with a sintered ceramic frit at the bottom through which air is bubbled. Figure 3.4 below shows the froth stability column and the ancillary equipment used to investigate the froth phase.

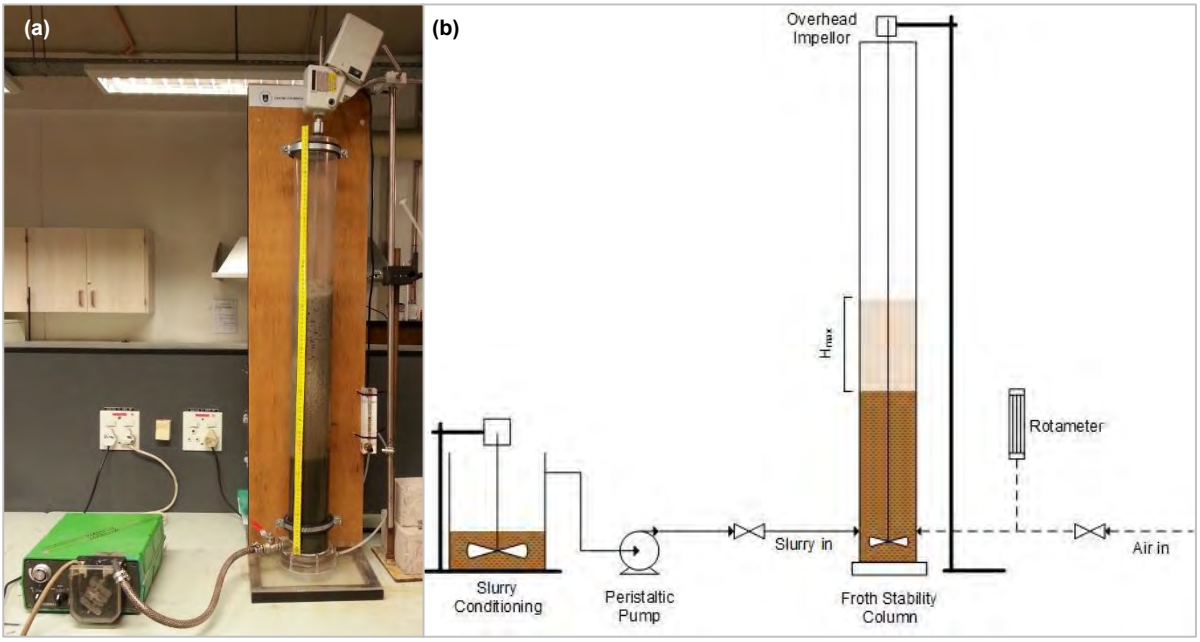

Figure 3.4: The froth stability column and ancillary equipment (a) and a schematic representation of the experimental setup (b).

3.3.2 Experimental Procedure

The milled slurry of 66% pulp density was transferred into a conditioning vessel using either deionised water or synthetic plant water. The slurry pulp density was adjusted to 33% solids by addition of the required quantity of water. An impellor was used to keep the solids in suspension. SIBX was then added as a 1.1 x 10^{-2} M solution and the slurry was conditioned for 5 minutes. 150 ppm of frother was added and conditioned for 1 minute. Using a peristaltic pump, the slurry was fed to the froth stability column. The column was filled to the 30 cm mark to give a total volume of 2.37 L. The slurry in the column was continuously agitated using an overhead impellor at a constant speed to ensure a homogenous suspension of solids.

To commence the generation of froth within the column for the dynamic test, the air was switched on to give a constant flow rate of 6 l/minute which corresponds to a superficial gas velocity (J_g) of 1.27 cm/s. The froth height relative to the pulp-froth interface was recorded after every 5 seconds up to the 2nd minute and in 30 second intervals up to the 5th minute. The maximum froth height H_{max} was also recorded.

For the static test, the air supply was switched off and the froth height of the decaying froth recorded after every 2 seconds until the froth had completely collapsed. The time intervals between readings were shorter for the static test due to the fast rate of collapse of the froth. The experiments were conducted in triplicate to minimise experimental error. The ceramic frit at the bottom of the column was frequently ultra-sonicated to prevent blockages by ore particles which could reduce the air flow rate.

The copper sulphate was added in the mill prior to xanthate addition to minimise interactions of the activator with the xanthate in the pulp which prevents adsorption of the activator onto the mineral surface (Chandra & Gerson, 2009). This is supported by the work by Gerson and Jasieniak (2008) on copper activation of pentlandite and pyrrhotite where they found that there was less than 10% of the copper remaining in solution after 10 seconds. The conditions investigated in both synthetic plant water and deionised water are summarised in Table 3.6.

Table 3.6: Summary of reagent dosages used for the frothing column tests.

Condition	No Xanthate	Xanthate (80 g/t)
No Copper	✓	✓
Copper (90 g/t)	✓	✓

3.3.3 Scoping tests for air flow rate

The air flow rate is an operating factor that affects froth stability. As a result a constant flow rate was used for the work using the froth stability column to avoid variations in results due to the air flow rate. Initially, tests were done to determine the air flow rate for the tests which promotes steady growth of the froth. The air flow rate (Q) influences the superficial gas velocity in the froth, (J_g) which is defined in equation 3.1 where A is the cross-sectional area of the column.

$$J_g = \frac{Q}{A} \quad \text{.....3.1}$$

J_g is used to eliminate the differences in the size of the flotation column used in experimental work. Q was varied at 2, 4, 6 and 8 l/minute which corresponds to a superficial gas velocity (J_g) of 0.42, 0.85, 1.27 and 1.70 cm/s. According to Bikerman (1973), for the test to be suitable the J_g should be between 1 and 1.5 cm/s and there should be a linear relationship between H_{max} (the maximum froth height) and J_g. Figure 3.5 shows the variation of H_{max} with J_g.

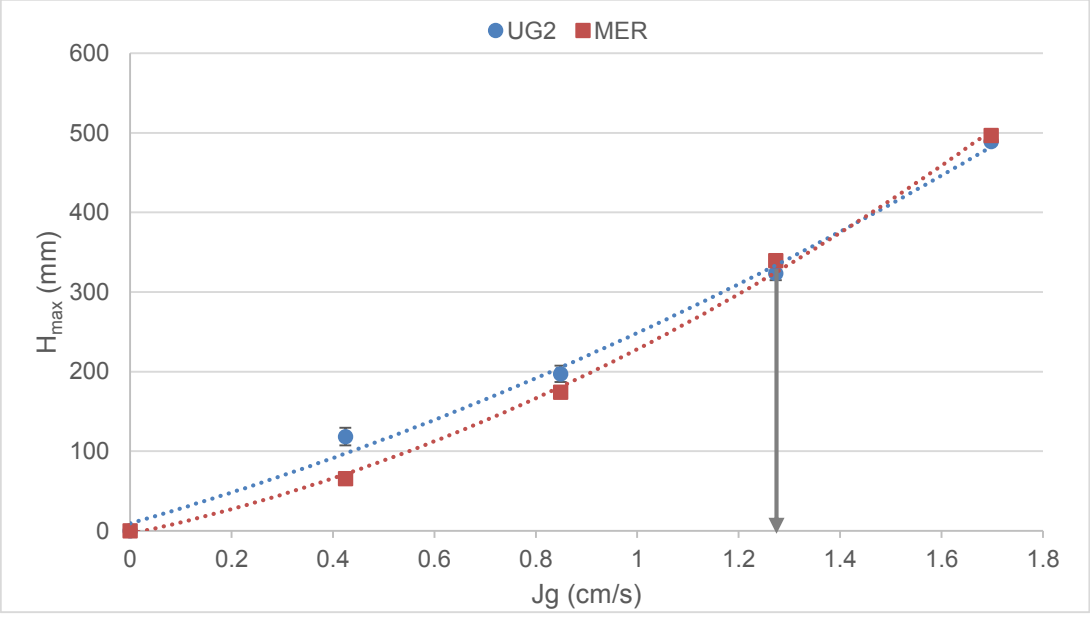

Figure 3.5: Scoping tests for air flow rate

The chosen air flow rate was 1.27 cm/s (6 l/minute) for the tests using both ores because it was in the recommended range of operation for the Bikerman test and it was in a linear region as shown in Figure 3.5.

3.4 Microflotation Tests

A microflotation cell was used to determine the flotation response of pure minerals under low solids densities. It enables the pulp phase effects of reagent adsorption to be studied in the absence of the froth phase. Competition of other minerals in the pulp is also not present since the studies are on single minerals.

3.4.1 The Microflotation Cell

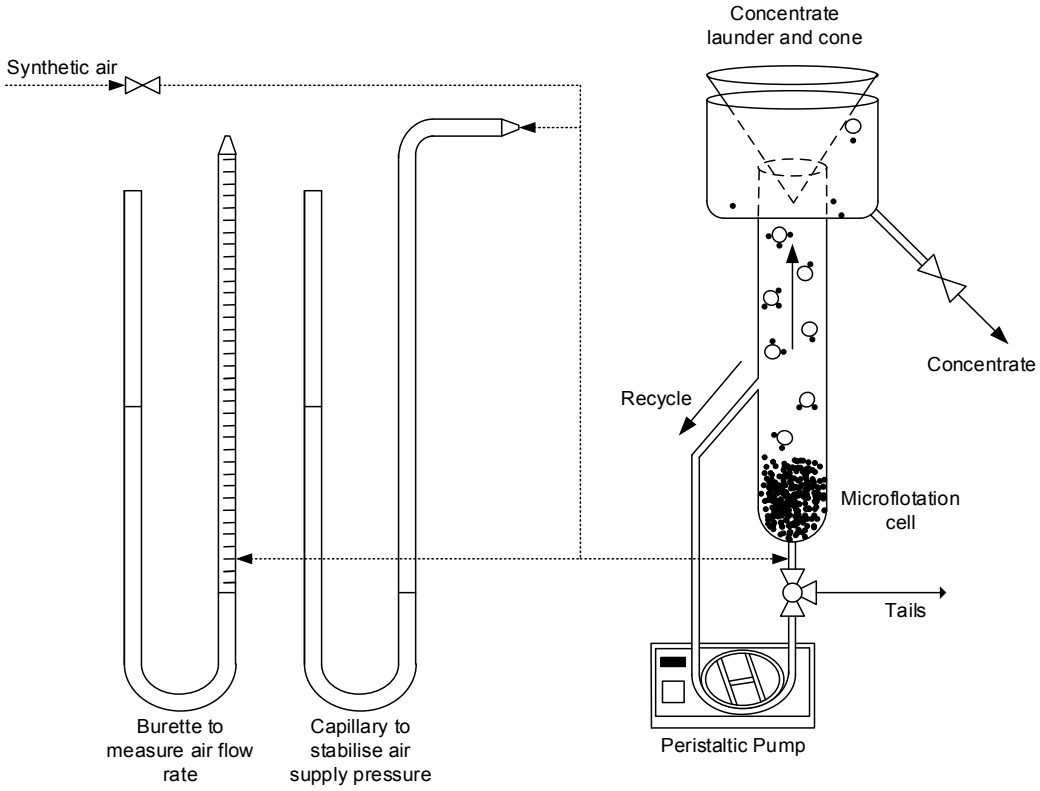

Figure 3.6: Schematic representation of microflotation equipment

The microflotation cell developed by Bradshaw and O'Connor (1996) shown in Figure 3.6 above consists of a tapered cylindrical cell with air introduced through a syringe at the base of the cell. The particle–bubble agglomerates rise to the top of the cell and are deflected off the cone at the top. The bubbles burst and drop into the launder where the concentrates are collected. The concentrates are then filtered, dried and weighed.

3.4.2 Experimental Procedure

The microflotation tests were carried out using 3 g talc or pyrrhotite samples with a particle size of +38-106 µm. The mineral sample was added to 50 cm^3 of deionised water and the pH adjusted to 9. The mineral suspension was ultra-sonicated for 5 minutes in a water bath to ensure a good dispersion of the mixture. The mineral suspension was transferred to the microflotation cell. The peristaltic pump was set at 90 rpm to uniformly disperse the particles in solution and to circulate the pulp.

Where reagent addition was required, 1 cm^3 of $CuSO_4$ and/or SIBX solution was added and conditioned for 2 minutes and 5 minutes respectively. The number of monolayers of copper and xanthate on each pure mineral was fixed whereas the concentrations were varied according to the surface area of the minerals. Two monolayers were used for copper surface coverage and 0.5 monolayers for xanthate surface coverage which gives an optimal coverage on the mineral surface (McFadzean et al., 2012). Deionised water adjusted to a pH of 9 was added to the cell to make a volume of 250 cm^3 and the cone was put in place.

Air was introduced through a syringe at the base of the cell at a flow rate of 7 cm^3/min. Concentrates were collected for 2, 4, 6 and 8 minutes and filtered. A tailings sample was collected at the end of each run. The experiments were conducted in duplicate to minimise experimental error.

The conditions investigated in both synthetic plant water and deionised water are summarised in Table 3.7.

Table 3.7: Summary of experimental conditions investigated for microflotation tests

Mineral	No Reagents	Cu Only	Xanthate Only	Cu + Xanthate
Talc	✓	✓	✓	✓
Pyrrhotite	✓	✓	✓	✓

3.5 Zeta Potential Determinations

Zeta potential was discussed in detail in section 2.3.2 of this dissertation. The zeta potential determinations were carried out on dilute dispersions of the individual minerals using the Malvern Zetasizer 4 shown in Figure 3.7.

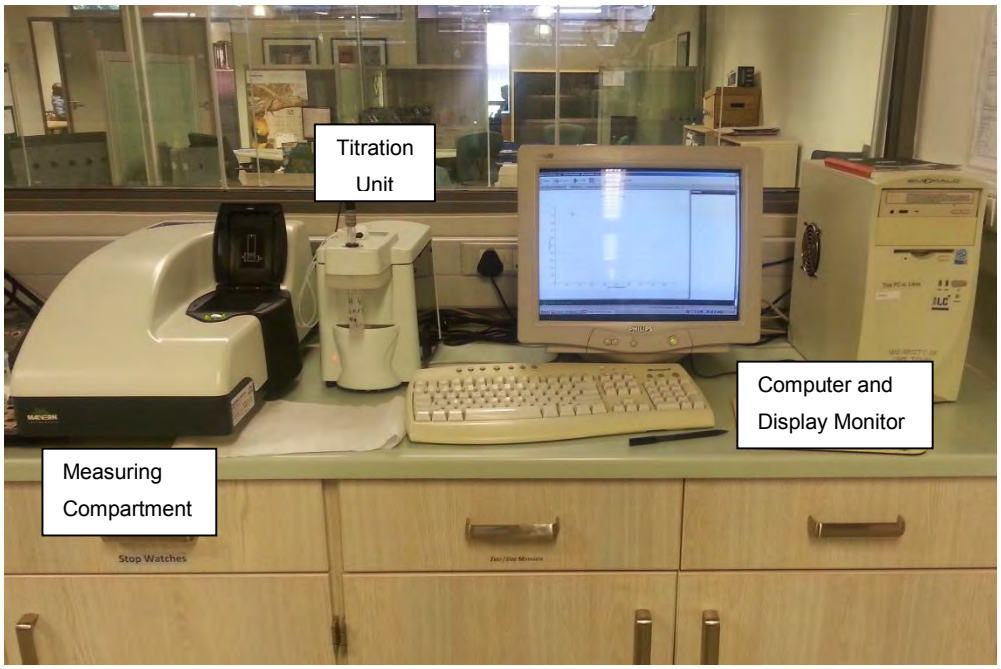

Figure 3.7: The Malvern Zetasizer 4 machine used to measure the zeta potential of minerals.

3.5.1 Technique description

The Malvern Zetasizer 4 measures the electrophoretic mobility which is related to the zeta potential by the Henry equation (3.2) shown below:

$$u_E = \frac{\zeta\varepsilon}{1.5\eta} f(\kappa a) \quad \text{.....3.2}$$

where u_E is the electrophoretic mobility, ε is the fluid dielectric constant, ζ is the zeta-potential, η is the dynamic viscosity, κ is the Debye-Huckel parameter and a is the particle radius. Henry's equation transforms into Smoluchowski's equation 3.3 when there are large particles in more concentrated electrolyte solutions since $\kappa a >> 1$ and $f(\kappa a)$ is 1.5 (Hunter, 1993).

$$u_E = \frac{\zeta\varepsilon}{\eta} \quad \text{.....3.3}$$

This reduces to equation 3.4 at 25°C where the units are millivolts (mV).

$$\zeta = 12.85u_E \quad \text{.....3.4}$$

3.5.2 Experimental Procedure

A mineral sample weighing 0.375 g with a particle size of 100% passing 25 µm was added to a 500 cm^3 beaker. 300 cm^3 of a 10^{-2} M background electrolyte ($Na_2B_4O_7.10H_2O$) was added to the beaker. The suspension was mixed with a magnetic stirrer and the solution split into 5 beakers each containing 50 ml. The pH in each beaker was adjusted to 2, 4, 6, 8 and 10 and the mixture conditioned for 20 minutes to ensure the pH remained constant. For experimental conditions requiring reagent addition, 1 cm^3 of $CuSO_4$ solution and/or SIBX solution was added and conditioned for 2 minutes and 5 minutes respectively. The xanthate and copper sulphate solutions were of concentration 5 x 10^{-3} M. Using a pipette, 2 cm^3 of the mineral suspension was transferred into the Malvern Zetasizer 4 folded capillary tube ensuring there were no bubbles in the cell. The capillary tube was placed into the Malvern Zetasizer 4 instrument to measure the electrophoretic mobility and in turn the zeta potential of particles in suspension at 25°C. The experiments were conducted in triplicate to minimise experimental error.

The conditions investigated are summarised in Table 3.8.

Table 3.8: Summary of experimental conditions investigated for zeta potential tests

Mineral	No Reagents	Cu Only	Xanthate Only	Cu + Xanthate
Talc	✓	✓	✓	✓
Chromite	✓	✓	✓	✓
Plagioclase	✓	✓	✓	✓
Pyrrhotite	✓	✓	✓	✓

3.6 Analysis of activation products

Several instrumental techniques have been used to identify the surface species before and after copper activation. Examples of these ex-situ techniques include XPS (X-ray photoelectron spectroscopy) and ToF-SIMS (Time-of-Flight Secondary Ion Mass Spectrometry) analyses. These methods are used to determine the atomic/molecular composition as well as the oxidation state of the species on the surfaces of minerals. The major concerns with these methods is that the mineral surfaces could be altered prior to or during sample analysis.

EDTA (Ethylenediaminetetraacetic acid) is a strong complexant used in mineral processing to determine the amount of oxidation products covering the surface of minerals by removal of these products (Clarke et al., 1995). If a metal ion on the surface of the mineral is extractable by EDTA then it is not chemically bound. As a result, EDTA extraction was used to determine the amount of Cu(II) on the mineral surface present as $Cu(OH)_2$. EDTA was chosen as a surface extractant due to its strong complexing abilities with hydroxides but lack of reaction with sulphides (Kant, 1997).

Shackleton et al. (2007) used EDA (Ethylenediamine) to examine surface products and the results showed that the copper and the copper xanthate species were not strongly bonded to the PGE mineral surfaces. This confirmed the presence of $Cu(OH)_2$ colloids on the surface as a result of precipitation rather than the chemical reaction between the copper and metal ions in the PGE mineral structure (Shackleton et al., 2007).

3.6.1 Experimental set-up

EDTA extractions were carried out on the feed slurry to the frothing column experimental work as well as on talc samples which was the feed to microflotation tests. The experimental apparatus is shown in Figure 3.8. It consists of a closed reaction vessel with a supply of pure nitrogen and a vent to prevent pressure build-up. A magnetic stirrer was used for uniform mixing during the reactions.

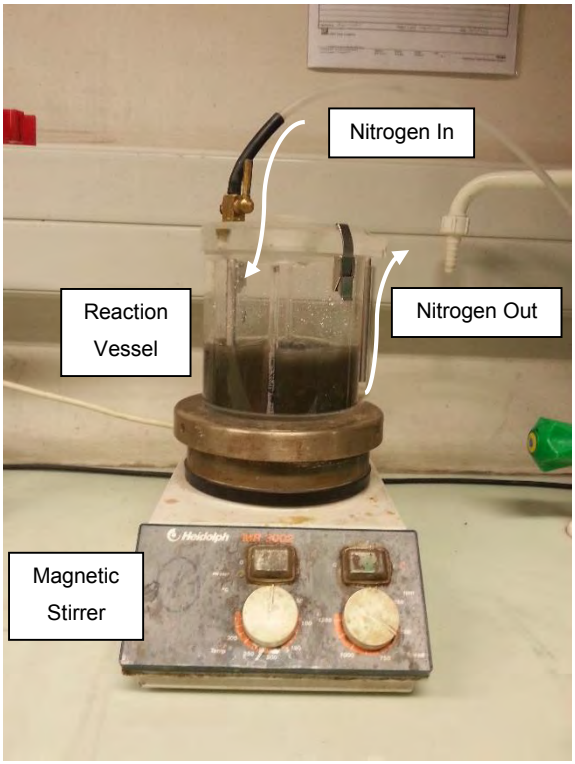

Figure 3.8: Experimental set-up for EDTA extraction

3.6.2 Experimental Procedure

A 0.03 M EDTA solution was made and its pH adjusted to 7.5 with NaOH. In a closed reaction vessel shown above, high purity nitrogen was bubbled through 250 ml of the EDTA solution for 20 minutes to purge the system of oxygen. A 20 ml frothing column feed slurry sample was collected after conditioning and filtered through a 0.45 µm Millipore filter. For the talc experiments, 3 g of the talc sample was reacted with reagents in 50 ml of deionised water. The reagents dosages used in microflotation of talc were used for these tests.

The slurry sample was filtered and the filtrate was sent for copper analysis using AAS – Atomic Absorption Spectroscopy. The residue was added to the EDTA solution while continuously mixing with a magnetic stirrer. The system was purged with high purity nitrogen for 30 minutes to avoid further oxidation of surface products. The suspension was filtered and the filtrate analysed for copper.

3.7 Reproducibility of results

3.7.1 Statistical Analysis Tools

The experiments were conducted in duplicate or triplicate for reproducibility and to minimise experimental error. The arithmetic mean, $\bar{x}$ was calculated using the following equation:

$$\bar{x} = \frac{1}{N}\sum_{x=i}^{N} x_i \quad \text{.....3.5}$$

where *N* represents the sample size.

Graphically, the errors associated with the mean were shown using error bars obtained from calculation of the standard error. The standard error is defined as follows:

$$Standard\ Error = \frac{\bar{x}}{\sqrt{N}} \quad \text{.....3.6}$$

3.7.2 Froth Stability Column

The experiments were conducted in triplicate to minimise experimental error. As discussed in chapter two, the maximum froth height H_{max} was determined from equation 2.4 by fitting experimental the data to the model and minimising the sum of errors.

$$H(t) = H_{max}(1 - e^{-\frac{t}{\tau}}) \quad \text{.....2.4}$$

The other parameter used to quantify froth stability was the froth half life time $t_{1/2}$ defined in equation 2.5 in the review of literature.

$$\frac{H_f}{H_{f\,max}} = \frac{1}{2} - \alpha ln\left(\frac{t}{t_{\frac{1}{2}}}\right) \quad \text{.....2.5}$$

The procedure followed to determine the values of H_{max} and $t_{1/2}$ is outlined in Appendix B. The froth rise and froth decay profiles for the two ores investigated are shown from Figure 3.9 to Figure 3.12 for Merensky ore using deionised water and UG2 ore using synthetic plant water.

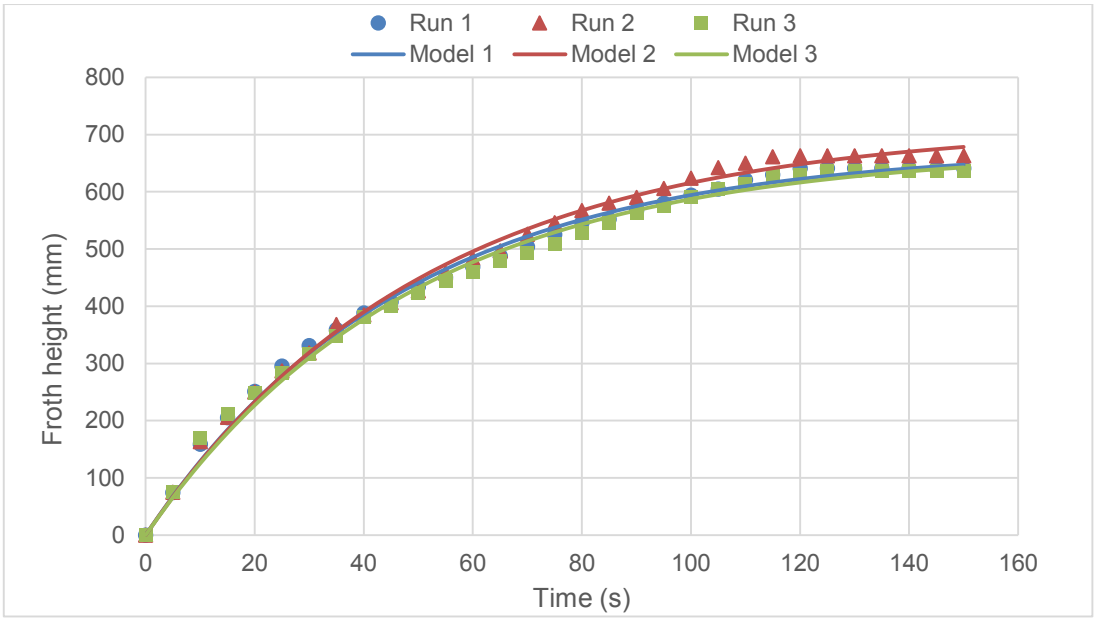

Figure 3.9: Variation of froth height with time for Merensky ore in deionised water

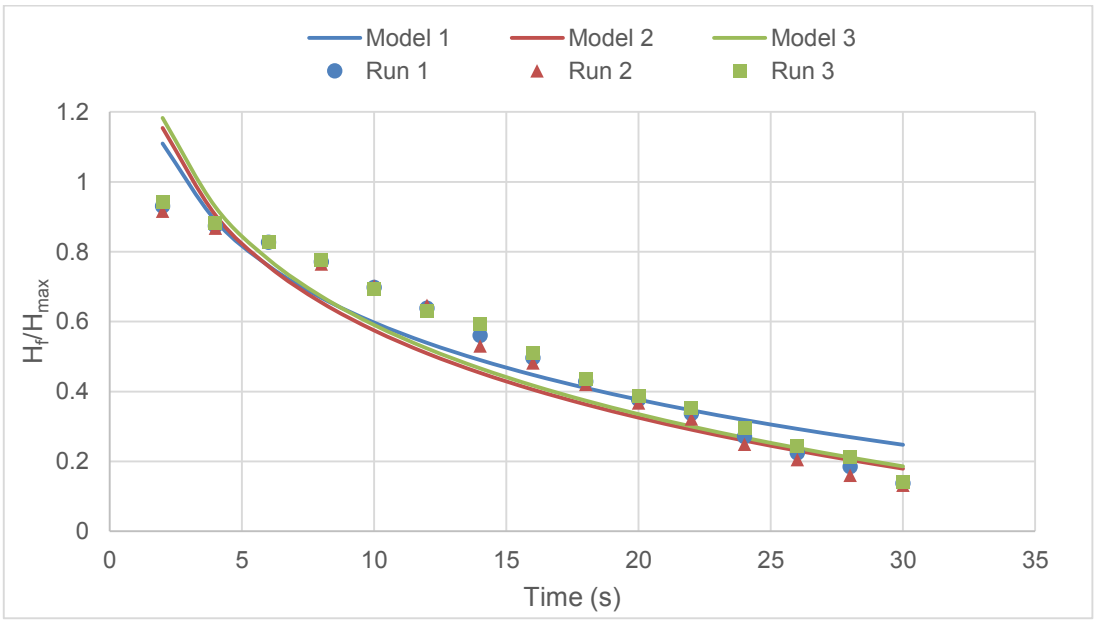

Figure 3.10: Decay profile for Merensky ore froth using deionised water

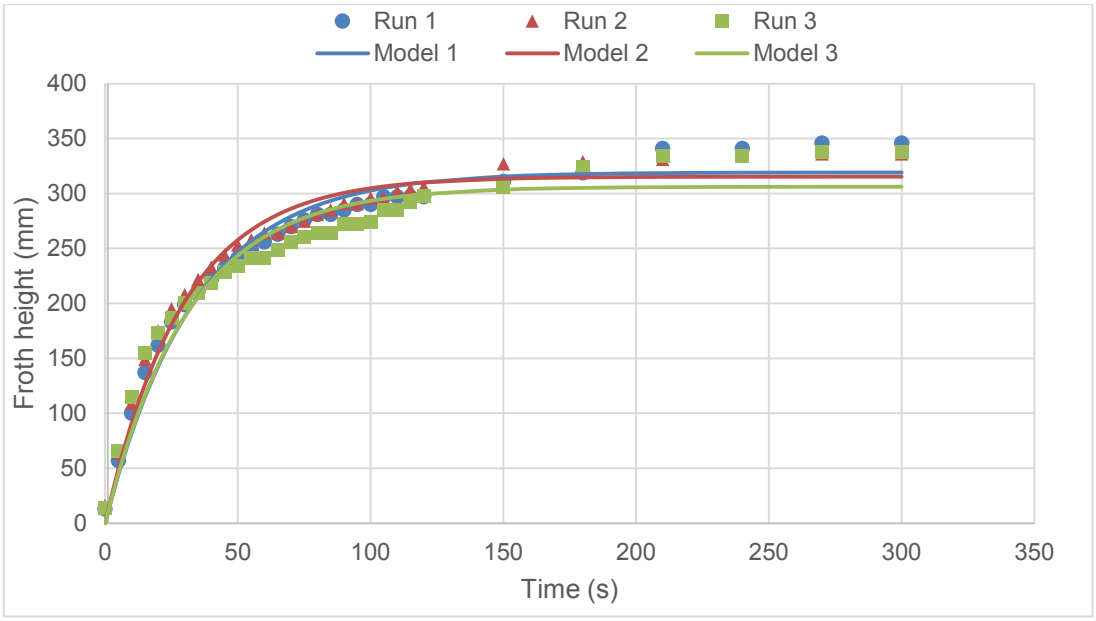

Figure 3.11: Variation of froth height with time for UG2 ore in synthetic plant water

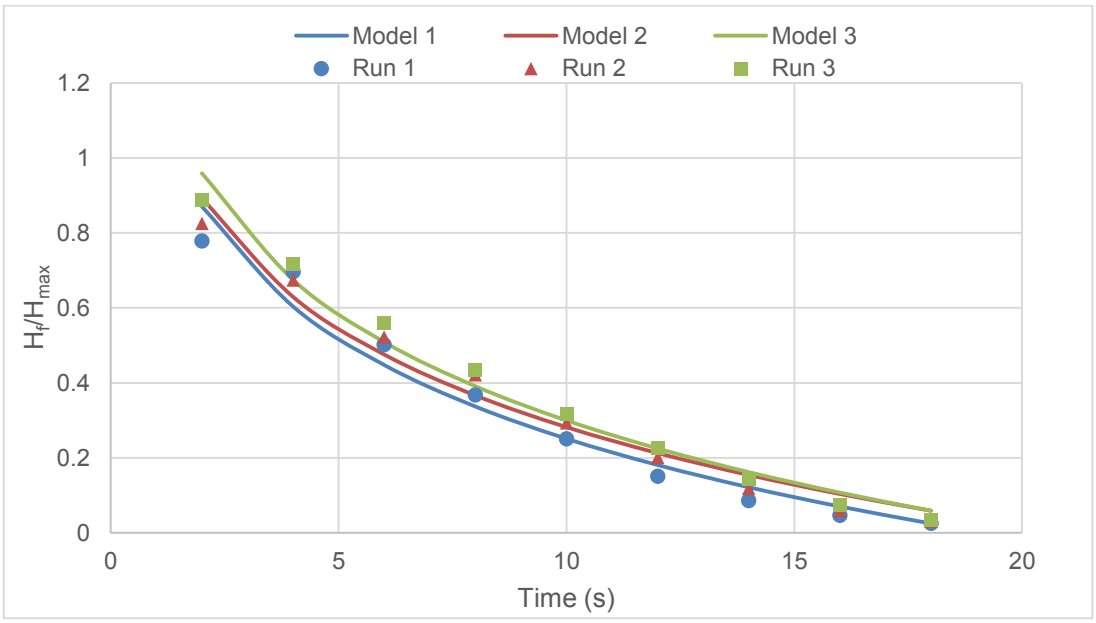

Figure 3.12: Decay profile for UG2 ore froth using synthetic plant water

The dynamic froth stability factor Σ and the froth half life time $t_{1/2}$ were used as proxies for froth stability as explained in Chapter 3. As discussed earlier, Σ was obtained from equation 2.3 below.

$$\sum = \frac{V_f}{Q} = \frac{A.H_{max}}{Q} \quad \text{.....2.3}$$

The comparison of the froth stability factor Σ and the froth half life time $t_{1/2}$ obtained for the different conditions is shown in Figure 3.13. Figure 3.13 shows the

reproducibility of froth stability results for Merensky and UG2 ores when no reagents were added.

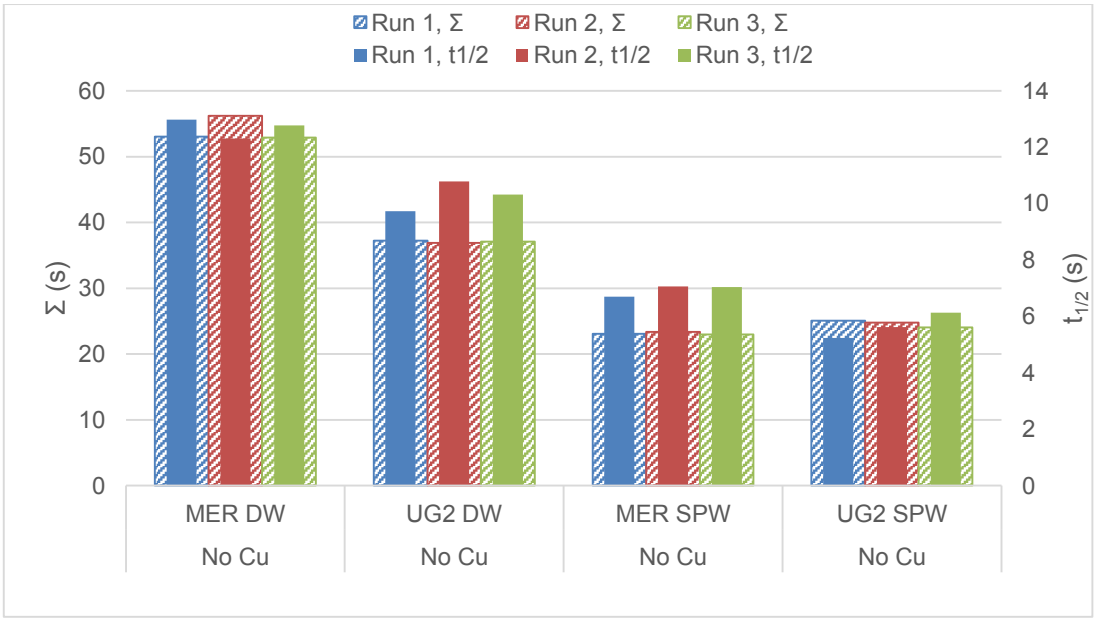

Figure 3.13: Reproducibility of the dynamic froth stability factor and froth half life time

Due to the consistency between the two sets of results, the froth stability results are shown in terms of the dynamic froth stability factor *Σ* in this dissertation.

3.7.3 Microflotation Cell

The microflotation experiments were conducted in duplicate to determine the reliability of the microflotation apparatus and procedure for the conditions with no reagent addition. Sources of experimental error could be the operation of the microflotation cell, the accuracy of the operator and the nature of the pure mineral samples used. The recoveries and total concentrate collected over a period of 20 minutes for talc and pyrrhotite in deionised water without reagent addition are shown in Table 3.9 and Table 3.10 respectively. The standard error was used to compute the error bars.

Table 3.9: Reproducibility of microflotation tests on talc in deionised water

Time (minutes)	0	2	6	12	20
Run 1, Talc	0	29.8	63.9	79.5	91.3
Run 2, Talc	0	24.7	57.6	82.9	92.0
Mean	0	27.3	60.8	81.2	91.7
Standard Error	0	2.5	3.1	1.7	0.3

Table 3.10: Reproducibility of microflotation tests on pyrrhotite in deionised water

Time (minutes)	0	2	6	12	20
Run 1, Pyrrhotite	0	11.2	27.6	44.1	53.6
Run 2, Pyrrhotite	0	12.0	28.7	43.6	54.1
Mean	0	11.6	28.1	43.9	53.9
Standard Error	0	0.4	0.5	0.3	0.2

As seen in Table 3.9 and Table 3.10, the tests were highly reproducible with the standard error lying within 4% of the mean. A graphical representation of the results is summarised in the recovery versus time graphs shown in Figure 3.14.

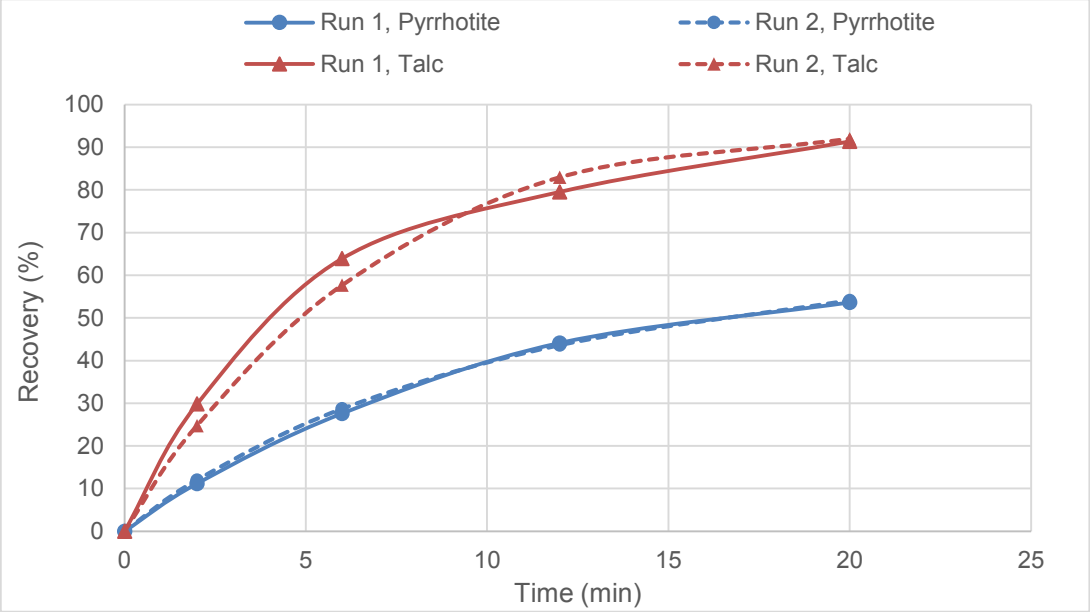

Figure 3.14: Microflotation reproducibility results for talc and pyrrhotite at pH 9

3.7.4 Zeta Potential Tests

Reproducibility tests were conducted in triplicate to determine the reliability of the procedure used to determine the zeta potential in this study. Possible errors could be due to consistency in the operation of the Malvern Zetasizer equipment as well as the operator's accuracy. Variations in the mineral samples could also contribute to experimental error. The standard error was also used to compute the error bars. The talc results for the condition with no reagent addition is shown in Table 3.11 and Figure 3.15.

Table 3.11: Talc zeta potential reproducibility

pH	Zeta Potential (mV)			Mean (mV)	Standard Error
	Run 1	Run 2	Run 3		
2	15.0	15.2	14.3	14.8	0.3
4	6.41	6.19	4.80	5.80	0.5
6	-23.9	-27.5	-29.4	-26.9	1.5
8	-52.1	-57.2	-61.3	-56.9	2.7
10	-55.1	-64.5	-68.7	-62.8	4.0

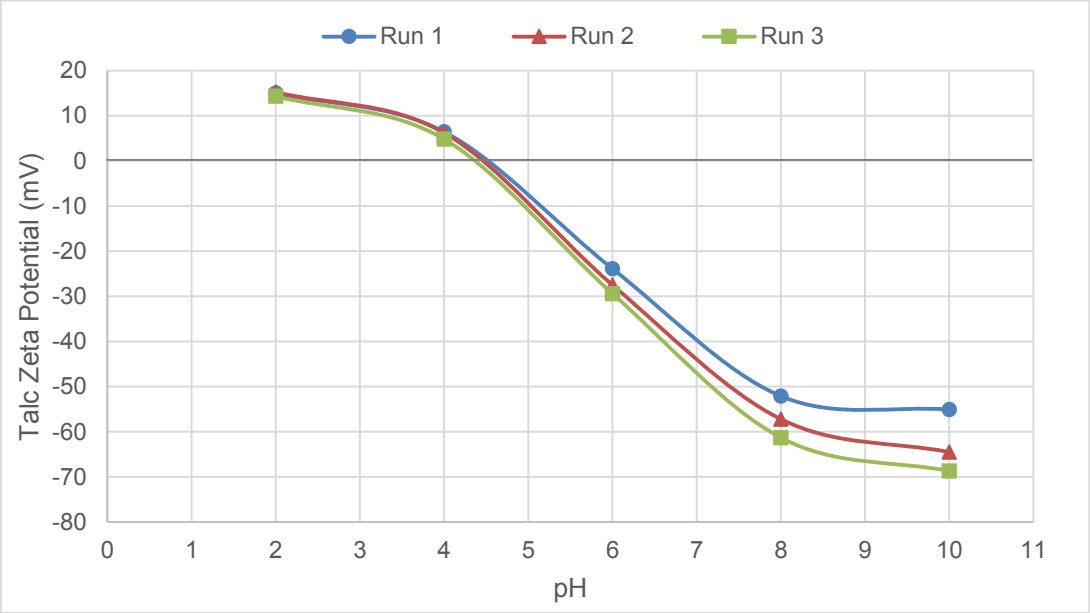

Figure 3.15: Talc zeta potential reproducibility in the absence of reagents in a 10^{-2} M $Na_2B_4O_7$ background electrolyte solution

The zeta potential tests for pyrrhotite with no reagent addition are shown in Table 3.12 and Figure 3.16.

Table 3.12: Pyrrhotite zeta potential reproducibility

pH	Zeta Potential (mV)			Mean (mV)	Standard Error
	Run 1	Run 2	Run 3		
2	17.2	15.4	16.7	16.4	0.5
4	16.5	17.2	16.7	16.8	0.2
6	-2.22	-3.40	-3.70	-3.10	0.6
8	-48.0	-53.0	-48.7	-49.9	1.6
10	-47.8	-52.4	-52.9	-51.0	1.6

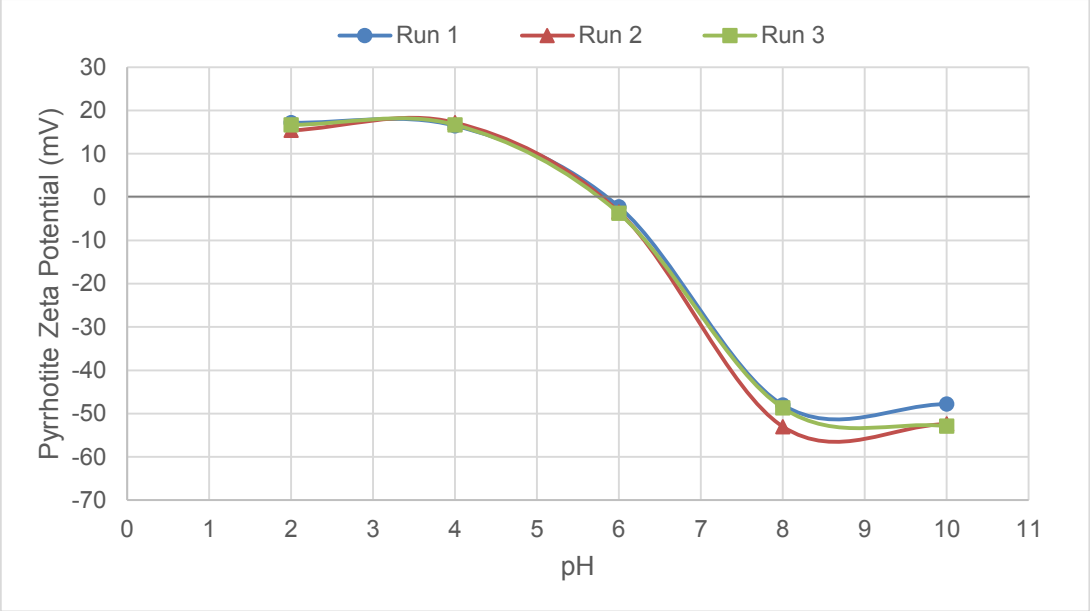

Figure 3.16: Pyrrhotite zeta potential reproducibility in the absence of reagents in a 10^{-2} M $Na_2B_4O_7$ background electrolyte solution

The zeta potential results for pyrrhotite also show a low standard error for each measured pH and that the technique and the procedure used gave reproducible results.

3.7.5 EDTA Extraction Tests

The EDTA experiments were conducted in duplicate for Merensky and UG2 ores using deionised water prior to the frothing column tests. Sources of error could be due to inconsistencies resulting from sample preparation, the experimental procedure and the EDTA extraction technique. Another source of error could be the Atomic Absorption Spectroscopy (AAS) method used to determine the amount of copper in solution. The reproducibility of the experiments is summarised in Table 3.13.

Table 3.13: Reproducibility of AAS and EDTA extraction results

Condition	Ore	Run 1	Run 2	Standard Error
EDTA Cu (%)	Merensky	59.5	59.2	0.16
Solution Cu (%)		0.23	0.19	0.02
EDTA Cu (%)	UG2	50.2	50.7	0.26
Solution Cu (%)		0.56	0.55	0.01

The low standard error shows reproducibility of the method used to determine the amount of copper in solution and extracted by EDTA.

4 RESULTS

The results of the tests that were conducted to meet the objectives of this study are presented in this chapter. In order to assess the link between activation in the pulp phase of flotation to the stability of the froth phase, four types of tests were conducted. These were (i) froth stability tests using the froth stability column, (ii) floatability tests using the microflotation cell, (iii) surface charge determination using zeta potential measurements and (iv) analysis of the products of activation in the pulp phase using the EDTA extraction method as outlined in Chapter Three. In this chapter, the results from the froth stability tests are presented first followed by microflotation tests, zeta potential tests and finally the activation product analysis tests.

The following abbreviations are used in the graphical representation of the data:

DW – Deionised Water
SPW – Synthetic Plant Water
MER – Merensky ore
UG2 – Upper Group 2 ore

4.1 Froth Stability Tests

In this section the particle effects on froth stability are analysed first using two phase and three phase systems. This is followed by an analysis of the effect of reagent addition on the froth stability of the two ores. A comparison of the effect of water type on the each of the ores is then given. The froth stability for the ores is then compared for the water types investigated.

4.1.1 Effect of particles on froth stability

From the literature reviewed, particles have been found to have a significant influence on the froth phase. The effect of particles on the dynamic froth stability factor Σ was analysed by conducting a baseline test in a two phase system (water and air only) and comparing this to the froth stability in a three phase system (water, air and solids).

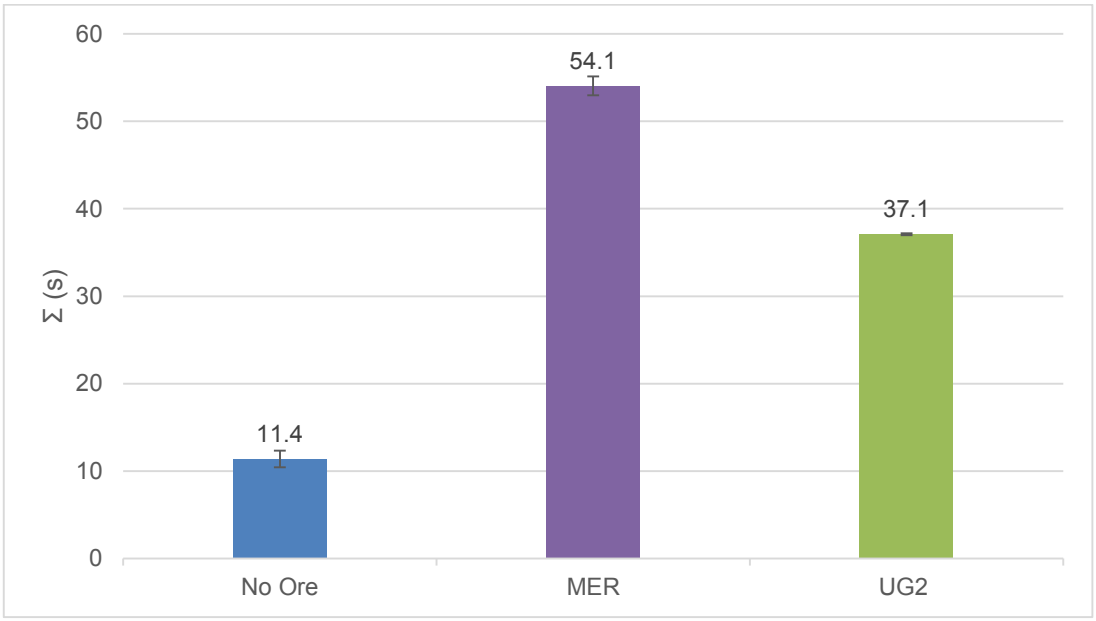

Figure 4.1: Effect of particles on froth stability in deionised water

Figure 4.1 shows the effect of particles on the froth stability of Merensky (MER) and UG2 ores when no reagents, other than frother, were added in deionised water. The frother concentration in the two phase system was 3.4 times higher than in the three phase tests in order to obtain reasonable froth height readings for a given period of time.

For the baseline test (no ore), the dynamic froth stability factor, *Σ,* was 11.4 seconds. The dynamic froth stability factor increased with the addition of particles indicating an increase in froth stability. The dynamic froth stability factor was higher for Merensky ore (54.1 seconds) than for UG2 ore which was 37.1 seconds for the given set of conditions. These tests show that although the frother dosage was much lower for the three phase tests than the two phase tests, more stable froth was obtained in the presence of particles.

Figure 4.2 below also shows an increase in froth stability for both ores in synthetic plant water.

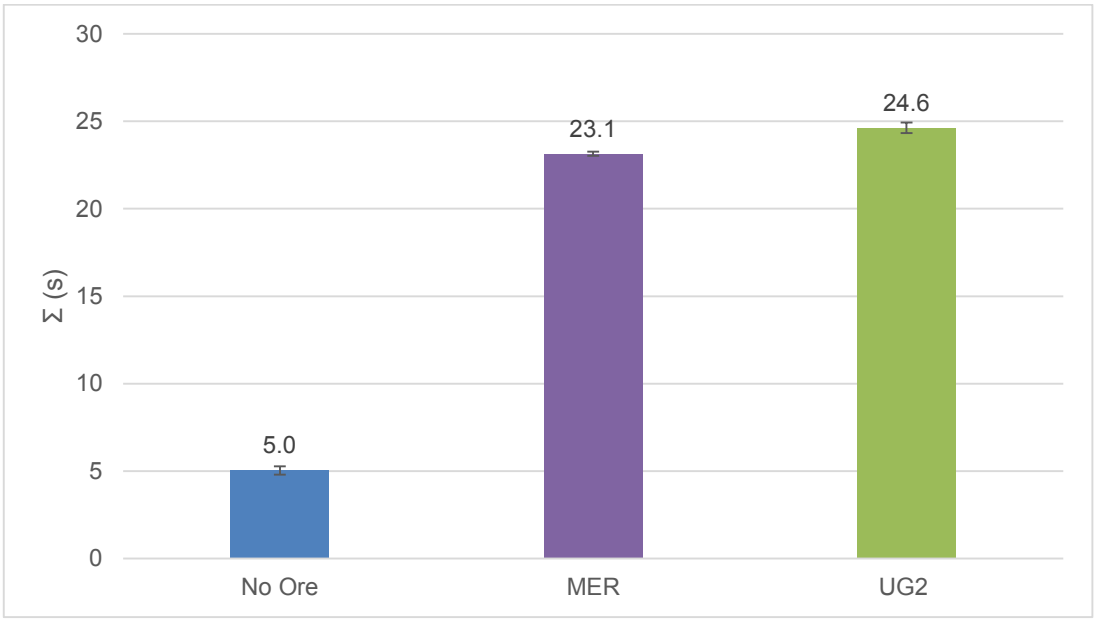

Figure 4.2: Effect of particles on froth stability in synthetic plant water

From Figure 4.2 it is also evident that the presence of particles results in a more stable froth for both ores when synthetic plant water is used. The dynamic froth stability factor when synthetic plant water was used was 5 seconds for the baseline test which increased to 23.1 seconds with Merensky ore and 24.6 seconds with UG2 ore. It is evident, when comparing Figure 4.1 and Figure 4.2, that the addition of ions in the synthetic plant water had a froth destabilising effect on both ore types, particularly the Merensky ore.

4.1.2 Effect of reagent addition on froth stability

The froth stability tests were conducted in deionised water to investigate the effect of addition of copper sulphate as an activator and xanthate as a collector to Merensky ore. Figure 4.3 shows the relationship between the dynamic froth stability factor and reagent addition in deionised water at pH 9.

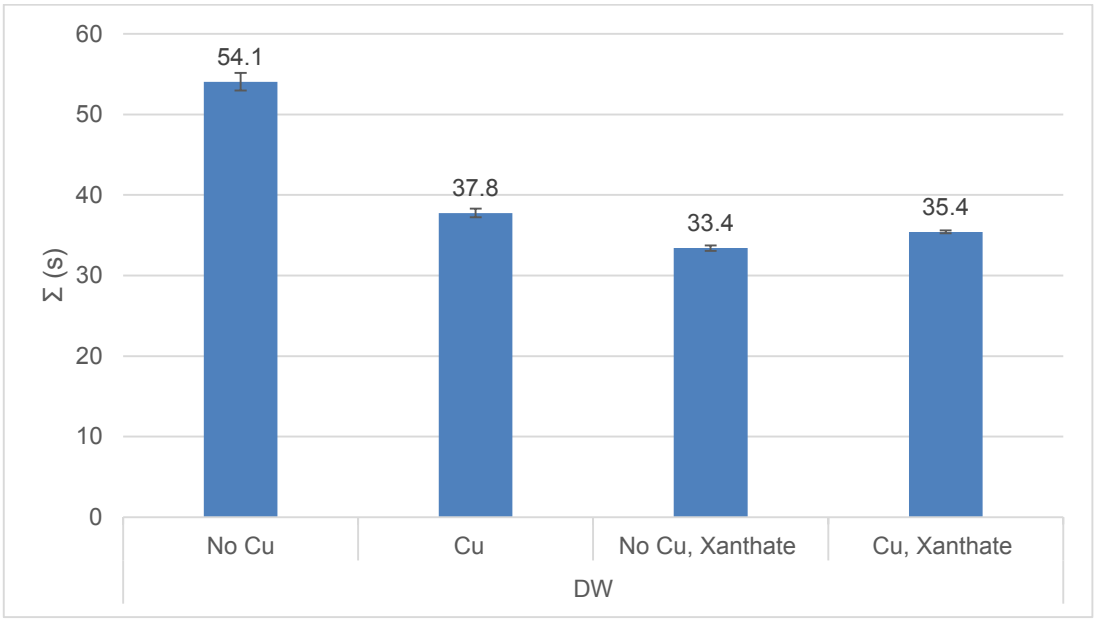

Figure 4.3: Froth stability of Merensky ore in deionised water at pH 9

The addition of only copper sulphate resulted in a less stable froth as evidenced by the decrease in the value of the dynamic froth stability factor *Σ* from 54.1 seconds to 37.8 seconds. When only xanthate was added, the froth became more unstable (33.4 seconds) than when only copper sulphate was present (37.8 seconds). When xanthate was added after copper activation, the froth was also destabilised (35.4 seconds) relative to the test with no reagent addition (54.1 seconds). However, both copper sulphate and xanthate slightly stabilised the froth more than the condition with xanthate addition only.

A separate test was conducted to determine the froth stability with an increased dosage of copper sulphate from 90 g/tonne to 120 g/tonne in the presence of xanthate. As seen in Figure 4.4, the value of *Σ* decreased to 23.5 seconds with a higher copper sulphate dosage. Figure 4.4 shows a local maximum in the value of *Σ* at 35.4 seconds when 90 g/tonne of copper sulphate was added prior to collector addition.

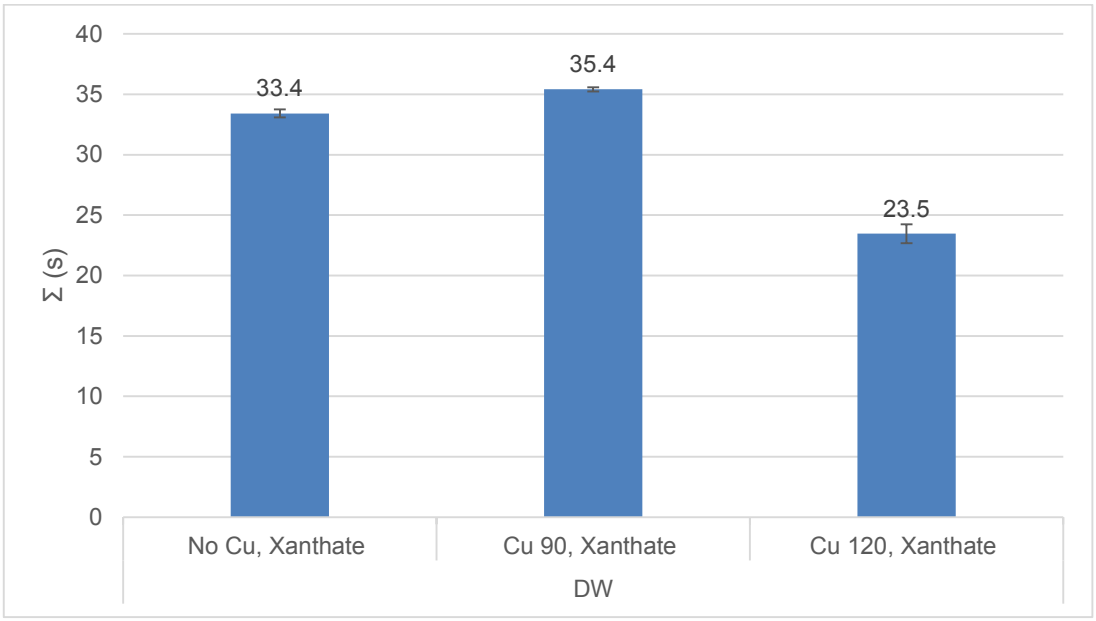

Figure 4.4: Effect of increasing copper sulphate concentration in the presence of xanthate collector at pH 9 (Merensky ore)

Froth stability tests were also conducted in synthetic plant water to investigate the effect of addition of copper sulphate to Merensky ore. Figure 4.5 shows the variation of Σ with addition of reagents in synthetic plant water at pH 9.

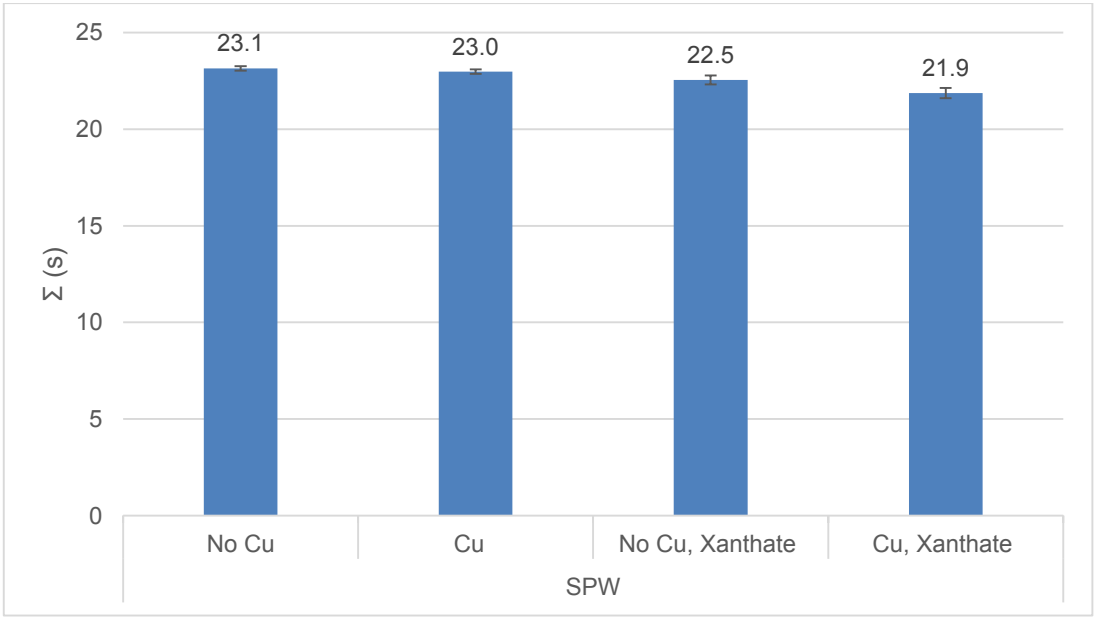

Figure 4.5: Froth stability of Merensky ore in synthetic plant water at pH 9

The use of synthetic plant water resulted in a generally less stable froth than in the deionised water, with little response to further reagent addition. The addition of reagents to Merensky ore in synthetic plant water destabilised the froth somewhat, which was the same trend obtained for Merensky ore deionised water. However, the

destabilisation of froth was less pronounced across the different tests than when deionised water was used. The addition of copper sulphate had no effect on the dynamic froth stability factor and the addition of xanthate only also decreased it slightly further to 22.5 seconds. The lowest froth stability and lowest value of Σ of 21.9 seconds was observed for the condition when both copper sulphate and xanthate were present.

Figure 4.6 shows the effect of reagent addition on the froth stability of UG2 ore in deionised water at pH 9.

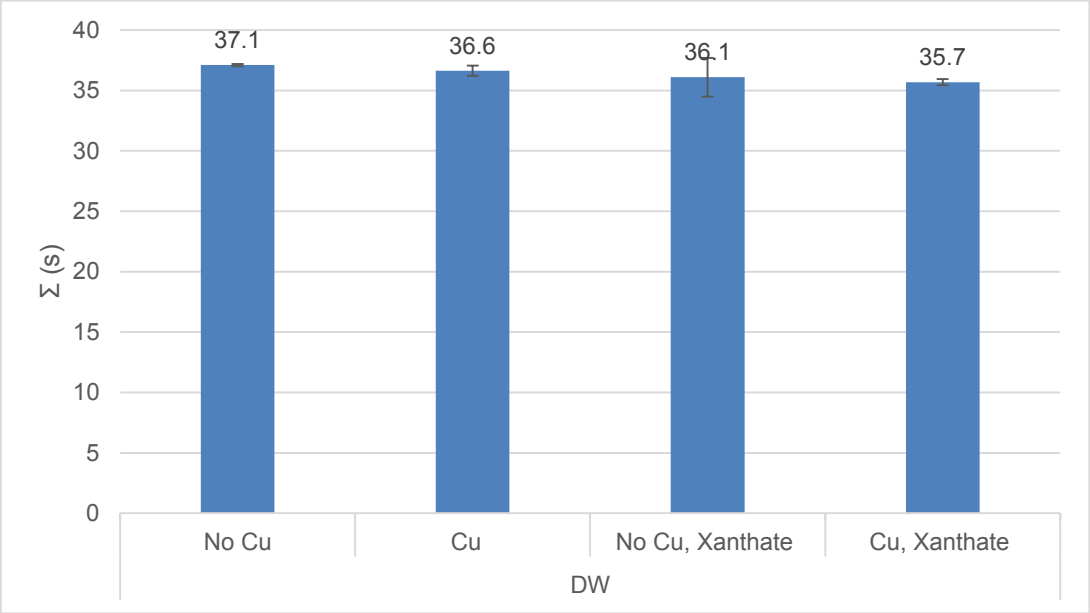

Figure 4.6: Froth stability of UG2 ore in deionised water at pH 9

The addition of copper sulphate resulted in a decrease in the dynamic froth stability factor, Σ, to 36.6 seconds from 37.1 seconds. The addition of xanthate only decreased Σ further to 36.1 seconds. The lowest froth stability factor was observed when both copper sulphate and xanthate were added where the value of Σ is 35.7 seconds.

Figure 4.7 shows the effect of reagent addition on the froth stability of UG2 ore in synthetic plant water at pH 9.

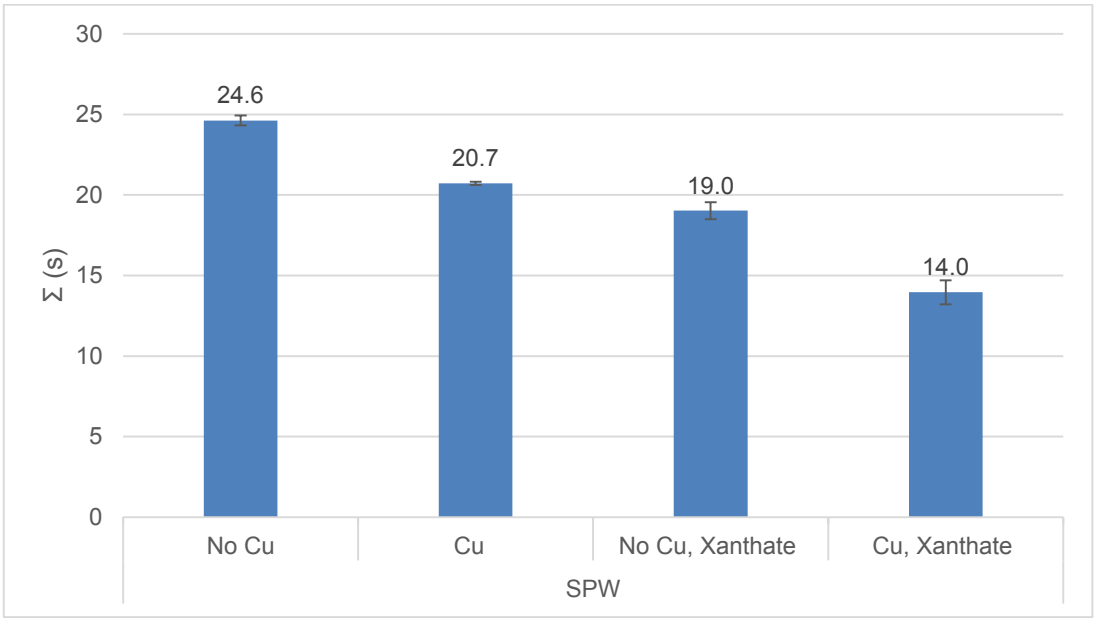

Figure 4.7: Froth stability of UG2 ore in synthetic plant water at pH 9

As observed in deionised water, the froth stability followed a similar trend in synthetic plant water when reagents were added for UG2 ore. Copper sulphate destabilised the froth as Σ decreased from 24.6 seconds to 20.7 seconds. The addition of only xanthate destabilised the froth further as evidenced by the decrease in the value of the dynamic froth stability factor to 19 seconds. The lowest froth stability was observed when both copper sulphate and xanthate were added, with Σ equal to 14 seconds.

4.1.3 Effect of water type on froth stability

Figure 4.8 shows the comparison of the froth stability of a Merensky ore in deionised water and in synthetic plant water.

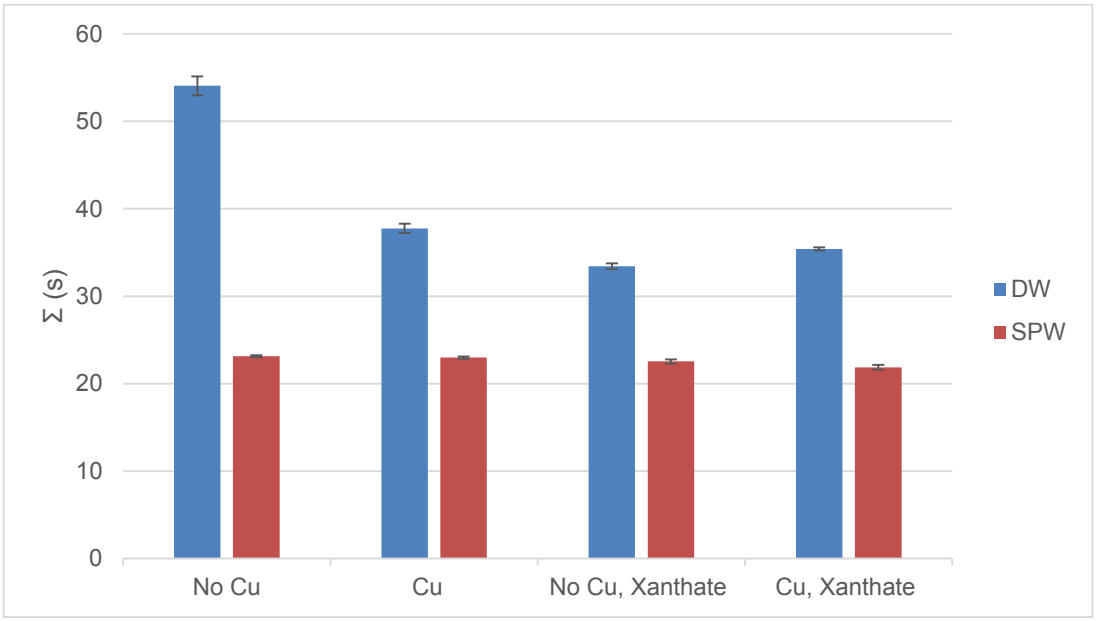

Figure 4.8: Froth stability of Merensky ore in deionised water and synthetic plant water at pH 9

Figure 4.8 shows the froth was more destabilized in synthetic plant water than in deionised water for the Merensky ore. The differences caused by reagent addition were more pronounced in deionised water than in synthetic plant water.

Figure 4.9 shows the comparison of the froth stability of UG2 ore in deionised water and in synthetic plant water.

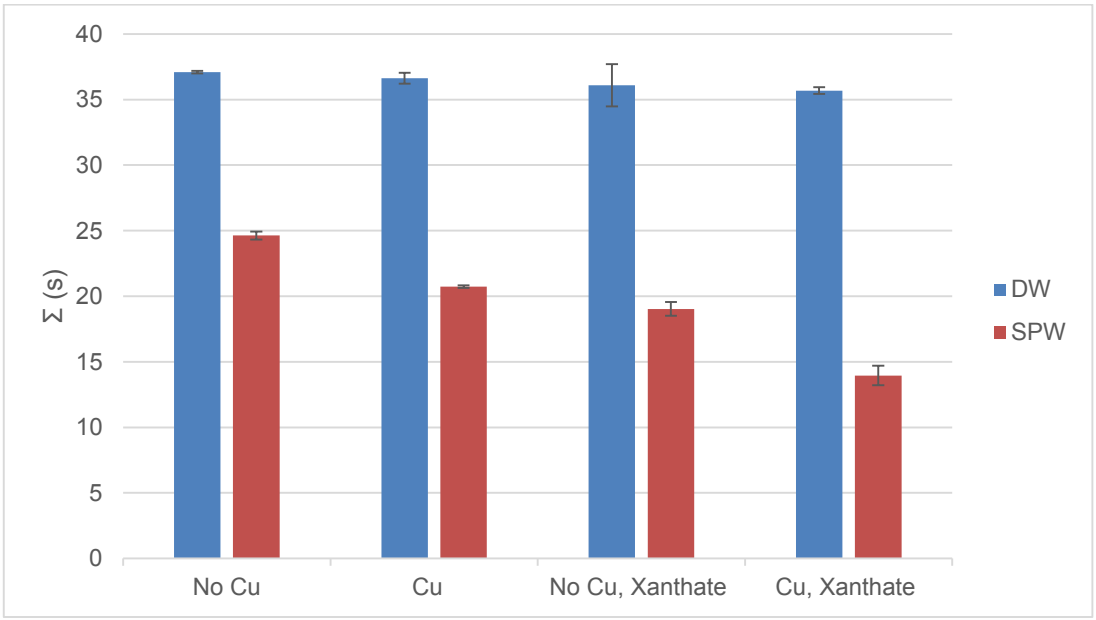

Figure 4.9: Froth stability of UG2 ore in deionised water and synthetic plant water at pH 9

It is evident from the figure above that the froth was less stable in synthetic plant water than in deionised water for UG2 ore. The effects of reagent addition were more

pronounced in synthetic plant water than in deionised water. This was similar to the trend observed for the Merensky ore where more stable froth was obtained with deionised water than with synthetic plant water.

4.1.4 Effect of ore type on froth stability

Figure 4.10 shows the comparison between the froth stabilities of the Merensky and UG2 ores in deionised water at pH 9.

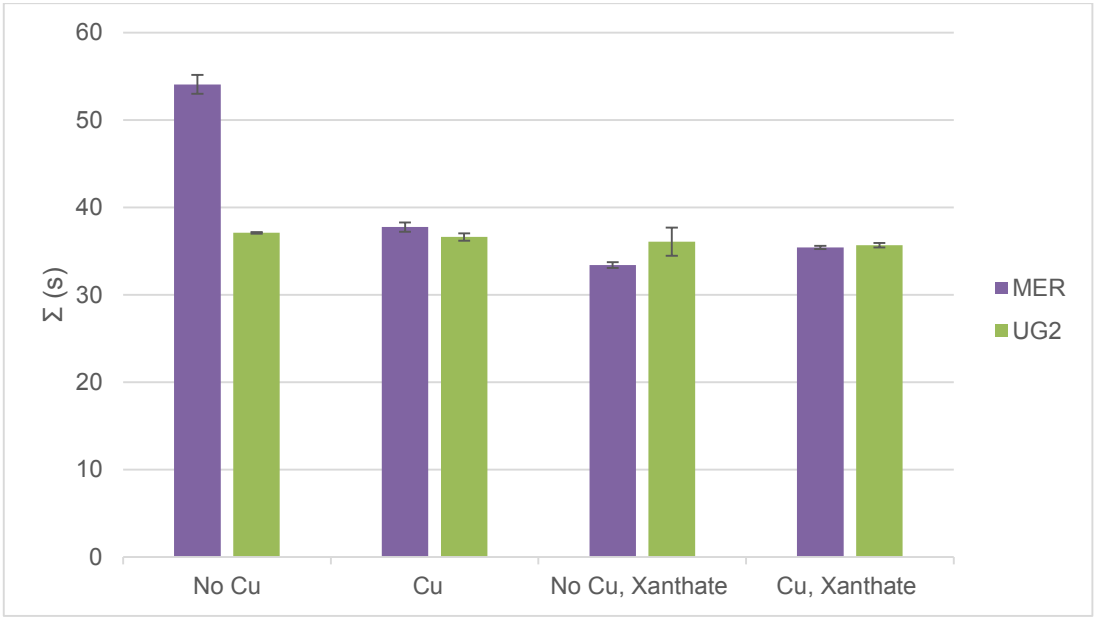

Figure 4.10: Froth stability of Merensky ore versus UG2 ore in deionised water at pH 9

The froth stability of UG2 ore remained fairly constant when compared to Merensky ore in deionised water. Merensky ore froth was more destabilised than the UG2 ore froth only when xanthate was present.

Figure 4.11 shows the comparison between the froth stability of Merensky and UG2 ores in synthetic plant water.

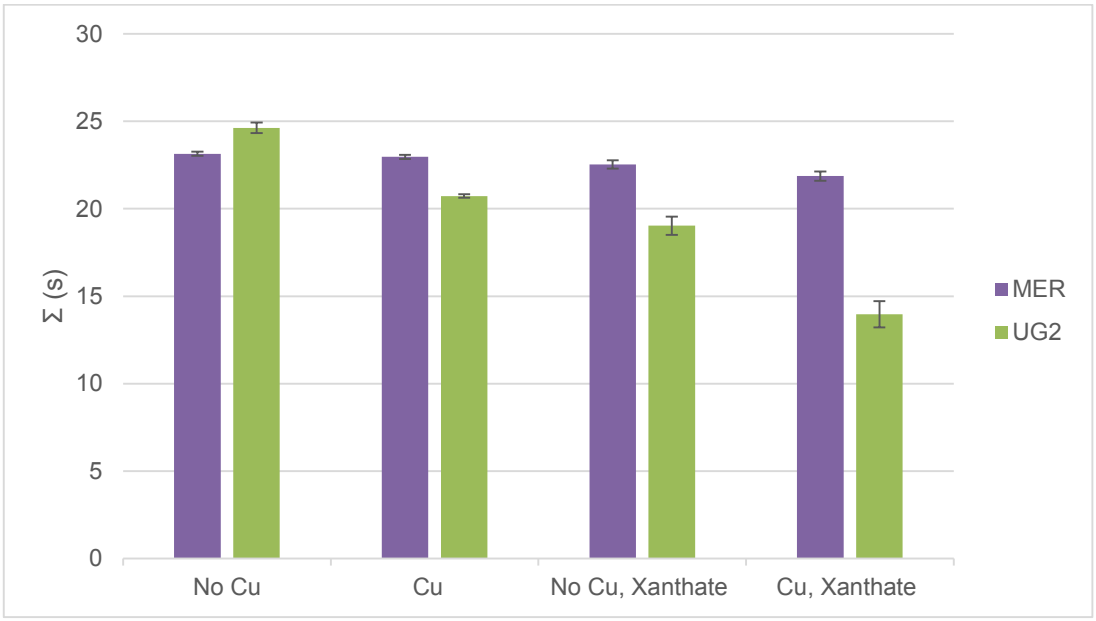

Figure 4.11: Froth stability of Merensky versus UG2 ore in synthetic plant water at pH 9

Merensky ore resulted in more stable froth than UG2 ore for all conditions except for when no reagents are added. The largest difference in froth stability of the two ores was obtained when both copper sulphate and xanthate are present.

4.2 Microflotation Tests

Microflotation tests were conducted using pure minerals to investigate the effect of copper sulphate and xanthate on floatability in the absence of the froth phase. The microflotation tests were also used as a proxy for particle hydrophobicity which was correlated with mineral floatability. Since all pulp phase effects such as turbulence, air flow rate and particle density were maintained constant and since there are no froth effects in microflotation tests, the mineral recovery is related to the hydrophobicity of the particles.

Talc and pyrrhotite were used to test the hypothesis that copper hydroxide at pH 9 would precipitate non-selectively onto non-sulphide gangue and reduce the floatability, whereas the copper(II) species would be reduced to copper(I) on a sulphide surface, interact with xanthate and enhance floatability.

In this section the microflotation results are analysed in terms of the flotation kinetics and the cumulative mass recovery, which is the mass of mineral obtained at the end of the test i.e. after 20 minutes. The error bars represent the standard error of the tests.

The Klimpel flotation model was used to fit the microflotation data in order to assess the flotation kinetics by predicting the flotation rate constant as well as the maximum recovery. The following equation describes the model (Klimpel, 1980):

$$R = R_{max}(1 - \frac{1}{kt}(1 - e^{-kt})) \quad \text{.....4.1}$$

Where R is the percentage recovery time, R_{max} is the final percentage recovery, t the time in minutes and k the initial rate constant (minutes^{-1}).

According to Mineral Technologies International, Inc. (2010), the Klimpel model is one of two of the most successful flotation models. The other model, the distributed rate constant model is used for flotation plant simulation whereas the Klimpel model is suitable for modelling single flotation cells. The Klimpel model, which is a simplified formulation of the distributed rate constant model, is based on an observation that not all particles with infinite residence time in a flotation system will be recovered by true flotation. There are two kinetic parameters required for each type of particle namely the ultimate recovery and the kinetic constant. The model however does not take into account factors such as the particle size and froth behaviour (MTI, 2010).

Firstly, the effect of reagent addition on talc floatability is investigated followed by the effect of water type on talc floatability. An analysis of the effect of reagent addition and water type is also made for pyrrhotite.

4.2.1 Effect of reagent addition on talc floatability

The effect of reagent addition on talc floatability in deionised water is shown in Figure 4.12.

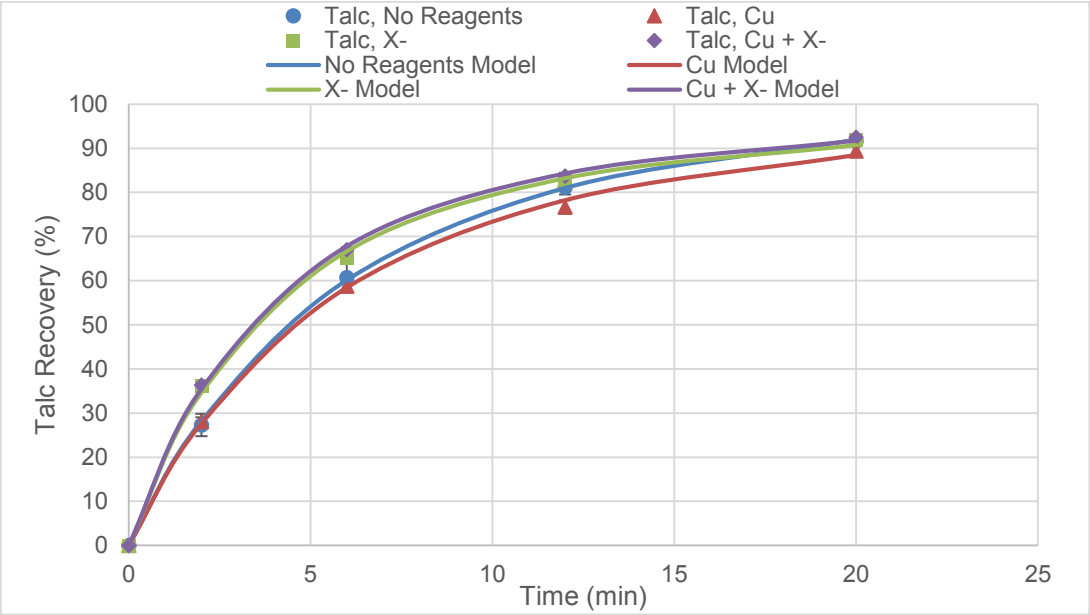

Figure 4.12: Talc microflotation with deionised water at pH 9. The error bars are shown but they are obscured by the markers

The theoretical maximum recovery (R_{max}) and the flotation rate constants obtained from fitting the data to the Klimpel model are shown in Table 4.1.

Table 4.1: Theoretical maximum recovery and flotation rate constant for talc in deionised water

Condition	R_{max} (%)	k (min^{-1})
No Reagents	100	0.314
Copper	100	0.323
Xanthate	100	0.447
Copper + Xanthate	100	0.456

From Figure 4.12 it is evident that overall the addition of reagents did not significantly change the cumulative mass recovery of talc since the value of R_{max} obtained was the same for the conditions investigated. The graph shows a slight decrease in the actual recovery at 20 minutes when copper sulphate was added. However, there was not a large decrease in recovery as hypothesised by the non-selective precipitation of copper hydroxide. The Klimpel model constants show the addition of only copper sulphate, only xanthate and both copper sulphate and xanthate increased the reaction kinetics as evidenced by the increasing rate constant values.

Figure 4.13 shows the effect of reagent addition on talc floatability in synthetic plant water.

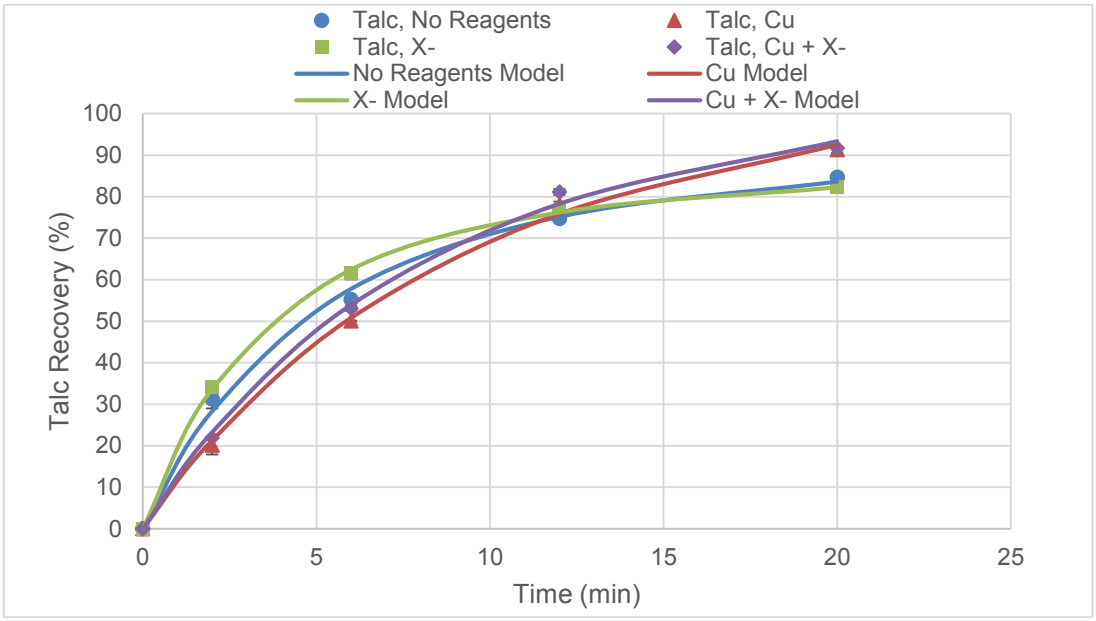

Figure 4.13: Talc microflotation with synthetic plant water at pH 9. The error bars are shown but they are obscured by the markers.

The Klimpel constants are shown in Table 4.2

Table 4.2: Theoretical maximum recovery and flotation rate constant for talc in synthetic plant water

Condition	R_{max} (%)	k (min^{-1})
No Reagents	97	0.369
Copper	100	0.196
Xanthate	91	0.500
Copper + Xanthate	100	0.224

It is evident from Figure 4.13 that the floatability of talc was not significantly affected by the addition of reagents in synthetic plant water. This is similar to the results obtained for the floatability of talc in deionised water. The highest talc recoveries were obtained when only copper sulphate was added and when both copper sulphate and xanthate were added.

As seen in Table 4.2, the highest theoretical maximum values for talc floatability were obtained when copper sulphate was added in the presence of both copper sulphate and xanthate. These conditions correspond to the lowest rates of flotation.

4.2.2 Effect of water type on talc floatability

A comparison of the floatability of talc in deionised versus synthetic plant water is shown in Figure 4.14. The Klimpel flotation model for talc in deionised water is represented by the solid lines and the Klimpel flotation model for talc in synthetic plant water is represented by the broken lines. The solid markers represent the conditions for talc in deionised water and the empty markers represent conditions for talc in synthetic plant water.

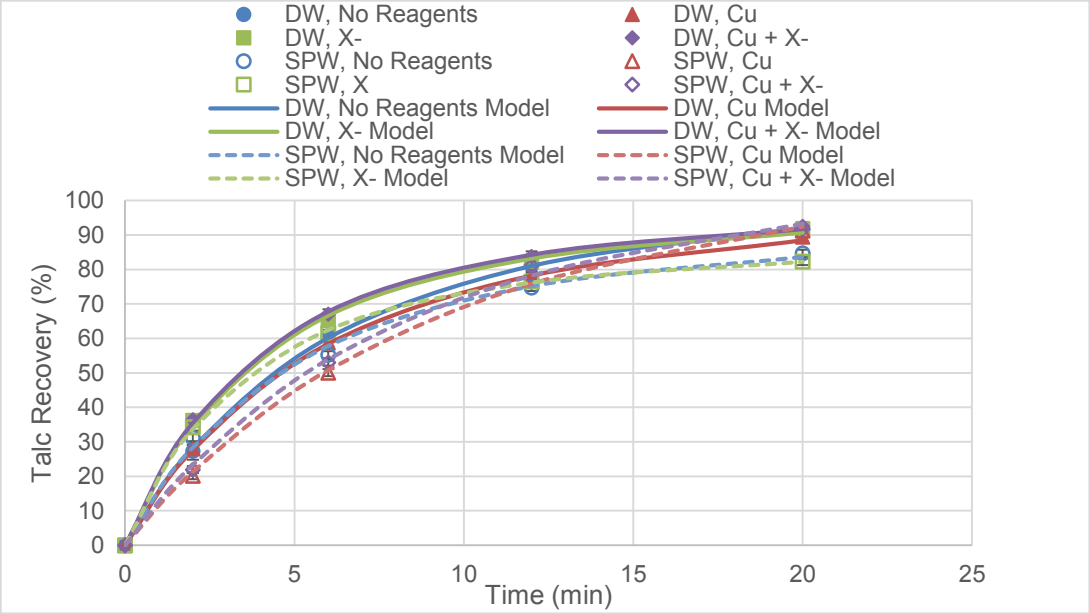

Figure 4.14: Talc flotation with deionised water and synthetic plant water at pH 9

The Klimpel constants are shown in Table 4.3.

Table 4.3: Theoretical maximum recovery and flotation rate constant for talc in synthetic plant water

Condition	Water Type	R_{max} (%)	k (min^{-1})
No Reagents	DW	100	0.314
	SPW	97	0.369
Copper	DW	100	0.323
	SPW	100	0.196
Xanthate	DW	100	0.447
	SPW	91	0.500
Copper + Xanthate	DW	100	0.456
	SPW	100	0.224

According to Figure 4.14, the overall talc recovery was slightly higher in deionised water than in synthetic plant water for the conditions when no reagents were added and when xanthate only was added. However, there was little difference in the

recoveries for all other conditions. These observations were reinforced by the Klimpel model constants in Table 4.3.

4.2.3 Effect of reagent addition on pyrrhotite floatability

The effect of addition of reagents on the floatability of pyrrhotite in deionised water is shown in Figure 4.15.

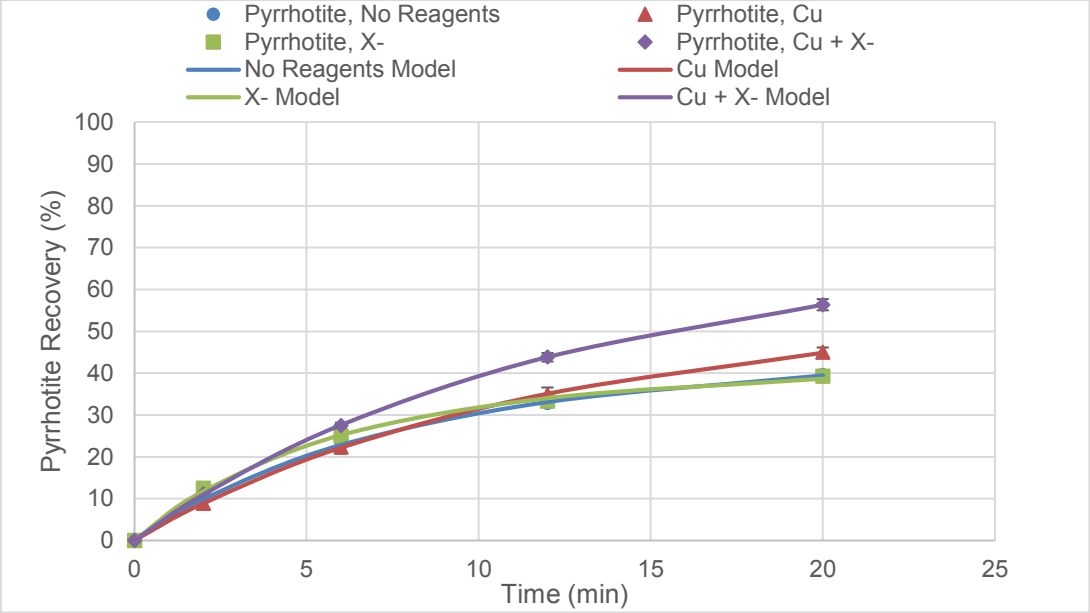

Figure 4.15: Pyrrhotite microflotation with deionised water results at pH 9

The Klimpel constants are shown in Table 4.4.

Table 4.4: Theoretical maximum recovery and flotation rate constant for pyrrhotite in deionised water

Condition	R_{max} (%)	k (min^{-1})
No Reagents	51	0.225
Copper	66	0.146
Xanthate	46	0.310
Copper + Xanthate	84	0.142

According to Figure 4.15, floatability of pyrrhotite was not enhanced in the presence of xanthate only. The addition of copper sulphate improved the overall pyrrhotite recovery but reduced the initial flotation rate constant *k*. When the xanthate was added after copper sulphate activation, there was a significant increase in the pyrrhotite mass recovery.

The effect of reagent addition on the floatability of pyrrhotite in synthetic plant water is shown in Figure 4.16.

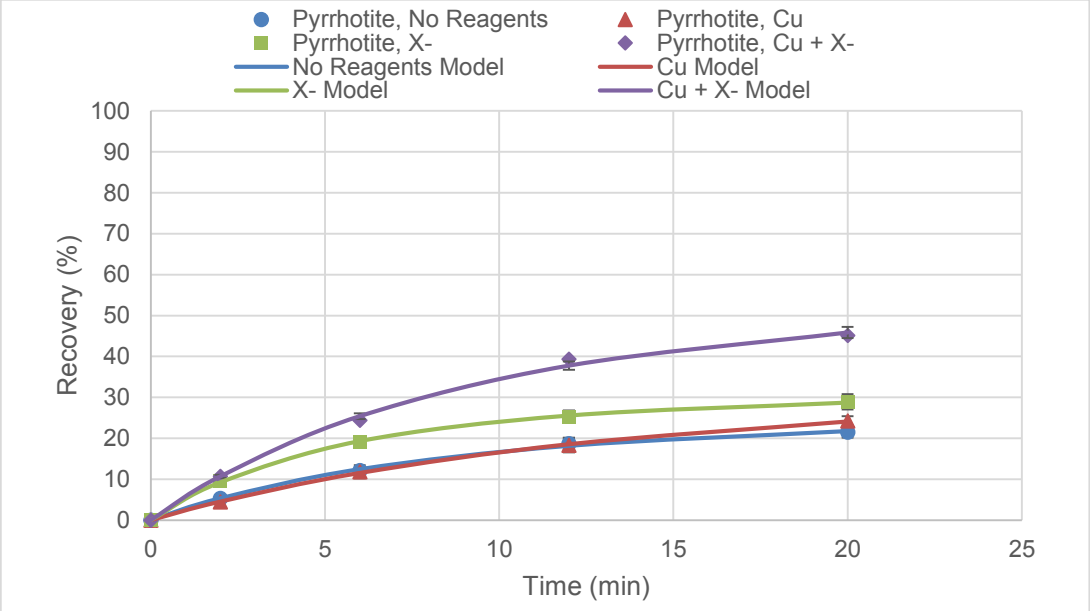

Figure 4.16: Pyrrhotite microflotation with synthetic plant water results at pH 9

The Klimpel constants are shown in Table 4.5.

Table 4.5: Theoretical maximum recovery and flotation rate constant for pyrrhotite in synthetic plant water

Condition	R_{max} (%)	k (min^{-1})
No Reagents	28	0.218
Copper	37	0.133
Xanthate	34	0.340
Copper + Xanthate	61	0.200

The addition of copper sulphate alone slightly increased the overall recovery of pyrrhotite in synthetic plant water. The addition of xanthate increased the flotation kinetics and the overall pyrrhotite recovery slightly. As seen in Figure 4.16, the presence of both copper sulphate and xanthate in the system increased the floatability of pyrrhotite significantly.

4.2.4 Effect of water type on pyrrhotite floatability

Figure 4.17 shows flotation of pyrrhotite with deionised water and with synthetic plant water. The solid lines represent Klimpel flotation model obtained for pyrrhotite in deionised water and the broken lines represent the Klimpel flotation model for

pyrrhotite in synthetic plant water. The solid markers represent pyrrhotite floatability in deionised water and the open markers represent pyrrhotite floatability in synthetic plant water.

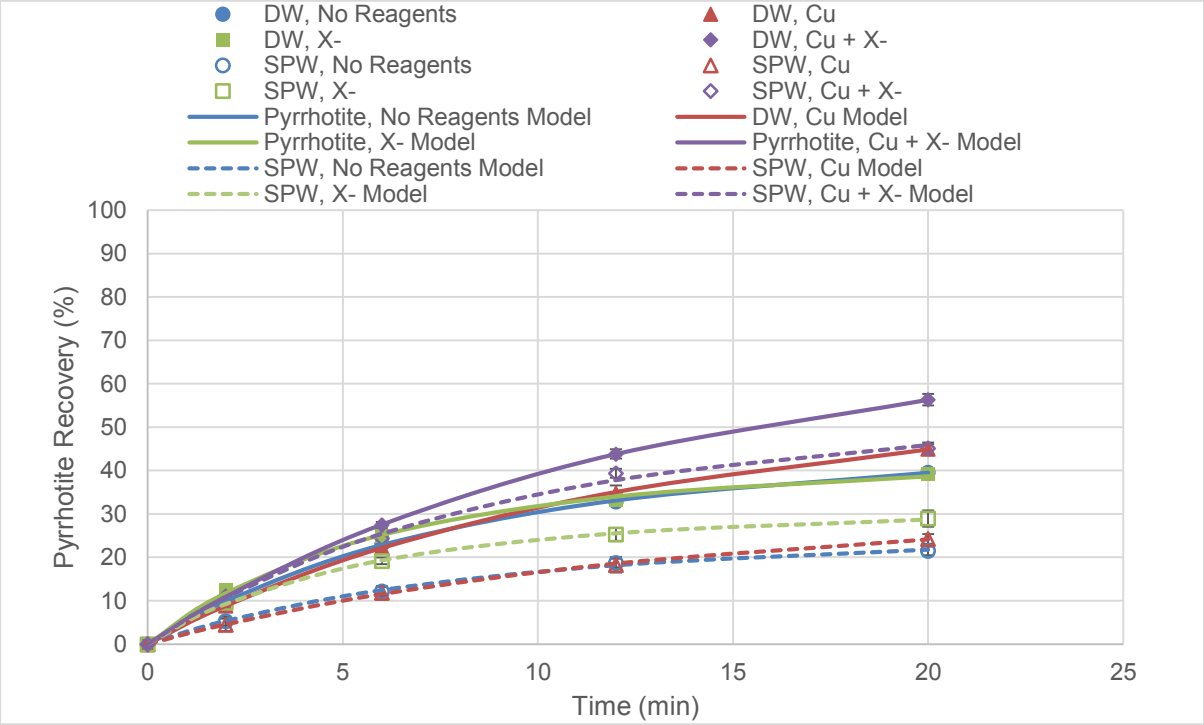

Figure 4.17: Pyrrhotite flotation with deionised water and synthetic plant water at pH 9

The Klimpel constants are shown in Table 4.6.

Table 4.6: Theoretical maximum recovery and flotation rate constant for pyrrhotite in deionised and synthetic plant water

Condition	Water Type	R_{max} (%)	k (min^{-1})
No Reagents	DW	51	0.225
	SPW	28	0.218
Copper	DW	66	0.146
	SPW	37	0.133
Xanthate	DW	46	0.310
	SPW	34	0.340
Copper + Xanthate	DW	84	0.142
	SPW	61	0.200

Overall, the flotation performance (mass recovery) was decreased when synthetic plant water was used in place of deionised water for all conditions as seen in Figure 4.17. This was also evidenced by the decrease in R_{max} values shown in Table 4.6. The flotation rates were higher in deionised water than in synthetic plant water as evidenced by the increase in the slopes and the rate constant *k* values with the

exception of the conditions when xanthate was added with and without copper sulphate.

4.3 Zeta Potential Determinations

In this study, zeta potential measurements were used to attempt to identify the surface copper species responsible for pure mineral activation since the extent of adsorption is dependent on the charge and type of species present in the bulk solution. The error bars represent the standard error of the tests.

Firstly, the effect of pH on the zeta potential is presented followed by the effect of reagent addition on each of the pure minerals investigated (talc, chromite, plagioclase and pyrrhotite). The effect of addition of copper sulphate on all of the minerals is then assessed in the presence and absence of xanthate.

4.3.1 Effect of pH on the zeta potential of pure minerals

Figure 4.18 shows the variation of zeta potential with pH for the four minerals investigated.

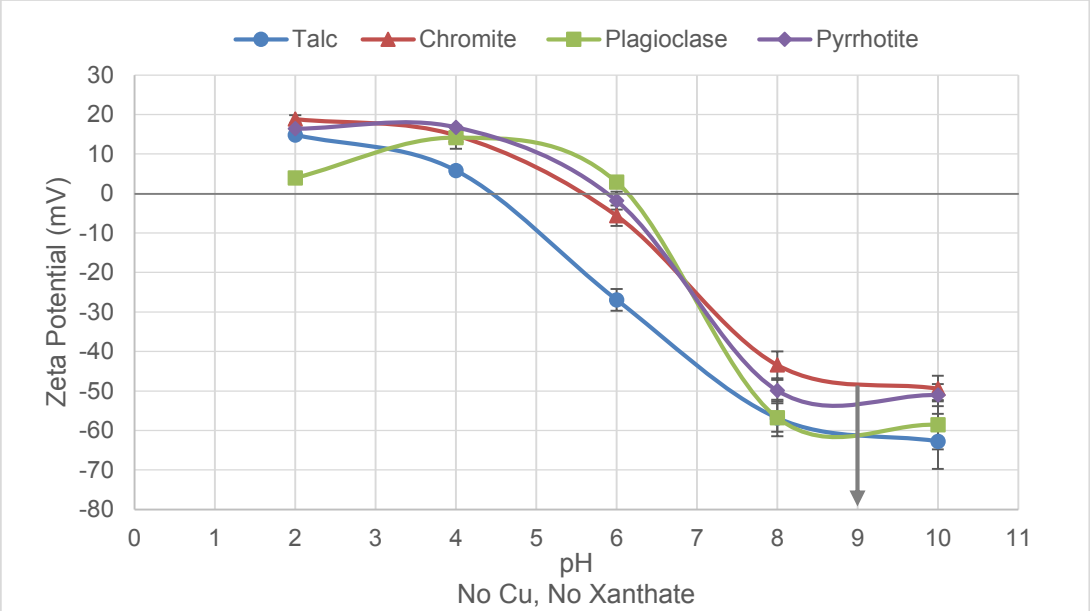

Figure 4.18: Mineral zeta potentials in the absence of reagents in a 10^{-2} M $Na_2B_4O_7$ background electrolyte solution

As expected, the zeta potential versus pH curves for the minerals studied have a sigmoid shape. The zeta potential decreased with increasing pH. It is evident from the graph that talc had the lowest isoelectric point pH ($pH_{i.e.p}$) which is close to 4.5

and the $pH_{i.e.p}$ of chromite, pyrrhotite and plagioclase are around 5.6, 5.9 and 6.2 respectively. All of the minerals exhibited a negative charge (between -48 mV and -63 mV) at pH 9 as shown in Figure 4.18.

4.3.2 Effect of reagent addition on talc zeta potential

Figure 4.19 shows the effect of reagent addition on the zeta potential of talc. The open markers and broken lines represent conditions with copper sulphate addition.

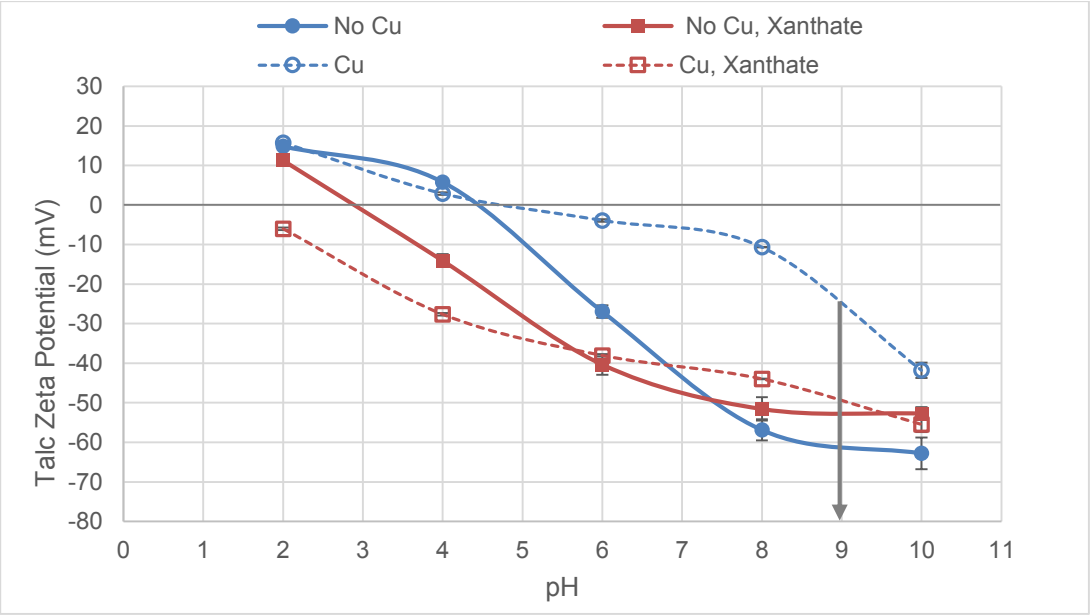

Figure 4.19: Talc zeta potential determinations in a 10^{-2} $Na_2B_4O_7$ M background electrolyte solution. All reagent concentrations were 5 x 10^{-3} M

Figure 4.19 shows the addition of copper sulphate resulted in a shift of the zeta potential to less negative values above pH 5. The addition of copper sulphate did not shift the $pH_{i.e.p}$ of talc. The addition of xanthate (with no copper sulphate) makes the zeta potential more negative in acidic conditions (below pH 7) and slightly more positive above pH 7 with respect to the bare talc surface. For the condition with both xanthate and copper sulphate, the zeta potential was more negative below pH 7 and slightly more positive above pH 7, similar to the xanthate only system.

At pH 9, which was used for the microflotation tests and is the natural pH of the UG2 and Merensky ores, it is clear that both xanthate and copper adsorbed onto the talc surface. The addition of copper sulphate resulted in the largest shift in zeta potential to a less negative value.

4.3.3 Effect of reagent addition on chromite zeta potential

The effect of reagent addition on the zeta potential of chromite is shown in Figure 4.20.

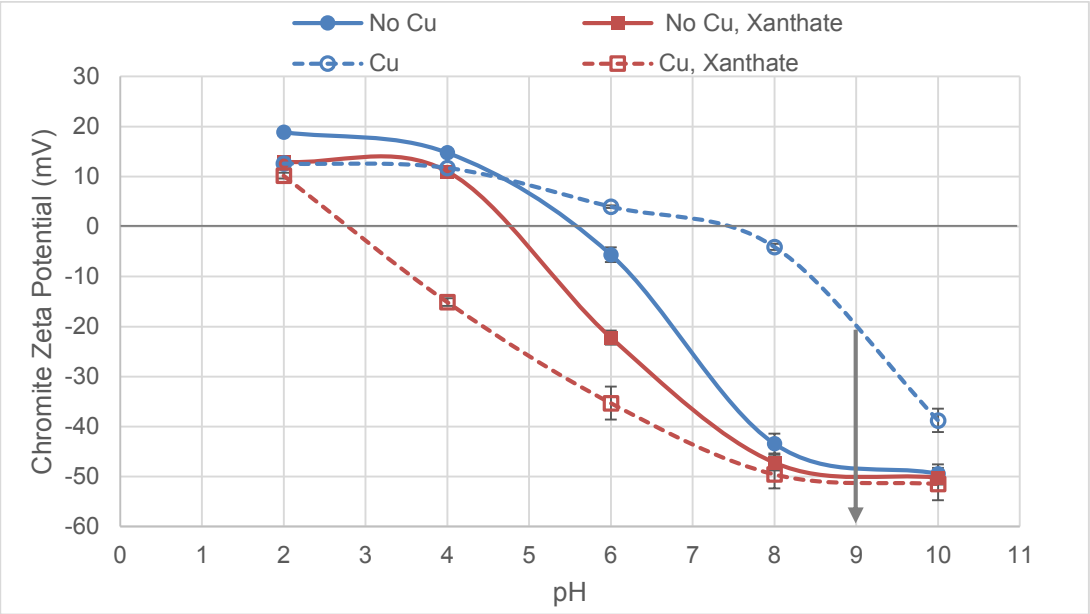

Figure 4.20: Chromite zeta potential determinations in a 10^{-2} $Na_2B_4O_7$ M background electrolyte solution. All reagent concentrations were 5 x 10^{-3} M

Addition of copper sulphate shifted the zeta potential of chromite to more positive values above pH 5. At pH 9, the addition of copper sulphate shifted the zeta potential of chromite to significantly less negative values, indicating that the copper was adsorbing onto the chromite surface. The addition of xanthate alone did not significantly change the zeta potential of chromite, suggesting that xanthate alone did not adsorb on the chromite surface, as expected. Copper in the presence of xanthate had a lower zeta potential at pH's less than 8, but did not significantly change the zeta potential of chromite above pH 8.

4.3.4 Effect of reagent addition on plagioclase zeta potential

The effect of reagent addition on the zeta potential of plagioclase is shown in Figure 4.21.

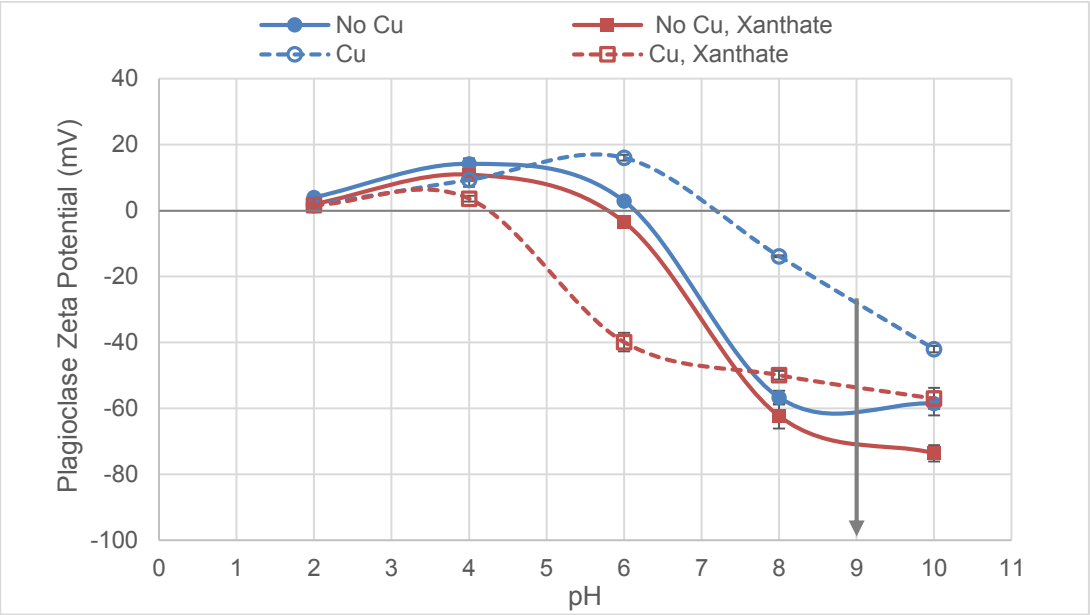

Figure 4.21: Plagioclase zeta potential determinations in a 10^{-2} $Na_2B_4O_7$ M background electrolyte solution. All reagent concentrations were 5 x 10^{-3} M

As seen in Figure 4.21, the presence of copper sulphate caused the zeta potential to shift to more positive values in the alkaline pH range, indicating the adsorption of copper species. The addition of xanthate did not significantly alter the zeta potential throughout the whole pH range. The addition of copper sulphate and xanthate shifted the zeta potential to intermediate values at pH 9.

4.3.5 Effect of reagent addition on pyrrhotite zeta potential

The effect of reagent addition on the zeta potential of pyrrhotite is shown in Figure 4.22.

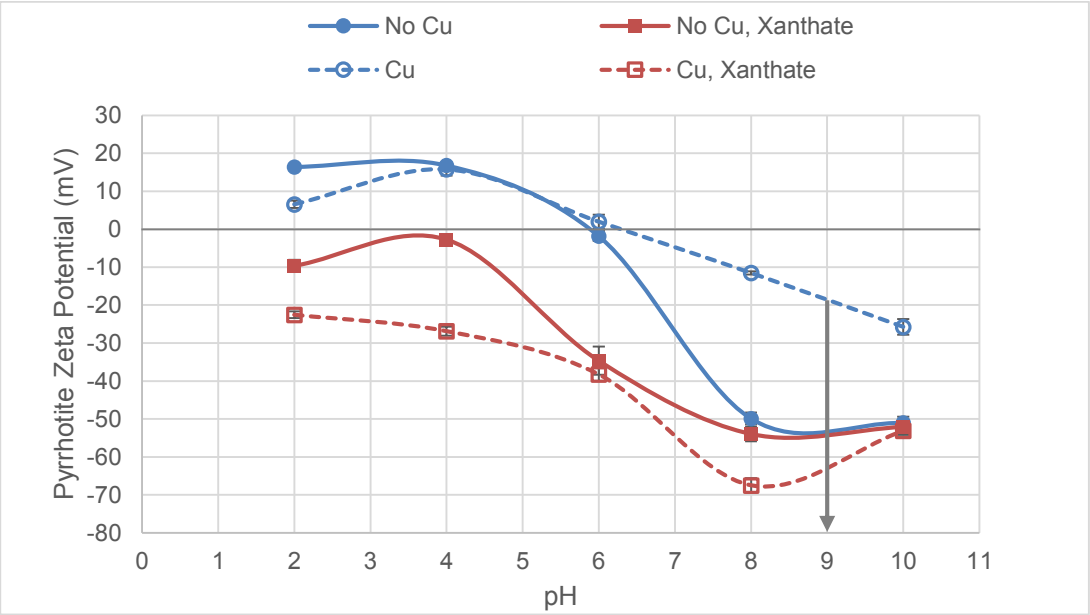

Figure 4.22: Pyrrhotite zeta potential determinations in a 10^{-2} $Na_2B_4O_7$ M background electrolyte solution. All reagent concentrations were 5 x 10^{-3} M

It is evident from Figure 4.22 that the addition of copper sulphate to the system makes the surface of pyrrhotite less negatively charged above pH 6. When only xanthate is added, the zeta potential becomes more negative across most of the pH range, indicating some xanthate adsorption. However, the surface charge of the bare pyrrhotite surface and that with xanthate added is the same at pH 9. When xanthate is added to pyrrhotite activated with copper, the zeta potential is most negative.

4.3.6 Effect of copper sulphate on the zeta potential of pure minerals

The effect of the addition of copper sulphate on the zeta potential was investigated in the presence and in the absence of xanthate collector.

The effect of copper sulphate on the four minerals in the absence of xanthate is shown in Figure 4.23.

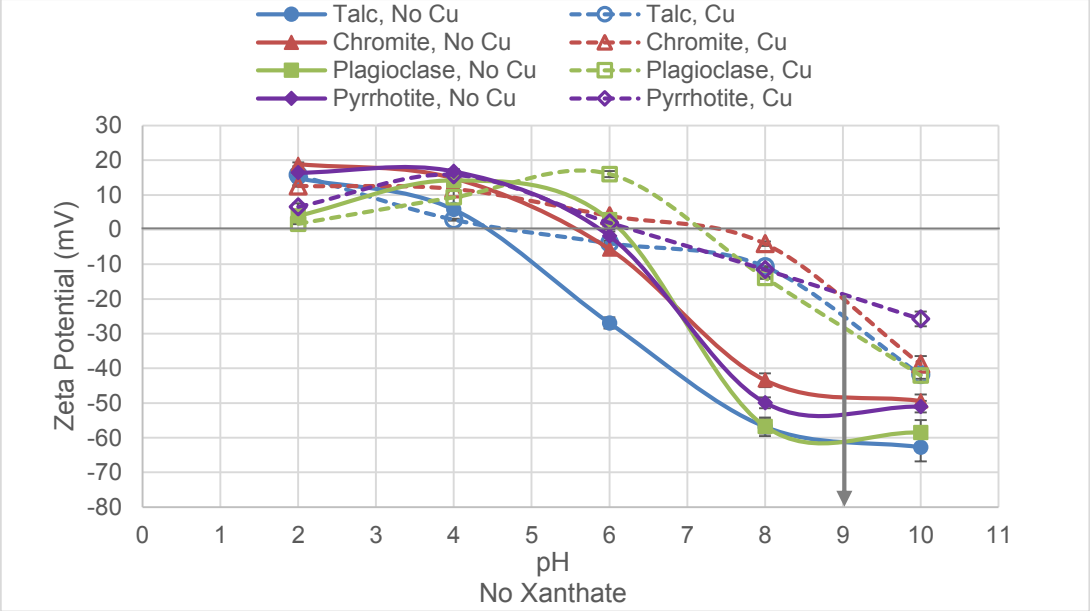

Figure 4.23: Effect of Cu on minerals in the absence of xanthate in a 10^{-2} $Na_2B_4O_7$ background electrolyte solution. All reagent concentrations were 5 x 10^{-3} M

It is evident from Figure 4.23 that the presence of copper sulphate caused the zeta potential of the minerals to shift to more positive values at pH 9, the pH of interest. Initially, before copper sulphate activation, the minerals' zeta potentials were between -48 mV and -63 mV. These were shifted to between -19 mV and -30 mV as represented by the broken lines in Figure 4.23 above. The addition of copper sulphate also shifted the isoelectric point pH ($pH_{i.e.p}$) to higher pH values for all of the minerals with the exception of talc. The effect of copper sulphate on the four minerals investigated in the presence of xanthate is shown in Figure 4.24.

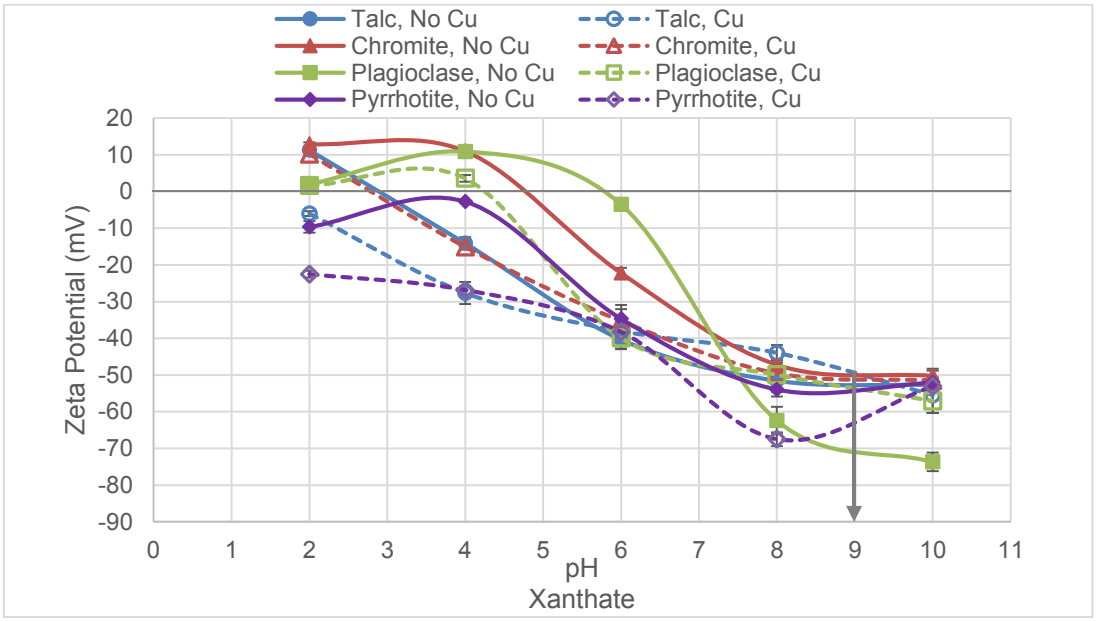

Figure 4.24: Effect of Cu on minerals in the presence of xanthate in a 10^{-2} M $Na_2B_4O_7$ background electrolyte solution. All reagent concentrations were 5 x 10^{-3} M

The addition of copper sulphate does not appear to have a significant effect on the zeta potential of chromite and talc in the presence of xanthate at pH 9. The zeta potential becomes less negative for plagioclase and more negative for pyrrhotite at pH 9 when copper sulphate and xanthate are present. The zeta potentials of the minerals with and without copper sulphate activation lie in the range between -48 mV and -72 mV. This is significantly lower than the range of zeta potential obtained when copper sulphate was added in the absence of xanthate which was between -19 mV and -30 mV. Since xanthate was added after copper sulphate activation, the more negative zeta potential values obtained indicate adsorption of xanthate onto activated mineral surfaces.

4.4 Activation products analysis

From the literature reviewed, it is clear that the nature of the activation species influences the floatability of the minerals and this was investigated in the microflotation test work. The zeta potential tests gave an indication of the extent to which the surface charge was altered as a result of copper sulphate activation and xanthate adsorption. In order to determine the nature of the activating species on the mineral surfaces, analyses were done using EDTA, a complexing agent.

For the froth stability tests, a dosage of 90 g/tonne of copper sulphate was used. This is equivalent to 46 g/tonne of Cu and approximately 10 mg/L if all the copper sulphate was in solution. The following mass balance was used for the total copper in the system.

$$Cu_{total} = Cu(OH)_{2,surface} + Cu_{solution} + Cu_{surface} \quad \text{.....4.2}$$

The $Cu_{surface}$ is Cu(I) or Cu(II) that has chemically reacted with the mineral surface and cannot be extracted with EDTA. $Cu(OH)_{2,surface}$ is a non-selective copper hydroxide precipitate that can be extracted from the surface using EDTA. $Cu_{solution}$ is the residual copper left in the solution. The copper extracted via the EDTA procedure ($Cu(OH)_2$), the copper in the bulk solution and the surface copper were expressed as a percentage of the copper added to the system. The standard deviation for the AAS (Atomic Absorption Spectroscopy) tests used to determine the relative amounts of copper was 4%. The detailed calculations used to determine the copper species present in the system are shown in Appendix D.

In this section of the dissertation, the copper activation products from Merensky ore are first determined followed by Merensky ore iron analysis. The results for copper activation products from UG2 ore are then given and lastly, an analysis of the products of talc activation.

4.4.1 Merensky ore copper analysis

Figure 4.25 shows results for analysis of the copper content in the conditioned Merensky pulp prior to the froth stability tests.

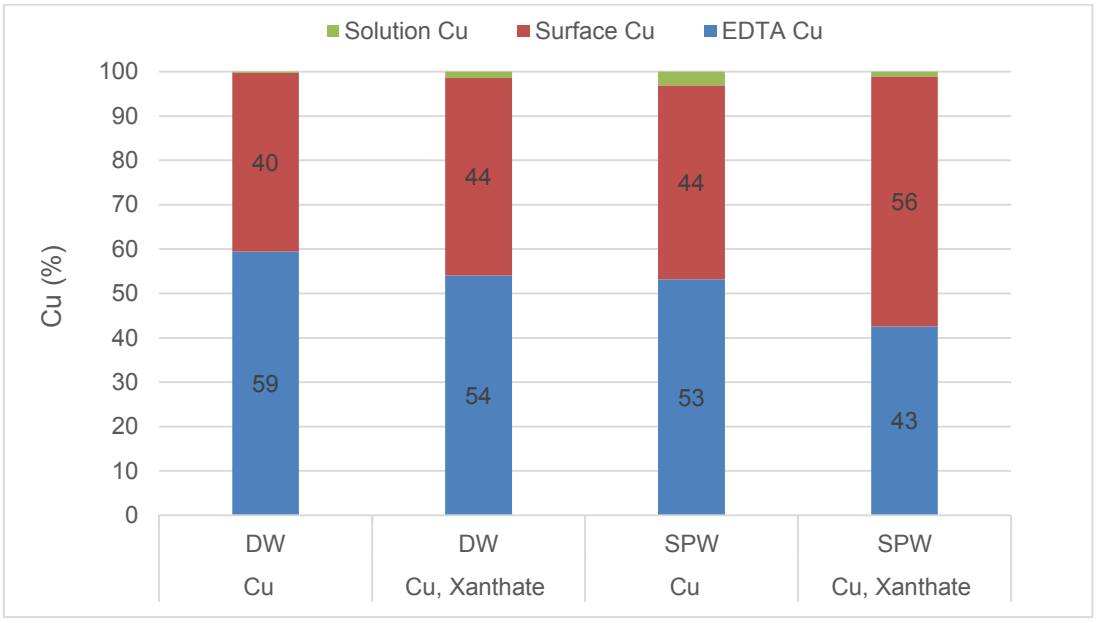

Figure 4.25: Merensky ore copper analysis

According to Figure 4.25, more EDTA extractable copper ($Cu(OH)_2$) was recovered in deionised water than in synthetic plant water. The highest amount of $Cu(OH)_2$, as represented by the blue bars, was found when only copper is added in the absence of xanthate in deionised water. The least amount of $Cu(OH)_2$ was observed when both copper and xanthate are present in synthetic plant water. This was also the condition with the most chemically reacted copper on the mineral surface, represented by the red bars. The surface copper was possibly in the form of copper(I) sulphide. When xanthate was present, both in synthetic plant water and deionised water, the amount of copper extractable by EDTA was lower than when there is no xanthate added. For all of the conditions investigated in Figure 4.25 the amount of residual copper left in solution was minimal as evidenced by the green bars.

4.4.2 Merensky ore iron analysis

Some studies have suggested an ion exchange reaction occurs between the sulphide mineral lattice iron and the Cu(II) in solution (Buswell & Nicol, 2002; Finkelstein, 1997). Figure 4.26 shows the total iron (iron in solution and EDTA extractable iron) for the conditions investigated in deionised and synthetic plant water. Iron analysis was not done for UG2 ore because of the low content of iron-bearing base metal sulphides in the ore.

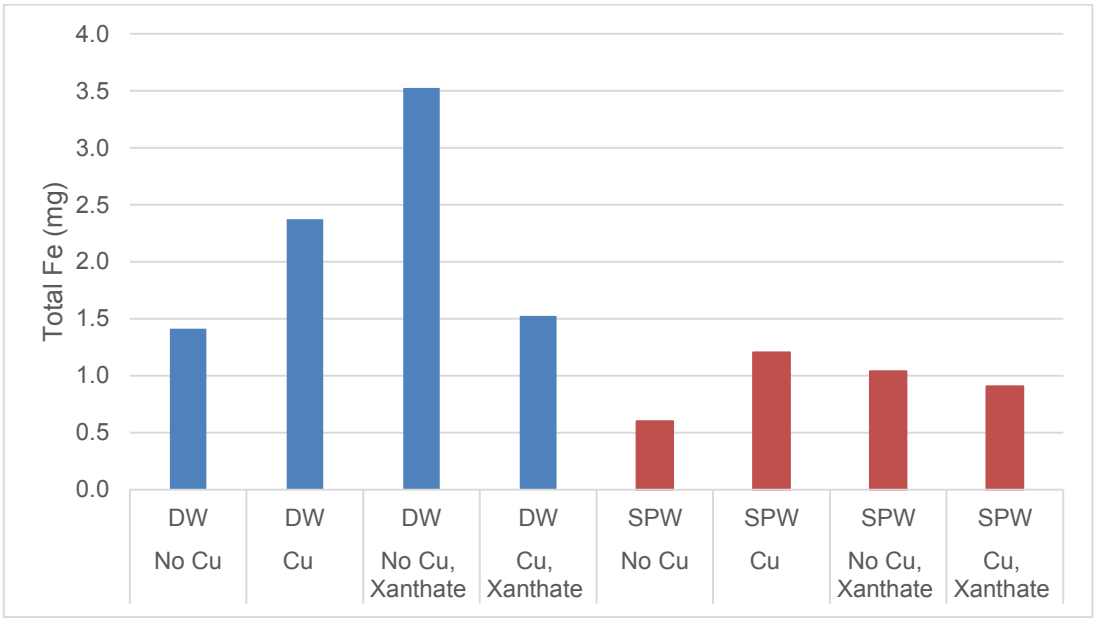

Figure 4.26: Iron Analysis of Merensky ore

Figure 4.26 shows the total amount of iron in deionised water was higher than in synthetic plant water. The higher amounts of iron expected if the copper were exchanging for iron in the mineral lattice, were not observed.

The amount of iron extractable by EDTA from Merensky ore is shown in Figure 4.27.

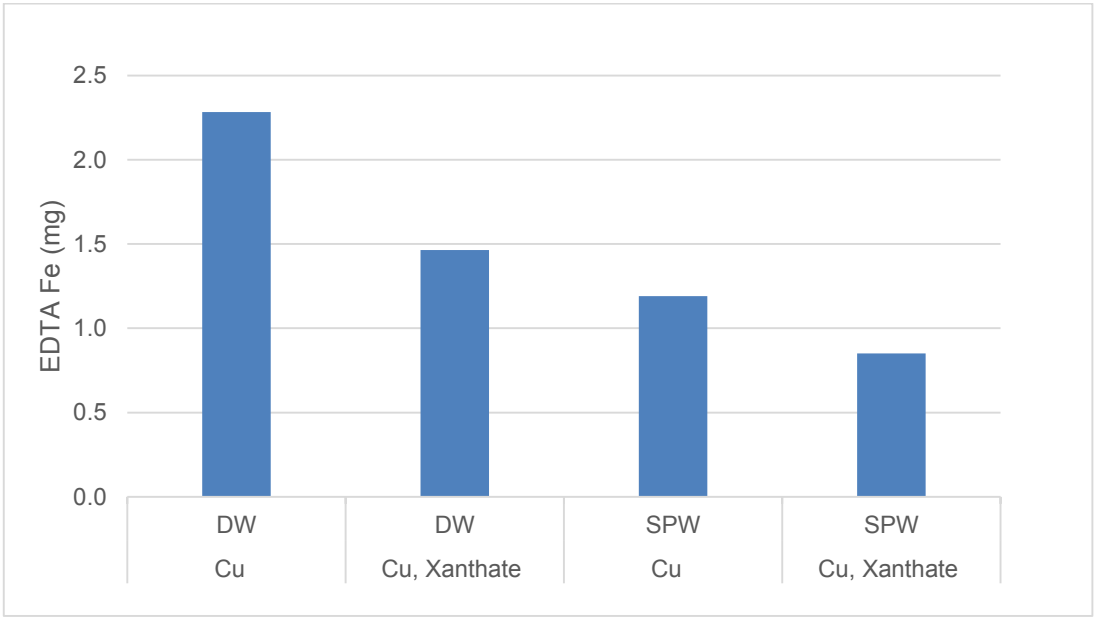

Figure 4.27: EDTA extractable Fe in Merensky ore using 0.03 M EDTA solution

It is evident there was more iron extracted by EDTA when deionised water was used than when synthetic plant water was used. Less copper hydroxide was extracted by EDTA in the presence of xanthate.

4.4.3 UG2 ore copper analysis

Figure 4.28 shows results for analysis of the copper content in the conditioned UG2 pulp prior to the froth stability tests.

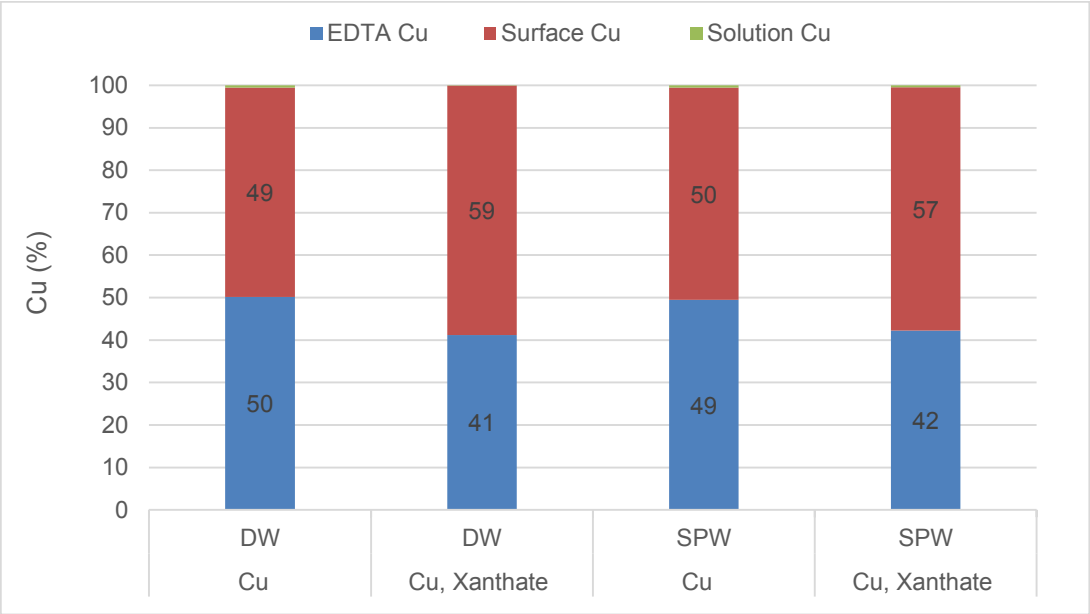

Figure 4.28: UG2 ore copper analysis

The copper extracted by the EDTA ($Cu(OH)_2$) and the chemically reacted surface copper did not change significantly comparing the conditions when synthetic plant water or deionised water was used. This is shown by the blue bars in Figure 4.28. As observed for the Merensky ore, the presence of xanthate resulted in lower amounts of $Cu(OH)_2$ extracted in both water types. Consequently, the highest amounts of chemically reacted copper was also obtained for the conditions with both copper and xanthate present in both deionised and synthetic plant water as shown by the red bars. When only copper was present, approximately half of the copper species are present as $Cu(OH)_2$ and half as surface-reactive copper. For all of the conditions, the amount of copper left in solution was negligible as shown by the green bars.

4.4.4 Ore comparison of surface activation products

A comparison of copper extracted by EDTA from Merensky and UG2 ores is shown in Figure 4.29.

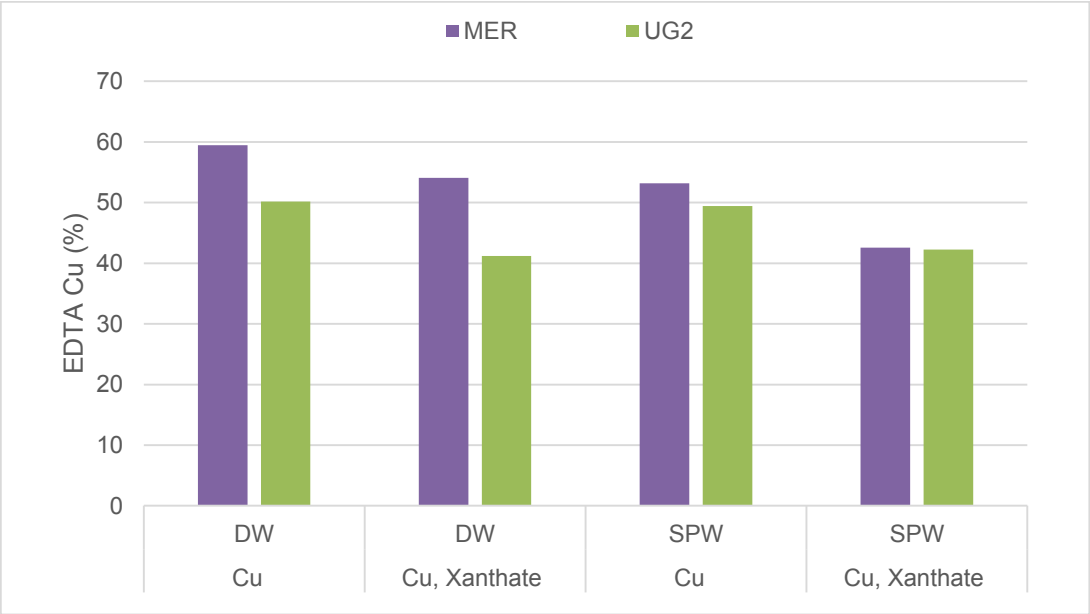

Figure 4.29: Comparison of EDTA extractable copper from Merensky and UG2 ores. The concentration of the EDTA solution was 0.03 M.

It is evident from all of the conditions investigated that more EDTA extractable copper was obtained from Merensky ore mineral surfaces than from UG2 ore. This holds for both synthetic plant water and deionised water. This was unexpected since it was expected that most of the copper would precipitate on UG2 ore as non-selective $Cu(OH)_2$, since there are very few sulphides present with which to react. In the case of Merensky ore, it was expected that the copper would react with the sulphide minerals to form chemically adsorbed Cu(I) or Cu(II) species.

Figure 4.30 shows the variation of chemically reacted copper for the different reagent conditions for the Merensky and UG2 ores.

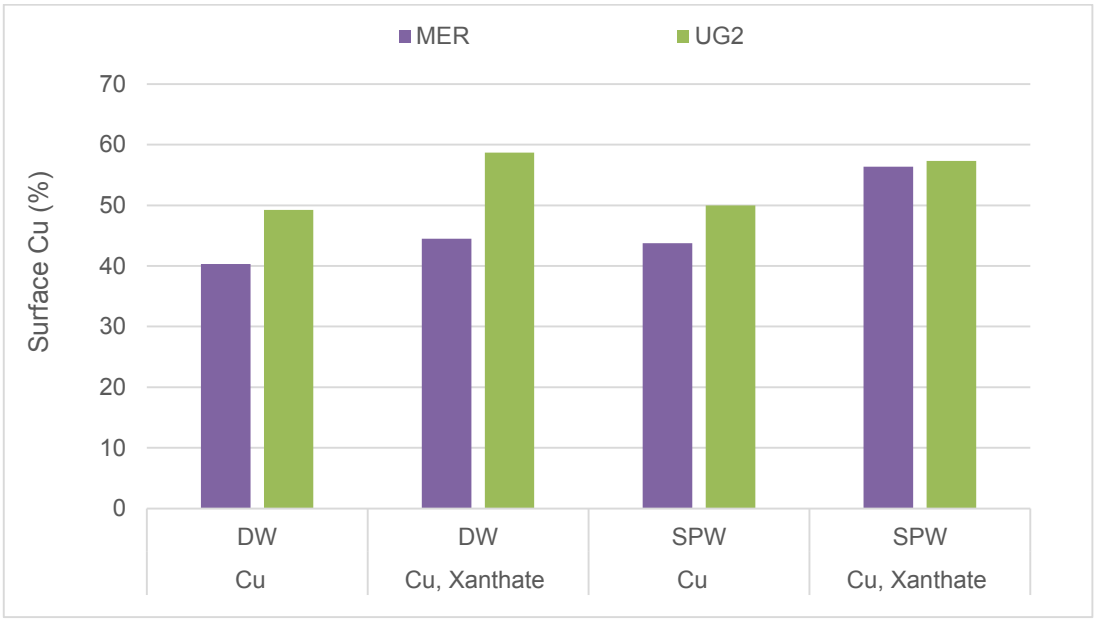

Figure 4.30: Comparison of surface copper from Merensky and UG2 ores

Figure 4.30 suggests more chemically reacted copper was on the UG2 ore mineral surfaces than Merensky ore. This is the case for both of the two water types.

4.4.5 Talc copper analysis

EDTA extraction tests were conducted on talc samples using the copper dosage of 2 monolayers and xanthate dosage of 0.5 monolayers which are the same conditions used for the microflotation tests.

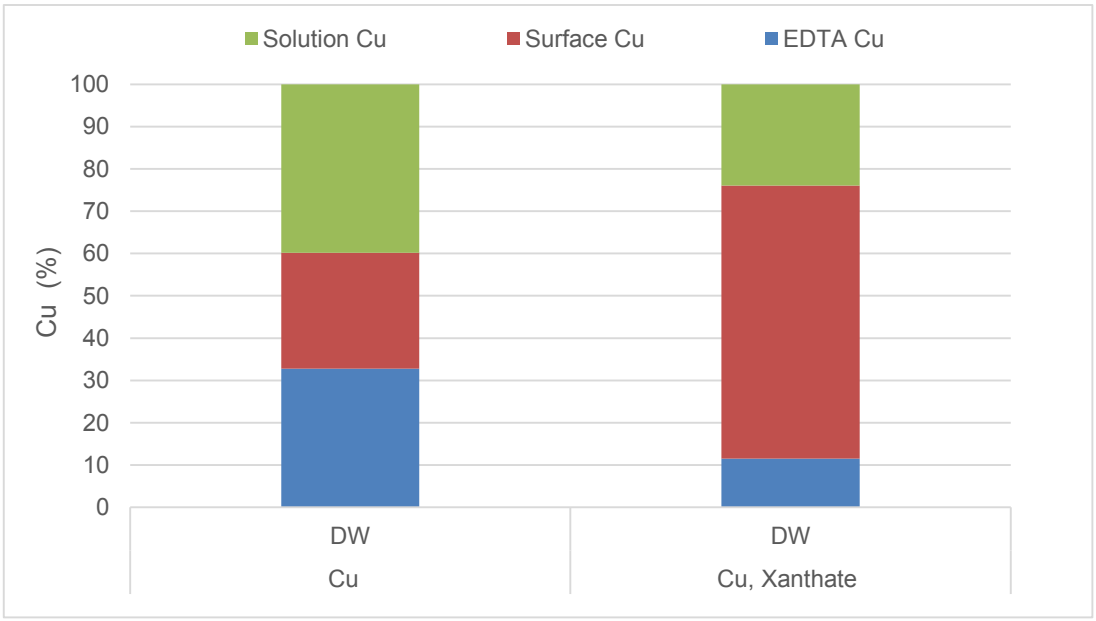

Figure 4.31: Talc copper analysis

Figure 4.31 shows the copper adsorbed onto the talc surface with and without xanthate. Contrary to the Merensky ore and UG2 ore residual copper analysis, there was more copper in solution for the talc tests as evidenced by the green bars. Unexpectedly, relatively large amounts of surface-reacted copper was present on the talc surface. As with the UG2 ore and Merensky ore EDTA extractions, less copper hydroxide was found in the presence of xanthate as indicated by the blue bars. Figure 4.31 also shows the highest amount of chemically reacted copper on the mineral surface was when both copper and xanthate are present as shown by the red bars.

4.5 Summary of results

In summary, the froth stability tests showed the froth was most stable in the absence of activator or collector and least stable in the presence of both reagents. This trend was observed for both ore types and for the two water types – deionised water and synthetic plant water. The key findings from the tests conducted in this study are summarized below.

Copper Sulphate

The froth stability results showed the use of copper sulphate as an activator destabilised the froth for both Merensky and UG2 ores. Copper sulphate, however, did not change the floatability of talc and pyrrhotite as seen in the microflotation tests. However, there was clearly adsorption of copper onto the mineral surfaces as shown by the zeta potentials of the pure minerals, which shifted to more positive values when copper sulphate was added. In addition, no residual copper was found in solution, indicating copper adsorption onto the mineral surfaces for the UG2 and Merensky ores either as $Cu(OH)_2$ or as chemically reacted copper. The EDTA extraction experiments showed that the copper was present on the mineral surfaces - between 40 and 60% as $Cu(OH)_2$ and also between 40 and 60% as chemically reacted copper for both Merensky and UG2 ores. More residual copper was found in solution for talc, but there were still approximately equal amounts of $Cu(OH)_2$ and chemically reacted copper on the talc mineral surface for the condition with copper only.

Xanthate

The use of xanthate as a collector, in the absence of copper sulphate, resulted in a more destabilised froth in comparison to when only copper sulphate was used as an activator for both ores and for the two water types. From the microflotation work, xanthate slightly improved the floatability of pyrrhotite in synthetic plant water but not in deionised water. The floatability of talc was not changed by the presence of xanthate in both synthetic plant water and deionised water. The zeta potential of the pure minerals with no reagent addition was relatively similar to the zeta potential values obtained with xanthate added.

Copper sulphate and xanthate

The froth was least stable when both copper sulphate and xanthate were present for UG2 and Merensky ores both in deionised water and synthetic plant water. The microflotation tests showed the highest recoveries of pyrrhotite when both copper sulphate and xanthate were present. The same trend was observed from the microflotation tests using talc although the floatability of talc was improved to a lesser extent than pyrrhotite. Zeta potential was lower at more acidic pH's when both copper sulphate and xanthate were present on the mineral surface compared to when no reagents were present. At pH 9 however, since xanthate was added after copper sulphate activation, the zeta potential became more negative again indicating non-selective xanthate adsorption onto the minerals' surfaces. EDTA extraction experiments showed that there was less EDTA extractable copper and more chemically reacted copper present on the mineral surfaces when xanthate was present. This suggests that the xanthate was chemically reacting with copper on the mineral surface and anchoring it.

Water type

Deionised water yielded a more stable froth as evidenced by the higher dynamic froth stability factors obtained for all of the conditions investigated. Synthetic plant water had a depressant effect on flotation as evidenced by the lower recoveries obtained under all conditions for pyrrhotite when using synthetic plant water. Talc floatability was also slightly reduced in synthetic plant water for all of the conditions investigated. The water type did not appear to have an effect on the relative amounts

of EDTA extractable copper ($Cu(OH)_2$) or the chemically reacted surface copper on the Merensky and UG2 ore surfaces.

Merensky iron analysis

Iron hydroxides were found to be present on the Merensky ore mineral surfaces. The total iron (in solution and extracted by EDTA) was found to vary with each condition and it did not appear to follow any trend. For the two types of water investigated, more iron hydroxides were obtained in the absence of xanthate than when xanthate was present.

5 DISCUSSION

This chapter presents a discussion of the results shown in Chapter 4. The zeta potential results are analysed first to show the effect of reagents on the surface charge of the pure minerals investigated. The microflotation results are then discussed to investigate the effect of copper sulphate on floatability in the absence of the froth phase. The EDTA extraction results are then discussed in order to investigate the form of the products on the mineral surface. Lastly, all of the results on pulp phase activation are linked to the froth stability test results.

5.1 Zeta Potential Determinations

Zeta potential measurements were assumed to be indicative of the mineral surface charge. The differences in the mineral surface charge in the absence of additional reagents arise from the differences in the chemical structure of each mineral (Mhlanga et al., 2012).

In the case of sulphide minerals, the isoelectric point pH ($pH_{i.e.p}$) can be used as a good indication of the extent of sulphide surface coverage with metal hydroxide/oxides species or surface oxidation (Healy & Moignard, 1976). $Cu(OH)_2$ has an $pH_{i.e.p}$ of around 9.4 and above this pH, it is negatively charged (Parks, 1965). A low $pH_{i.e.p}$ value indicates the surface is lightly oxidised, but the $pH_{i.e.p}$ close to that of the corresponding metal hydroxide/oxide indicates that the surface is heavily oxidised (Fullston et al., 1999).

5.1.1 Effect of pH on zeta potential of pure minerals

Figure 4.18 which shows a sigmoid variation of the zeta potential of the pure minerals with increasing pH. For all of the minerals, the zeta potential generally decreased with increasing pH. Increasing pH decreased zeta potential due to the presence of more negative OH^- ions on the mineral surface whereas the increase in the amount of H^+ in acidic pH resulted in a more positive zeta potential.

Oxidation levels of pure sulphide minerals can be detected using zeta potential tests since it is known that some unoxidised sulphides have a $pH_{i.e.p}$ of about 2 (Acar & Somasundaran, 1992). A comparison of the $pH_{i.e.p}$ of the different minerals from literature and from this study are summarised in Table 5.1.

Table 5.1: Isoelectric points of the pure minerals

Mineral	Literature $pH_{i.e.p}$	Researcher	Measured $pH_{i.e.p}$
Talc	2.5 – 3	Burdukova, 2007	4.5
Chromite	5.6 – 7.2	Somasundaran & Wang, 2006	5.6
Plagioclase	5.6 – 6.4	Parsons, 2012	5.9
Pyrrhotite	6.5	Montalti, 1994	6.2

Table 5.1 shows the $pH_{i.e.p}$ for the minerals investigated in this study are similar to the ones obtained from previous findings with the exception of talc. The deviations in the $pH_{i.e.p}$ values for the talc could be due to several reasons. Firstly, the composition of the talc may be different coming from different sites. Secondly, there could be a variation in the concentration and type of background electrolytes used which could compress the electrical double layer to different extents. Also, $pH_{i.e.p}$ of silicate minerals (talc and plagioclase) is affected by crystal chemistry and selective leaching of metal cations or silica from the surface (Fuerstenau & Pradip, 2005). The pyrrhotite used in this study could have been oxidised to some extent bearing in mind that the $pH_{i.e.p}$ of $Fe(OH)_3$ is around 6.7 according to Smart at al. (1998).

5.1.2 Effect of copper sulphate on the zeta potential of pure minerals

For all of the minerals, there was no substantial change in zeta potential below ~pH 5 – 6 when compared to the conditions with no reagent addition as shown in Figure 4.23. This is in agreement with the findings of Fornasiero and Ralston (2005) and James and Healy (1972) who found no adsorption of copper species on metal oxide surfaces at acidic pH's. Thus, it appears that, below pH 5 – 6, no copper species were adsorbing onto the talc, chromite or plagioclase. In the case of pyrrhotite, Chang et al. (1954) found that at pH 5.1, there was a direct ion exchange of Cu^{2+} for Fe^{2+} in the crystal lattice of pyrrhotite. Thus, if Cu^{2+} exchanged for Fe^{2+} there would be no net change in surface charge, which is what was observed for pyrrhotite.

Figure 2.7 (Cu speciation diagram) shows that above pH 6 $Cu(OH)_2$ (s) is the predominant copper species. The zeta potential becomes less negative at this pH (Figure 4.23), indicating precipitation or adsorption of the neutral molecule, $Cu(OH)_2$, which shields the minerals' negative charge. The addition of copper species shifts the zeta potentials from between -48 mV to -63 mV to between -19 mV to -30 mV at

pH 9. The $pH_{i.e.p}$ of $Cu(OH)_2$ is 9.4 which reinforces the assumption that copper adsorbs on all the minerals in the form of $Cu(OH)_2$ above pH 6. This was evidenced by the shift in the $pH_{i.e.p}$ of all of the minerals to higher values with the exception of talc.

The shift in the zeta potential of pure minerals above pH 6 shown in Figure 4.23 suggests inadvertent activation of the minerals as the activation by copper is non-selective. This is similar to the findings by Martinovic and co-workers (2005) in their studies on surface properties of gangue minerals in PGM bearing ores. Ekmekçi et al. (2006) proposed the nature of the adsorption of copper species was likely to be electrostatic.

Wesseldijk et al. (1999) showed that chromite can be activated by the typical platinum concentrator reagent suite and that the copper species adsorbed on the chromite surface at alkaline pH values was $CuOH^+$ which was formed in solution. Positively charged complexes such as $Cu(OH)^+$ could contribute to the less negative zeta potential observed when the pH is increased. This means that the minerals are most likely to be covered in copper hydroxides in alkaline conditions. The presence and amounts of copper hydroxides on the mineral surfaces were further investigated using the EDTA extraction method in this study. The EDTA extraction tests showed in addition to copper hydroxide species, chemically reacted copper species were also present on the mineral surfaces indicating that some of the copper hydroxide species formed at pH 9 may have been reduced on the mineral surface. This will be discussed in more detail in section 5.3.

5.1.3 Effect of xanthate on the zeta potential of pure minerals

When only xanthate was added, the zeta potentials of the minerals in alkaline conditions did not change significantly. This could be due to the mineral surfaces being negatively charged as a result of the adsorption of OH^- ions which reduces xanthate adsorption.

Xanthate addition slightly changed the surface charge of chromite, an oxide mineral. This probably means that little xanthate adsorbed onto the chromite surface in the absence of copper sulphate. There was a slight decrease in zeta potential for interaction of xanthate with pyrrhotite which is similar to the findings by Montalti

(1994) that low concentrations of xanthate did not affect pyrrhotite surface charge. Copper sulphate however is thus expected to enhance the floatability of pyrrhotite to some extent because of its interaction with the base metal sulphides which could be an ion exchange reaction with the lattice Fe or an electrochemical reaction on the mineral surface. For the silicate minerals – talc and plagioclase, the addition of xanthate slightly altered the zeta potentials of the minerals at alkaline conditions perhaps indicative of adsorption of a small amount of xanthate although it has been found previously that xanthate collectors do not exhibit any affinity for siliceous minerals before activation (Malysiak et al., 2004).

5.1.4 Effect of copper sulphate and xanthate on the zeta potential of pure minerals

It was already shown that copper adsorbs onto all the minerals above ~pH 6 making the surface more positively charged. Adsorption of the negatively charged xanthate neutralises the more positive copper species and brings the zeta potential back to similar values as those in the absence of reagents. Fornasiero and Ralston (2005) saw similar results for quartz activated with copper and nickel and using xanthate as a collector.

Overall, it can be seen from Figure 4.24 that the zeta potential of all of the four minerals does not change significantly when both copper sulphate and xanthate are added when compared to the condition with no reagents. The zeta potential of the minerals without xanthate addition was between -48 mV and -63 mV. With xanthate addition after activation of the minerals with copper sulphate, the range of zeta potential was between -48 mV and -72 mV. This is in contrast to the change in zeta potential when only copper sulphate was added as seen in Figure 4.23 which resulted in zeta potential values between -19 mV and -28 mV. Since the addition of xanthate to copper sulphate activated minerals did not significantly change the zeta potential, it is expected that the surface hydrophobicity of the particles becomes the dominant factor affecting bubble-particle attachment rather than particle charge.

5.2 Microflotation Tests

The degree of surface oxidation determines particle hydrophobicity or hydrophilicity hence the selectivity and recovery in the processing of sulphide ores (Shackleton et

al., 2007). Since the experiments were conducted at pH 9, the activation species are expected to be $Cu(OH)_2$ which could have an effect on the particle hydrophobicity and the amount of solids reporting to the froth phase. In the preceding section of this discussion chapter, adsorption of copper species at pH 9 was confirmed by the zeta potential measurements. In the presence of collector, a more hydrophobic copper xanthate species is expected to form on the mineral surface increasing the contact angle and hence the recovery of the particles through increased particle hydrophobicity.

5.2.1 Talc floatability

Talc is a naturally hydrophobic mineral and the reagents (copper sulphate and xanthate) were added to investigate their effect on the mineral's floatability. The results showed the addition of reagents did not substantially change the floatability of talc as shown in Figure 4.12 and Figure 4.13 in both deionised water and synthetic plant water. This is despite the fact that the zeta potential tests showed that copper (and copper and xanthate) adsorb onto the talc surface in alkaline conditions. In addition, Martinovic et al. (2005) suggested that relatively stable copper xanthate complexes are formed on gangue minerals and Malysiak (2004), using zeta potential and ToF-SIMS measurements, found pyroxene and feldspar (siliceous gangue minerals in Merensky ore), were coated by copper species at pH 9. This observation was also confirmed by the EDTA extraction tests on talc discussed later in this chapter.

Thus, the floatability of talc was largely unaltered despite the adsorption of copper and copper with xanthate on the talc surface. It was expected that the floatability of the talc may decrease due to non-selective precipitation of copper hydroxide precipitates at pH 9. The fact that this did not occur may mean that the copper did not react with the talc hydrophobic basal planes but with the already hydrophilic edges (Burdukova et al., 2008).

Talc floated at all of the conditions investigated, therefore, a significant amount of talc is thus expected to report to the froth phase during froth stability tests, since no depressant was used in this study to reduce talc floatability. A froth stabilising effect of particles was observed as seen in the results section and this is addressed later in this chapter.

Talc was slightly depressed in synthetic plant water meaning the overall floatability was reduced as shown in Figure 4.14. The lower floatability observed in synthetic plant water may be due to hydrophilic metal hydroxides which could have formed on the mineral surfaces which render the pure minerals hydrophilic hence reducing floatability.

5.2.3 Pyrrhotite floatability

The floatability of pyrrhotite was not enhanced by the addition of xanthate in deionised water as seen in Figure 4.15. This was not expected since iron sulphides are generally known to have good floatabilities with xanthates as collectors (Wang et al., 1989). Oxidation products on the surfaces of minerals could influence the floatability as collector adsorption is affected by the extent of oxidation. The $pH_{i.e.p}$ of 6.2 obtained in this study suggested possible oxidation of the mineral although the pyrrhotite was treated and stored prior to experiments to reduce oxidation. The pyrrhotite $pH_{i.e.p}$ of 6.2 is close to that of $Fe(OH)_3$ found to be around 6.7 by Smart et al. (1998). Montalti (1994) found the $pH_{i.e.p}$ of pyrrhotite to be 6.5 which is close to a value found in this study. The presence of iron hydroxides on the mineral surfaces could retard collector adsorption as well as pyrrhotite floatability.

Copper has been found to promote collectorless flotation in acidic conditions but not in alkaline conditions (Wang et al., 1989). The results in Figure 4.15 are in agreement with these findings since at pH 9 the addition of copper sulphate did not significantly change the floatability of pyrrhotite. The floatability of pyrrhotite was only increased when xanthate was added after copper activation. The copper activation of the pyrrhotite surface resulted in anchor points for xanthate adsorption to the mineral surface and the formation of hydrophobic copper-xanthate species on the pyrrhotite surface.

Similarly to the talc microflotation results, synthetic plant water depressed pyrrhotite flotation compared to deionised water (Figure 4.17). Cations in synthetic plant water have been found to adsorb onto the mineral surfaces. Ikumapayi (2013) found the recoveries of chalcopyrite, galena and sphalerite to be lower in process water than in deionised water at pH 9. Muzenda (2010) found process water to reduce the concentrate recovery and mass pull while tap/potable water increased these two parameters. It is speculated that the decrease in the floatability of pyrrhotite in

synthetic plant water is due to the adsorption of metal hydroxide complexes onto the mineral surfaces.

Similar to the flotation of pyrrhotite in deionised water, addition of copper sulphate did not enhance recovery in synthetic plant water. However, the addition of xanthate, without copper sulphate, resulted in increased recovery of pyrrhotite as seen in Figure 4.16. In synthetic plant water, the charged ions would adsorb onto the pyrrhotite surface, activating the surface and providing anchor points for xanthate adsorption in much the same way that copper activation does. However, copper species are clearly better activators than the species present in synthetic plant water, since the addition of copper(II) prior to xanthate addition in synthetic plant water resulted in a large increase in pyrrhotite recovery.

As seen from the zeta potential measurements, the surface charge was not significantly altered in the presence of both copper sulphate and xanthate. This suggests the main driver for particle-bubble attachment and enhancement in the floatability of pyrrhotite was the hydrophobicity of the copper-xanthate species formed on the mineral surface as opposed to the surface charge.

Some researchers claim copper activation is not possible at high pH's since copper ions are essentially insoluble in alkaline solution and thus not available for reaction (Buswell & Nicol, 2002). Contrary to these observations, the highest recovery of pyrrhotite was observed in both synthetic plant water and deionised water only with the addition of copper(II) prior to xanthate addition at pH 9. This confirms activation of the pyrrhotite in alkaline conditions and this could be due to the conversion of hydrophilic $Cu(OH)_2$ to copper-xanthate species.

5.3 Activation products analysis

In this study, it was hypothesised that the surface copper species would differ between the Merensky ore and UG2 ore due to the differences in mineralogy between the two ore types. It was hypothesised that, since the Merensky ore has a relatively high grade of sulphide minerals present, the copper(II) species would be reduced on the sulphide mineral surfaces to a chemically reacted copper(I) species. In contrast, the UG2 ore has almost no sulphide minerals present and, therefore,

there would be non-selective precipitation of copper hydroxide on the particle surfaces.

The EDTA extraction method was used to detect metal hydroxyl species on the mineral surfaces and the presence of copper and iron species was determined analytically using Atomic Absorption Spectroscopy. It was assumed the copper hydroxides were not susceptible to photo-reduction in the sample preparation for these tests.

5.3.1 Merensky and UG2 ore copper analysis

The Merensky ore had a relatively large percentage of copper hydroxide on the mineral surface (between 53 and 59%) compared to the chemically reacted copper (40 – 44%) as shown in Figure 4.25. Chemically reacted copper has been found by Malysiak (2003) in the interaction between copper (II) ions in solution and pentlandite surfaces. This involves charge transfer as opposed to an electrostatic attraction between opposite charges. Figure 5.1 shows how Cu(II) ion oxidises the sulphur of the mineral and it is itself reduced to Cu(I).

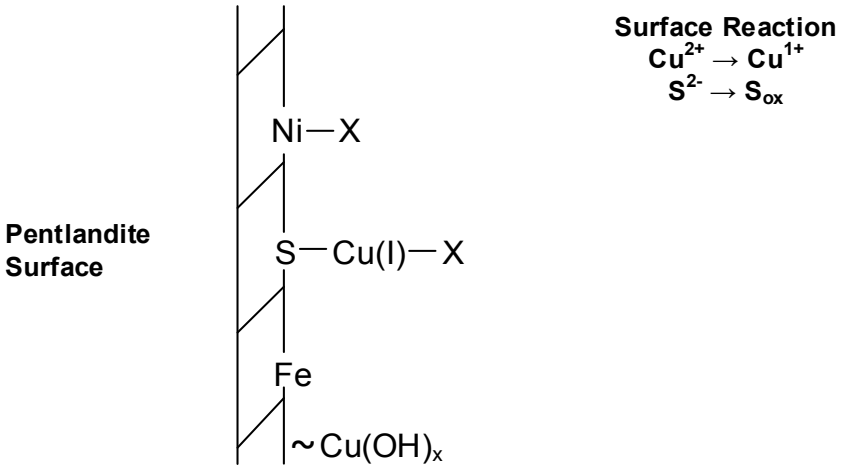

Figure 5.1: Schematic representation of copper ion and xanthate adsorption onto a pentlandite surface. Adapted from (Malysiak 2003; Shackleton et al. 2003) where ─ denotes strong bond and ~ denotes weak bond.

Previous evidence for the presence of copper hydroxide on sulphide mineral surfaces comes from Gerson et al. (1999). These authors conducted secondary ion mass spectrometry (SIMS) to determine the lateral distribution of copper on individual sphalerite particle surfaces and their work confirmed the formation of colloidal $Cu(OH)_2$ (s) on the sphalerite surface after conditioning with copper nitrate

at pH 8.5. A similar reaction of the sulphide minerals in the Merensky ore with copper sulphate at pH 9 may have occurred instead of the bulk of the copper being electrochemically reduced on the mineral surface as expected.

Figure 4.25 shows the percentage of copper in the bulk solution was very low since most of the copper added to the system was either chemically reacted on the Merensky ore surfaces or extracted in the form of copper hydroxides. Some of the chemically reacted copper on the mineral surfaces might have migrated into the lattice of the Merensky ore minerals. The studies by Prestige et al. (1994) suggested that copper ions were mobile, migrating through the sphalerite lattice. Buckley et al. (1989) also showed the presence of copper several layers below the surface of pyrrhotite. The low concentration of copper ions in solution could be an indication of minimal leaching out of copper from the surface layers of minerals.

Figure 4.28 showed that about half the surface copper on the UG2 ore was chemically reacted copper. The formation of chemically reacted copper on the UG2 ore surface was unexpected as the amount of base metal sulphides in the ore are much lower than in Merensky ore. Thus, the copper species must have reacted with oxide minerals in the UG2 ore in order to remain bound to the surface. The fact that chemically reacted copper was also found on the talc mineral surface (Figure 4.31) is further evidence of the possibility of this reaction occurring.

There is evidence in literature of metal ions chemically reacting with non-sulphide minerals. Al-Abadleh and Grassian (2003) reported that it is possible for lead ions to occupy calcium sites in a calcite ($CaCO_3$) surface atomic layer. Mackenzie and O'Brien (1969) confirmed the adsorption of nickel and cobalt ions from aqueous solution onto the quartz (oxide mineral) surface using zeta potential measurements. Nagaraj and Brinen (1996), with the use of XPS, found that Cu(I) rather than Cu(II) was present on copper activated pyroxene (a silicate mineral) after collector treatment. Shackleton et al. (2003) using ToF-SIMS analysis in addition to XPS and zeta potential findings also confirmed copper activation of pyroxene and true flotation of the mineral in the presence of xanthate (via microflotation tests). The formation of Cu(I)-X complexes on the activated silicate mineral surfaces is illustrated in Figure 5.2.

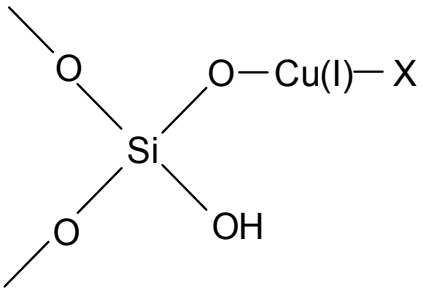

Figure 5.2: Schematic representation of xanthate adsorption onto a copper activated silicate mineral. Adapted from (Malysiak, 2003)

The formation of chemically reacted copper on the UG2 ore surface is also expected to promote the adsorption of xanthate which may increase the particle hydrophobicity. This may then reduce the froth stability due to an increase in contact angle beyond the optimum angle to confer stability.

For both Merensky and UG2 ores, the amount of EDTA extractable copper decreased when xanthate was present both in deionised water and synthetic plant water as shown in Figure 4.29. This could be due to adsorption of copper onto the mineral surfaces and attachment of xanthate onto these sites resulting in stable copper xanthate complexes on the mineral surface, which were not extractable by EDTA. The copper hydroxide species are known to act as sites for collector adsorption (Fornasiero & Ralston, 2005). This would result in better floatability in the presence of xanthate since more collector molecules preferentially adsorb onto the copper sites on the mineral surface increasing the hydrophobicity as observed in Figure 4.16 for pyrrhotite flotation. However, in some instances for example when the copper sulphate concentration is high, copper hydroxide may precipitate on the mineral surface and impart hydrophilic characteristics in the particles which reduces their floatability.

5.3.2 Merensky ore iron analysis

From Figure 4.26, it can be seen the total iron (solution and EDTA extractable) varies significantly for all of the conditions investigated. According to the ion exchange mechanism, the amount of iron in solution when copper sulphate is added is expected to be higher than the iron obtained for the conditions with no copper due to displacement of lattice Fe which increases the amount of iron in the bulk solution. In the absence of copper sulphate, the iron extracted is due to leaching of Fe ions

from the Merensky ore. The data therefore does not support the ion exchange activation mechanism of sulphides since the iron obtained in both deionised and synthetic plant water when both copper sulphate and xanthate were present was lower than the iron for the condition with xanthate only. The adsorption mechanism is thus proposed to be electrochemical on the sulphide sites.

The total amount of EDTA extractable iron is shown in Figure 4.27. Iron hydroxides are hydrophilic and should reduce the mineral particle hydrophobicity. Microflotation tests show that the recovery of pyrrhotite was higher in deionised water than in synthetic plant water (Figure 4.17). Although the amount of iron hydroxides formed on the Merensky surfaces was higher in deionised water than in synthetic plant water, a reduction in the floatability of pyrrhotite was not observed in deionised water as expected due to increased hydrophilicity. In the presence of xanthate, the iron hydroxides could have caused inadvertent activation of the mineral surfaces improving the recovery of pyrrhotite.

The presence of both copper sulphate and xanthate also resulted in a decrease in the amount of iron hydroxides extractable as seen with the reduced copper hydroxide extracted from the ore surfaces in the presence of xanthate. Again, this is evidence of the collector molecules forming stable species with the iron hydroxides which act as sites for collector adsorption.

Hydrophilic iron hydroxides and colloidal metallic iron produced when mild steel is used for milling Merensky ore as opposed to stainless steel could affect the froth in two different ways. Iron hydroxides could either stabilise the froth by optimising froth mineralisation or reduce the froth stability by coating mineral surfaces and lowering their floatability (Ekmekçi et al., 2006). The presence of ferric hydroxides on the mineral surfaces could also have a negative effect on the froth stability as this could result in less froth stabilising particles being are recovered from the pulp phase to the froth phase.

5.3.3 Talc copper analysis

The talc copper analysis results in Figure 4.31 showed the presence of copper hydroxide on the talc surface in the presence or absence of xanthate. There is less copper hydroxide obtained in the presence of xanthate which is the same result

obtained for the Merensky and UG2 ores. This was also possibly due to formation of more stable copper-xanthate species which are not easily extractible by EDTA. There is a significant amount of chemically reacted copper on the talc surface in the presence of xanthate. This is unusual since talc, a silicate gangue mineral is not expected to chemically react with copper and to form stable complexes. This has already been addressed in section 5.3.1.

Although chemically reacted copper was found on the talc surface, an increase in the hydrophobicity of the talc was however not observed from the microflotation tests on talc with both copper sulphate and xanthate present. This could be due the fact that talc is naturally hydrophobic and its floatability was not significantly changed with the addition of reagents. The zeta potential tests in Figure 4.19 also showed no significant change in the surface charge when both copper sulphate and xanthate were added to talc. A significant shift in the zeta potential was however observed when only copper sulphate was added which is indicative of copper adsorption onto the mineral surface.

5.4 Froth Stability Tests

An attempt is made in this section of the dissertation to link the key findings from the pulp phase tests to the froth phase. Two parameters with respect to particles were found to be applicable to explain changes in froth stability. These were particle hydrophobicity and the amount of particles reporting to the froth phase. Tsatouhas et al. (2006) observed that the froth stability decreased down the flotation bank and that the froth from the rougher cells was more stable than the scavenger cells. These authors linked the froth stability to the amount of particles in the froth. The rougher cell froth was stabilised due to the presence of more particles reporting to the froth phase than in the scavenger cells.

The same trend of decreasing froth stability with addition of copper sulphate, xanthate and both copper sulphate and xanthate was observed for the two ores investigated in deionised water and synthetic plant water. It is assumed this is due to the increase in hydrophobicity of the complexes formed as a result of pulp phase interactions. Based on the microflotation results discussed earlier, the increase in hydrophobicity of the complexes formed is proposed below:

Mineral < Mineral-Cu < Mineral-Xanthate < Mineral-Cu-Xanthate

It is assumed that the decrease in the froth stability as a result of the addition of reagents is due to an increase in contact angle and increasing hydrophobicity which promotes thinning of films and coalescence of bubbles. The froth is destabilised by increasing the contact angle beyond an optimum angle to confer stability on the froth. This relationship was shown by Johansson and Pugh (1992) and it is illustrated in Figure 5.3.

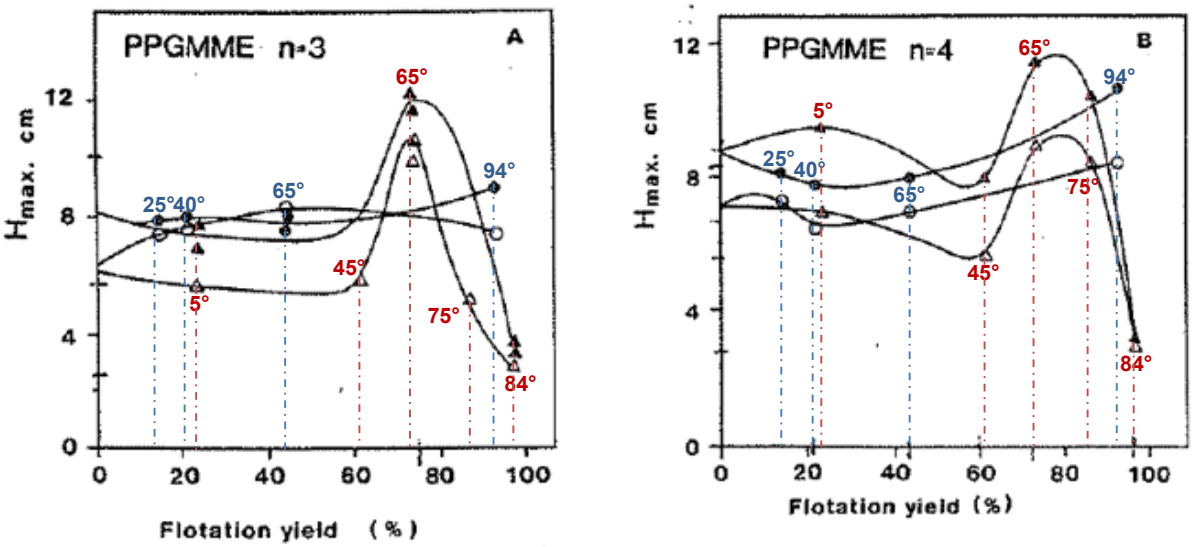

Figure 5.3: Relationship between maximum froth height (H_{max}) versus hydrophobicity (flotation yield) of quartz particles using polyglycol frothers; △ -26 – 44 µm size fraction, 20 mg/L froth concentration; ▲ -26 – 44 µm size fraction, 50 mg/L froth concentration; ○ -74 – 106 µm size fraction, 20 mg/L froth concentration; ● -74 – 106 µm size fraction, 50 mg/L froth concentration (Johansson & Pugh, 1992).

In these studies, Johansson and Pugh (1992) used quartz particles from two size fractions with varying hydrophobicity. A contact angle of 65° was found to yield the maximum froth stability for the finer size fraction (-26 – 44 µm) and more hydrophobic particles were found to destabilise the froth. These effects were not pronounced for the larger size fraction (-74 – 106 µm).

Based on the particle size distributions of the two ores used in this study, sixty percent of the particles were less than 75 µm in size meaning most of the particles were of small to medium size. The destabilisation effects of the froth observed could be due to increase in the contact angle beyond an optimum maximum, in this case the optimum point being the condition when no reagents are added.

5.4.1 Copper sulphate effect on froth stability

The addition of copper sulphate to both Merensky and UG2 ores destabilised the froth. This was most pronounced for Merensky ore in deionised water and UG2 ore in synthetic plant water. It was hypothesized that the destabilisation of froth with the addition of copper sulphate to Merensky ore was due to the increase in the hydrophobicity of particles which would accelerate coalescence of bubbles. It has been shown that an increase in hydrophobicity beyond an optimum point can decrease the stability of froth due to an increase in bubble coalescence (Aveyard et al., 1994; Johansson & Pugh, 1992) due to possible formation of a more hydrophobic copper(I) sulphide species.

The shift in zeta potential of the minerals to more positive values showed that copper was adsorbed onto the pure mineral surfaces. The EDTA extraction results in Figure 4.30 showed that more than 40% of the copper on the Merensky ore mineral surfaces was in the form of chemically reacted copper. The chemically reacted copper was presumably in the form of Cu(I) and this was expected to have a higher hydrophobicity than the unreacted mineral. The microflotation tests did not support this however since the floatability of pyrrhotite was not improved by copper sulphate activation. This suggests the main factor affecting froth stability could be the decrease in the amount of particles in the froth phase rather than particle hydrophobicity. Copper hydroxide species on the mineral surfaces could have depressed pyrrhotite reducing its floatability which could be similar to what was observed in microflotation tests using synthetic plant water (explained below).

The microflotation tests showed the synthetic plant water reduced the amount of solids reporting to the concentrate since R_{max} was reduced for pyrrhotite (Figure 4.17). Synthetic plant water also resulted in a reduced froth stability. Thus, it is postulated that the addition of copper sulphate may have the same effect on both Merensky and UG2 ores. The addition of copper sulphate in the absence of xanthate reduced the amount of hydrophobic froth stabilising particles reporting to the froth phase. This is in agreement with the findings by Moolman et al. (1995) that the addition of copper sulphate reduced the solids concentration in the froth phase which resulted in a reduction in the froth stability.

5.4.2 Xanthate effect on froth stability

The addition of only xanthate generally destabilised the froth further than when only copper sulphate was added for both Merensky and UG2 ores. This could be due to the formation of the mineral-xanthate complex which could be more hydrophobic than the copper(I) sulphide. The microflotation results for pyrrhotite in the presence of xanthate in synthetic plant water (Figure 4.16) showed an increase in the hydrophobicity and hence the recovery of pyrrhotite. The increase in contact angle and hydrophobicity may have contributed to the destabilisation effect shown with the addition of only xanthate.

The froth stability results however also showed for Merensky ore in synthetic plant water (Figure 4.5) and UG2 ore in deionised water (Figure 4.6) there was a slight decrease in froth stability with the addition of xanthate. No enhancement in the hydrophobicity of talc was observed in both deionised and synthetic plant water. Since the addition of xanthate to talc did not enhance its floatability, it is expected that similar amounts of talc report to the froth phase (for the condition with no reagents and the condition with xanthate only) and this results in similar froth stabilising effects by talc for the two conditions.

5.4.3 Copper sulphate and xanthate effect on froth stability

In general, the addition of both copper sulphate and xanthate to both Merensky and UG2 ores resulted in the most destabilised froth. This was the case for both deionised water and synthetic plant water. The hydrophobic Cu(I)-X species formed on the mineral surfaces may have further decreased the froth stability. As shown in the microflotation tests, pyrrhotite exhibited maximum recovery in the presence of both copper sulphate and xanthate. The EDTA extraction tests for both Merensky and UG2 ores showed that there was less EDTA extractable copper present after addition of xanthate which showed that the copper was “fixed” by the xanthate, presumably in the form of Cu(I)-X.

Increasing the copper sulphate concentration from 90 g/tonne to 120 g/tonne whilst maintaining the same xanthate dosage of 80 g/tonne was found to destabilise the froth (Figure 4.4). At 90 g/tonne of copper sulphate, the froth was more stabilised than at 120 g/tonne due to less collector molecules forming relatively stable

hydrophobic bonds with the copper sites on the mineral surface. When the copper sulphate concentration was increased to 120 g/tonne, it is speculated more sites became available for collector adsorption which increased the hydrophobicity of the particles. This increased hydrophobicity caused by Cu(I)-X on the mineral surface could have destabilised the froth.

5.4.4 The effect of water type on froth stability

The effect of water type on froth stability of Merensky and UG2 ores is shown in Figure 4.8 and Figure 4.9 respectively. The froth was more stable in deionised water than in synthetic plant water. The calcium content is considerably higher in synthetic plant water than deionised water as shown in Table 3.2 to Table 3.4 in the experimental section of this dissertation. Parsonage (1984) found that calcium sulphate reduced floatability of the desired minerals because it formed slime coatings on the sulphide minerals at alkaline pH's. The reduction in the floatability of particles may have resulted in less froth stabilising particles reporting to the froth phase due to a decrease in hydrophobicity.

Ions in synthetic plant water such as calcium and magnesium have also been found to promote heterocoagulation of particles which increases the size of the particles reporting to the froth phase which has an effect on froth stability (Parsonage, 1984). Froth stability has been found to decrease with increasing particle size (Flynn & Woodburn, 1987; Pugh, 2005; Aktas et al., 2008). The reduction in froth stability observed for the two ores with synthetic plant water could be due to an increase in particle size as a result of particle coagulation.

The synthetic plant water used in this study had a calcium content of about 137 ppm for Merensky ore and 105 ppm for UG2 ore (taking into account dissolution of ions from the mineral surfaces into solution). The combined effect of the ions in the synthetic plant water could contribute to the reduced floatability of talc as a consequence of reduced hydrophobicity. On the contrary, the ToF-SIMS and XPS data in the studies by Shackleton (2007) suggested the ions found in synthetic plant water were not strongly adsorbed to mineral surfaces. Shackleton (2007) showed increasing calcium concentration from 80 ppm to 500 ppm did not affect the flotation response of a merenskyite (platinum containing mineral) sample.

These findings can be linked to the microflotation results obtained for talc and pyrrhotite where the recoveries were higher in deionised water than in synthetic plant water. Ions in synthetic plant water were found to depress the floatability of pyrrhotite to a larger extent than talc. Pugh (2005) showed that the dynamic and static froth stability increased with increased particle concentration. Froth stability is expected to decrease because of a decrease in particle concentration resulting in less froth stabilising particles which prevent bubble coalescence. The decrease in froth stability of a Merensky and/or UG2 ore in synthetic plant water could be related to a decrease in the amount of floatable minerals reporting to the froth phase.

5.4.5 Particle effects on froth stability

Particles had a froth stabilising effect as seen in Figure 4.1 and Figure 4.2. The higher froth stability observed for Merensky ore could be due to more floatable sulphides in the ore with an optimum hydrophobicity to stabilise the froth.

The stabilisation of froth by solid particles has been well established and linked to an increase in surface viscosity of films (Subrahmanyam & Forssberg, 1988). In a review on the factors affecting froth stability in mineral processing, Farrokhpay (2011) suggested that froth stability is mainly governed by particles, rather than surfactant molecules. Particle stabilisation has been attributed to creation of a stearic barrier preventing coalescence (Hunter et al., 2008).

Johansson and Pugh (1992) investigated the effect of quartz particles hydrophobicity on mineralised froths using polyglycol frothers. As seen in Figure 5.4, the addition of particles within the particle size range 22 – 44 μm increased the dynamic froth stability factor throughout the range of frother concentration. These results are consistent with the findings of this study since a polyglycol frother was used in this study.

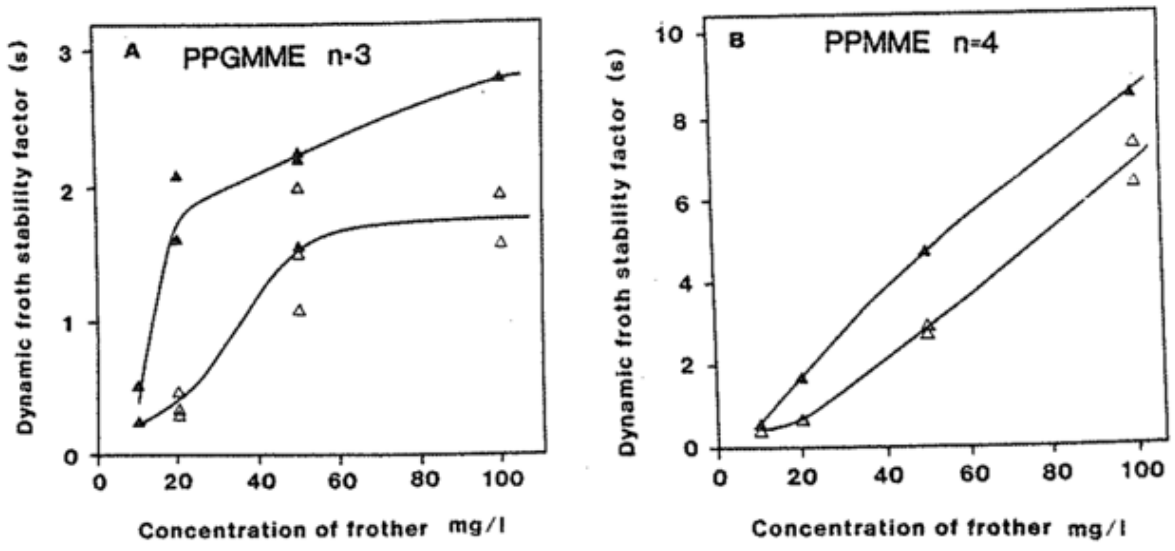

Figure 5.4: The relationship between the dynamic froth stability factor (Σ) and frother concentration where △ represents experiments without particles and ▲ represents experiments with 22-44 µm size quartz particles with a contact angle of 65° (Johansson & Pugh, 1992).

According to Figure 4.11, the froth is also more stabilised in Merensky ore than UG2 ore for all of the conditions expect for when no reagents are added. The base metal sulphides in Merensky ore could have formed hydrophobic species with copper sulphate and xanthate which stabilise the froth to a certain degree more than the UG2 ore particles. Ore mineralogy data shows Merensky ore has a higher talc content than UG2 ore. Since no depressant was used in this study, higher froth stabilities observed for Merensky ore could be due to the naturally hydrophobic talc increasing the recovery of other minerals to the froth phase which could confer additional stability.

5.5 Summary of discussion

Copper sulphate

The addition of copper sulphate to Merensky and UG2 ores destabilised the froth for both ores but because of different reasons. For the Merensky ore, it was expected for the destabilisation of froth to be due to formation of hydrophobic Cu(I) sulphide species on the mineral surfaces which would increase the contact angle and result in an increase in bubble coalescence. However, an increase in floatability of pyrrhotite in synthetic plant water was not observed from the microflotation tests. The zeta potential tests showed adsorption of copper onto the mineral surfaces and there was $Cu(OH)_2$ present on the mineral surfaces as evidenced by the EDTA tests. The

copper hydroxides could be suppressing the floatability of minerals resulting in less froth stabilising particles reporting to the froth phase.

The zeta potential results showed the addition of copper sulphate in the absence of xanthate, resulted in less negative zeta potential values for all of the minerals which is indicative of non-selective adsorption of copper onto the mineral surfaces. The $pH_{i.e.p}$ of chromite, pyrrhotite and plagioclase shifted closer to the $pH_{i.e.p}$ of $Cu(OH)_2$ suggesting formation of the copper hydroxyl species on the mineral surfaces.

From the EDTA extraction tests, the small amounts of copper left in solution for both Merensky and UG2 ores suggests the copper-containing minerals in these ores did not dissolve to form Cu(II) ions in the bulk solution. The EDTA results showed adsorption of copper chemically onto the UG2 mineral surfaces and this is first time this has been shown for a UG2 ore. Oxide minerals have been shown to form chemically reacted species with copper from previous studies. However, the higher froth stabilities observed for Merensky ore for most of the conditions investigated could be due more floatable sulphides in the ore which stabilise the froth more than activated oxide minerals found in UG2 ore.

The analysis of the residual solution for iron after copper activation did not support the ion exchange mechanism for copper activation. This is due to the inconsistencies in the amounts of iron obtained in solution. Fe ions were expected to increase in the bulk solution if they were exchanged with solution Cu ions but this was not found to occur.

Xanthate

The addition of xanthate resulted in more destabilised froth than the condition with only copper sulphate addition for both the Merensky and UG2 ores. This was attributed to the increase in hydrophobicity of the complex formed on the mineral surfaces. The zeta potentials of the pure minerals (talc and plagioclase) were slightly altered with the addition of xanthate possibly indicating some adsorption. The floatability of talc was not changed with the addition of xanthate as shown by the microflotation tests although the zeta potential tests suggested adsorption of xanthate onto the talc surfaces. Higher recoveries of pyrrhotite were only obtained in

synthetic plant water suggesting that the ions in the synthetic plant water could have increased sites for collector adsorption on the pyrrhotite surfaces.

The increase in hydrophobicity increases the contact angle which in turn results in an increase in bubble coalescence which was observed with the addition of xanthate as a collector to the two ores. The destabilisation of froth with the addition of xanthate was not pronounced for Merensky ore in synthetic plant water and UG2 ore in deionised water.

Copper sulphate and xanthate

The most destabilised froth was observed for the condition with both copper sulphate and xanthate present for both ores. The zeta potential test showed the addition of xanthate after copper activation of the minerals made the zeta potential more negative, which is indicative of xanthate adsorption after copper activation. The floatability of talc was not changed significantly with the addition of both copper sulphate and xanthate. However, talc is very naturally hydrophobic and it is possible that reagent addition has no further effect on hydrophobicity. Pyrrhotite floatability was highest in the presence of these two reagents. It presumed the addition of xanthate to copper activated sulphides in the Merensky ore increased the hydrophobicity and contact angle of particles. The films thin faster due to increased contact angle resulting in the observed decrease in froth stability.

The analysis of the mineral surface products using the EDTA extraction method revealed there was less $Cu(OH)_2$ on the mineral surfaces in the presence of both copper sulphate and xanthate than when only copper sulphate was present. This was evidence of xanthate forming stable complexes with the copper since minimal copper was left in the bulk solution. Besides the formation of copper xanthate species via $Cu(OH)_2$ reduction, significant amounts of chemically reacted copper were found on both ores. This was unexpected for the UG2 ore since the sulphide content of the ore is very low. Earlier findings in literature have shown that oxide and silicate minerals can react chemically with copper which explains the presence of chemically reacted copper on UG2 surfaces. This chemically reacted copper on the UG2 ore surfaces is also expected to react with xanthate resulting in the formation of the hydrophobic copper(I)-xanthate species resulting in the destabilisation of froth observed.

Water Type

It was assumed that the cations in synthetic plant water adsorb onto the mineral surfaces reducing the surface charge in the same way that copper reduced the surface charge in the zeta potential tests. A decrease in the floatability of the minerals was attributed to the precipitation of metal hydroxides on the mineral surfaces which reduced the hydrophobicity and hence floatability. Iron hydroxides were also found to be present on the Merensky ore surfaces. The reduction in floatability of minerals as a result of non-selective metal hydroxide precipitation was linked to the reduction in froth stability of the two ores when synthetic plant water was used.

The destabilisation of froth with the use of synthetic plant water could be related to the decrease in particle concentration in the froth phase due to inhibition of activation due to metal hydroxide precipitates on mineral surfaces which reduces floatability.

6 CONCLUSIONS

6.1 Conclusions

The main findings from the test work performed in this study are summarised in this chapter. The contribution of this research is to provide a better understanding of the effect of copper sulphate activation on the froth phase in the flotation of Merensky and UG2 ores. Each of the key questions posed in the first chapter (section 1.3) of this dissertation is addressed and conclusions drawn from this study are given, followed by recommendations for future work. The four key questions are presented as headings for subsections 6.1.1 to 6.1.4 to properly frame the responses.

6.1.1 Is there a difference in the effect of copper sulphate on the froth stability of a Merensky ore and a UG2 ore?

From the preceding findings it is evident that froth stability is dependent on the particle properties such as particle concentration and particle hydrophobicity. These factors were found to be directly linked to activation by copper sulphate.

At the commencement of this investigation, based on previous publications, it was hypothesised that Merensky ore froth would be destabilised due to the formation of Cu(I) on the base metal sulphide surfaces resulting in the formation of hydrophobic copper-xanthate species which increase the contact angle and promote bubble coalescence. The results showed the Merensky ore froth was not destabilised to a large extent with the addition of copper sulphate although chemically reacted copper species were found on the surface of Merensky ore. The base metal sulphides were rendered more hydrophobic as shown by the microflotation tests for pyrrhotite in synthetic plant water. The increased hydrophobicity was either at or below the optimum range for good froth stability (~65°), or the heavily mineralised Merensky ore froth was not that susceptible to the destabilising effects of increased contact angle.

For the UG2 ore, it was hypothesised that the addition of copper sulphate would also destabilise the froth but due to the non-selective formation of colloidal hydroxides on the mineral surfaces. Froth stability decreased with addition of copper sulphate which was not entirely due to non-selective hydrophilic copper hydroxide coating as

hypothesised. The formation of chemically reacted copper was unexpected and it is the first time that this has been shown for UG2 ore. It was postulated that the copper also chemically reacted with the oxide mineral in the UG2 ore. In the absence of xanthate, the froth was destabilised due to a decrease in the amount of hydrophobic froth stabilising particles and this was attributed to the copper hydroxide species found on the mineral surfaces from the EDTA tests. The decrease in froth stability in the presence of xanthate was attributed to the formation of hydrophobic copper-xanthate species, which have a destabilising effect in the sparsely mineralised UG2 froth.

6.1.2 How does the addition of copper sulphate change the surface charge of pure minerals?

The addition of copper sulphate to the pure minerals investigated (talc, chromite, plagioclase and pyrrhotite) made the zeta potentials less negative for all of the minerals. The addition of xanthate, after copper activation made the zeta potential values more negative again and these values were close to the zeta potential values obtained with no reagent addition. The shift in zeta potential values showed the surface charge of the pure minerals was changed with the addition of copper sulphate or xanthate which was indicative of adsorption of either reagent onto the mineral surfaces.

6.1.3 How does the addition of copper sulphate change the floatability of pure minerals?

From the microflotation tests, the floatabilities of talc and pyrrhotite were not improved with the addition of copper sulphate in the absence of xanthate. The floatability of pyrrhotite was only significantly improved with the addition of copper sulphate as well as xanthate. An increase in floatability of a mineral is linked to an increase in the contact angle of attachment between a particle and a bubble. The increase in the contact angle of pyrrhotite was therefore linked to an increase in hydrophobicity since the overall mass recovery was improved. It was assumed the other base metal sulphides in Merensky ore behave similarly to pyrrhotite when copper sulphate is used as an activator and this is in agreement with previous literature findings.

6.1.4 What activation products were formed on mineral surfaces when copper sulphate was added?

The EDTA extraction tests showed formation of several products on the pure talc mineral, the Merensky and UG2 ore surfaces. Significant amounts of copper were found to be present on the talc surface in the form of copper hydroxide and chemically reacted copper. The reduction in the amount of copper hydroxide extracted when xanthate was present was probably due to stable copper xanthate species on the mineral surface. Iron hydroxides were also found on the Merensky ore surfaces although this did not support the ion exchange copper activation mechanism with base sulphide minerals.

This study has shown that both the pulp and the froth zones are affected by copper sulphate addition and that they may behave differently at different conditions. The continued addition of copper sulphate at plant scale should be assessed in the light of these findings.

6.2 Recommendations for future work

The following recommendations are proposed for future test work based on the contributions and key findings of this study:

1. Analysis of flotation performance in continuous systems using water recovery and solids recovery as well as PGM or BMS assays.

   As seen from this study, copper sulphate adsorbs onto minerals non-selectively. The recovery of pyrrhotite was enhanced when pyrrhotite was activated by copper prior to collector adsorption. The recovery of talc also improved slightly with copper sulphate addition before xanthate addition which suggests possible activation of silicate gangue minerals which could reduce the grade and recovery of the concentrate.

2. Measuring the electrochemical potential (Eh) of the pulp.

   The Eh determines which form of the collector occurs in the pulp phase. Dixanthogen has been found to be formed above 200 mV. Different surface products may have been formed when the copper sulphate was added.

Electrochemical measurements of the rest potential of minerals could also be used to confirm the formation of copper sulphide species i.e. CuS or Cu_2S.

3. Analysis of residual xanthate in solution to determine if the copper hydroxide species affects xanthate adsorption onto the mineral surface.

4. Ex-situ surface analysis techniques can be implemented to analyse activation products. Examples of these techniques are XPS (X-ray Photoelectron Spectroscopy) and ToF-SIMS (Time-of-Flight Secondary Ion Mass Spectrometry).

5. Use of depressant to investigate the effect of gangue on froth stability.

REFERENCES

Acar, S. & Somasundaran, P., 1992. Effect of dissolved mineral species on the electrokinetic behaviour of sulfides. *Minerals Engineering*, 5(1), pp.27–40.

Adamson, A. & Gast, A., 1967. *Physical chemistry of surfaces* 6th ed., Wiley - Interscience.

Aktas, Z., Cilliers, J.J. & Banford, A.W., 2008. Dynamic froth stability: Particle size, airflow rate and conditioning time effects. *International Journal of Mineral Processing*, 87(1), pp.65–71.

Al-Abadleh, H.A. & Grassian, V.H., 2003. Oxide surfaces as environmental interfaces. *Surface Science Reports*, 52(3-4), pp.63–161.

Allison, S.A., Goold, L.A., Nicol, M.J. & Granville, A., 1972. A determination of the products of reaction between various sulphide minerals and aqueous xanthate. *Metallurgical Transactions*, 3(10).

Ata, S., 2012. Phenomena in the froth phase of flotation - A review. *International Journal of Mineral Processing*, 102-103, pp.1–12. Available at: http://dx.doi.org/10.1016/j.minpro.2011.09.008.

Ata, S., Ahmed, N. & Jameson, G.J., 2004. The effect of hydrophobicity on the drainage of gangue minerals in flotation froths. *Minerals Engineering*, 17(7-8), pp.897–901.

Averill, B. & Eldredge, P., 2012. Solubility-Product Constants (Ksp) for Compounds at 25 ° C. In *Principles of General Chemistry*. pp. 2984 – 2988.

Aveyard, R., Binks, B.P., Fletcher, P.D.I., Peck, T.G. & Rutherford, C.E., 1994. Aspects of aqueous foam stability in the presence of hydrocarbon oils and solid particles. *Advances in Colloid and Interface Science*, 48, pp.93–120.

Banford, A.W., Aktas, Z. & Woodburn, E.T., 1998. Interpretation of the effect of froth structure on the performance of froth flotation using image analysis. *Powder Technology*, 98(1), pp.61–73.

Barbian, N., Cilliers, J.J., Morar, S.H. & Bradshaw, D.J., 2007. Froth imaging, air recovery and bubble loading to describe flotation bank performance. *International Journal of Mineral Processing*, 84(1), pp.81–88.

Barbian, N., Hadler, K. & Cilliers, J.J., 2006. The froth stability column: measuring froth stability at an industrial scale. *Minerals Engineering*, 19(6), pp.713–718.

Barbian, N., Hadler, K., Ventura-Medina, E. & Cilliers, J.J., 2005. The froth stability column: linking froth stability and flotation performance. *Minerals Engineering*, 18(3), pp.317–324.

Barbian, N., Ventura-Medina, E. & Cilliers, J.J., 2003. Dynamic froth stability in froth flotation. *Minerals Engineering*, 16(11), pp.1111–1116.

Bartsch, O., 1924. Concerning Foam. *Kolloidchem.Beihefte*, 20, pp.1–49.

Bikerman, J., 1973. *Foams* 1st ed., Springer.

Binks, B.P., 2002. Particles as surfactants—similarities and differences. *Current Opinion in Colloid & Interface Science*, 7(1-2), pp.21–41.

Bradshaw, D.J., 1997. *Synergistic effects between thiol collectors used in the flotation of pyrite*. PhD Thesis. University of Cape Town.

Bradshaw, D.J. & O'Connor, C.T., 1996. Measurement of the sub-process of bubble loading in flotation. *Minerals Engineering*, 9(4), pp.443–448.

Buckley, A.N., Woods, R. & Wouterlood, H.J., 1989. An XPS investigation of the surface of natural sphalerites under flotation-related conditions. *International Journal of Mineral Processing*, 26(1-2), pp.29–49. Available at: http://www.sciencedirect.com/science/article/pii/0301751689900410 [Accessed June 8, 2015].

Bulatovic, S.M., 2007. *Handbook of Flotation Reagents Chemistry , Theory and Practice : Flotation of Sulfide Ores*, Elsevier.

Burdukova, E., 2007. *Surface Properties of New York Talc as a Function of pH, Polymer Adsorption and Electrolyte Concentration*. PhD Thesis. University of Cape Town.

Burdukova, E., Van Leerdam, G.C., Prins, F.E., Smeink, R.G., Bradshaw, D.J. & Laskowski, J.S., 2008. Effect of calcium ions on the adsorption of CMC onto the basal planes of New York talc - A ToF-SIMS study. *Minerals Engineering*, 21(12-14), pp.1020–1025.

Buswell, A.M. & Nicol, M.J., 2002. Some aspects of the electrochemistry of flotation of pyrrhotite. *Journal of Applied Electrochemistry*, 32, pp.1321 – 1329.

Castro, S. & Laskowski, J.S., 2011. Froth Flotation in Saline Water. *KONA Powder and Particle Journal*, 29(29), pp.4–15.

Chan, B. & Nyabeze, W., 2013. *The effect of copper sulphate on froth stability*, University of Cape Town. (Unpublished).

Chandra, A.P. & Gerson, A.R., 2009. A review of the fundamental studies of the copper activation mechanisms for selective flotation of the sulfide minerals, sphalerite and pyrite. *Advances in Colloid and Interface Science*, 145(1), pp.97–110.

Chang, C.S., Cooke, S.R. & Iwasaki, I., 1954. Flotation characteristics of pyrrhotite with xanthates. *Trans. AIME*, 199, p.209.

Chen, C., 2012. *Development of measurement of froth characteristics*. MSc Thesis. Chalmers University of Technology.

Chen, Z. & Yoon, R.-H., 2000. Electrochemistry of copper activation of sphalerite at pH 9.2. *International Journal of Mineral Processing*, 58(1), pp.57–66.

Cilliers, J.J. & Bradshaw, D.J., 1996. The flotation of fine pyrite using colloidal gas aphrons. *Minerals Engineering*, 9(2), pp.235–241.

Clarke, P., Fornasiero, D., Ralston, J. & Smart, R.S.C., 1995. A study of the removal of oxidation products from sulfide mineral surfaces. *Minerals Engineering*, 8(11), pp.1347–1357.

Collins, G.L. & Jameson, G.J., 1976. Experiments on the flotation of fine particles: the influence of particle size and charge. *Chemical Engineering Science*, 31(11), pp.985–991.

Corin, K.C., Reddy, a., Miyen, L., Wiese, J.G. & Harris, P.J., 2011. The effect of ionic strength of plant water on valuable mineral and gangue recovery in a platinum bearing ore from the Merensky reef. *Minerals Engineering*, 24(2), pp.131–137.

Craig, V.S.J., 2004. Bubble coalescence and specific-ion effects. *Current Opinion in Colloid and Interface Science*, 9(1-2), pp.178–184.

Deschenes, L.A., Barrett, J., Muller, L.J., Fourkas, J.T. & Mohanty, U., 1998. Inhibition of Bubble Coalescence in Aqueous Solutions. 1. Electrolytes. *The Journal of Physical Chemistry*, 102(26), pp.5115–5119. Available at: http://pubs.acs.org/doi/abs/10.1021/jp980828w.

Dippenaar, A., 1982. The destabilization of froth by solids. I. The mechanism of film rupture. *International Journal of Mineral Processing*, 9(1), pp.1–14.

Dudenkov, S. V., 1967. Effect of precipitates of metal xanthates and oleates on frothing. *Tsvetnye Metally*, 40, pp.18–21.

Ekmekçi, Z., Becker, M., Tekes, E.B. & Bradshaw, D., 2010. An impedance study of the adsorption of $CuSO_4$ and SIBX on pyrrhotite samples of different provenances. *Minerals Engineering*, 23, pp.903–907.

Ekmekçi, Z., Bradshaw, D.J., Allison, S.A. & Harris, P.J., 2003. Effects of frother type and froth height on the flotation behaviour of chromite in UG2 ore. *Minerals Engineering*, 16(10), pp.941–949.

Ekmekçi, Z., Bradshaw, D.J., Harris, P.J. & Buswell, a. M., 2006. Interactive effects of the type of milling media and $CuSO_4$ addition on the flotation performance of sulphide minerals from Merensky ore Part II: Froth stability. *International Journal of Mineral Processing*, 78(3), pp.164–174.

Farrokhpay, S., 2011. The significance of froth stability in mineral flotation - A review. *Advances in Colloid and Interface Science*, 166(1-2), pp.1–7. Available at: http://dx.doi.org/10.1016/j.cis.2011.03.001.

Farrokhpay, S. & Zanin, M., 2011. Effect of water quality on froth stability in flotation. In *Chemeca*. Sydney.

Finkelstein, N.P., 1997. Addendum to: The activation of sulphide minerals for flotation: A review. *International Journal of Mineral Processing*, 55(4), pp.283–286.

Flynn, S.A. & Woodburn, E.T., 1987. A froth ultra-fine model for the selective separation of coal from mineral in a dispersed air flotation cell. *Powder Technology*, 49(2), pp.127–142.

Fornasiero, D. & Ralston, J., 2005. Cu(II) and Ni(II) activation in the flotation of quartz, lizardite and chlorite. *International Journal of Mineral Processing*, 76(1-2), pp.75–81.

Fuerstenau, D.W., 1982. Sulphide Mineral Flotation. In R. P. King, ed. *Principles of flotation*. Johannesburg.

Fuerstenau, D.W. & Pradip, 2005. Zeta potentials in the flotation of oxide and silicate minerals. *Advances in Colloid and Interface Science*, 114, pp.9–26.

Fullston, D., Fornasiero, D. & Ralston, J., 1999. Zeta potential study of the oxidation of copper sulfide minerals. *Colloid and Interface Science*, 146, pp.113–121.

Gaudin, A.M., Fuerstenau, D.W. & Mao, G.W., 1959. Activation and deactivation studies with copper on sphalerite. *Minerals Engineering*, 11, p.430.

Gerson, A.R. & Jasieniak, M., 2008. The Effect of Surface Oxidation on the Cu Activation of Pentlandite and Pyrrhotite. , pp.1054–1063.

Gerson, A.R., Lange, A.G., Prince, K.E. & Smart, R.S.., 1999. The mechanism of copper activation of sphalerite. *Applied Surface Science*, 137(1-4), pp.207–223.

Goates, J.R., Gordon, M.B. & Faux, N.D., 1952. Calculated values for the solubility-product constants of the metallic sulfides. *Journal of the American Chemical Society*, 74(3), pp.835–836.

Grobler, W.A., Sondashi, S. & Chidley, F.J., 2005. Recent developments in flotation reagents to improve base metal sulphide recovery. *South African Institute of Mining and Metallurgy*, pp.2–7.

Harris, P.J., 1982. Frothing Phenomena. In *The Principles of Flotation*. pp. 237 – 248.

Hartland, S., 2004. *Surface and Interfacial Tension: Measurement, Theory and Applications* 1st ed., Marcel Dekker, Inc.

Hay, M.P. & Roy, R., 2010. A case study of optimising UG2 flotation performance. Part 1: Bench, pilot and plant scale factors which influence Cr2O3 entrainment in UG2 flotation. *Minerals Engineering*, 23(11-13), pp.855–867.

Healy, T. & Moignard, M., 1976. Review of Electrokinetic Studies of Metal Sulphides. *Flotation*.

Horozov, T.S., 2008. Foams and foam films stabilised by solid particles. *Current Opinion in Colloid and Interface Science*, 13(3), pp.134–140.

Hunter, R.J., 1993. *Introduction to modern colloid science*, Oxford University.

Hunter, T.N., Pugh, R.J., Franks, G. V. & Jameson, G.J., 2008. The role of particles in stabilising foams and emulsions. *Advances in Colloid and Interface Science*, 137(2), pp.57–81.

Ikumapayi, F.K., 2013. *Recycling Process Water in Complex Sulphide Ore Flotation Recycling Process Water in Complex Sulphide Ore Flotation*. PhD Thesis. Lulea University of Technology.

Ip, S.W., Wang, Y. & Toguri, J.M., 1999. Aluminum foam stabilization by solid particles. *Canadian Metallurgical Quarterly*, 38(1), pp.81–92. Available at: http://www.sciencedirect.com/science/article/pii/S000844339800024X [Accessed June 20, 2015].

James, R.O. & Healy, T.W., 1972. Adsorption of hydrolyzable metal ions at the oxide—water interface. III. A thermodynamic model of adsorption. *Journal of Colloid and Interface Science*, 40(1), pp.65–81.

Johansson, G. & Pugh, R.J., 1992. The influence of particle size and hydrophobicity on the stability of mineralized froths. *International Journal of Mineral Processing*, 34, pp.1–21.

Jones, R.T., 1999. Platinum smelting in South Africa. *South African Journal of Science*, 95.

Kant, C., 1997. *The effect of pulp potential and surface products on copper mineral flotation*. McGill University.

Kartio, I., Laajalehto, K., Kaurila, T. & Suoninen, E., 1996. A study of galena (PbS) surfaces under controlled potential in pH 4.6 solution by synchrotron radiation excited photoelectron spectroscopy. *Applied Surface Science*, 93, pp.167–177.

Kawatra, S.K., 2002. Froth Flotation-Fundamental Principles. *Research, Michigan Technical University*, pp.1–30.

Klimpel, R.R., 1980. Selection of chemical reagents for flotation. In *Mineral Processing Plant Design 2*. pp. 907 – 934.

Koh, P.T.L., Hao, F.P., Smith, L.K., Chau, T.T. & Bruckard, W.J., 2009. The effect of particle shape and hydrophobicity in flotation. *International Journal of Mineral Processing*, 93(2), pp.128–134.

Laskowski, J. & Castro, S., 2014. Flotation in highly concentrated electrolyte solutions. In *International Mineral Processing Congress*. pp. 1–12.

Laskowski, J.S., 2004. Testing flotation frothers. *Physicochemical Problems of Mineral Processing*, 38(June), pp.13–22.

Li, C. & Somasundaran, P., 1993. Reversal of bubble charge in multivalent inorganic salt solutions—effect of lanthanum. *Colloids and Surfaces A: Physicochemical and Engineering Aspects*, 81(2), pp.13–15.

Li, X., Shaw, R. & Stevenson, P., 2010. Effect of humidity on dynamic foam stability. *International Journal of Mineral Processing*, 94(1-2), pp.14–19.

Luttrell, G.H. & Yoon, R.H., 1984. Surface studies of the collectorless flotation of chalcopyrite. *Colloids and Surfaces*, 12, pp.239–254.

Mackenzie, J.M.W. & O'Brien, R.T., 1969. Zeta Potential of quartz in the presence of nickel (II) and cobalt (II). *Trans. AIME*, 244, pp.168 – 173.

Mailula, T.D., Bradshaw, D.J. & Harris, P.J., 2003. The effect of copper sulphate addition on the recovery of chromite in the flotation of UG2 ore. *Jounal of the South African Institute of Mining and Metallurgy*, (March), pp.143–146.

Malysa, K., 1992. Wet foams: formation, properties and mechanism of stability. *Advances in Colloid and Interface Science*, 40, pp.37–83.

Malysiak, V., 2003. *Pentlandite-pyroxene and pentlandite-feldspar interactions and their effect on separation by flotation*. PhD Thesis. University of Cape Town.

Malysiak, V., Shackleton, N.J. & O'Connor, C.T., 2004. An investigation into the floatability of a pentlandite-pyroxene system. *International Journal of Mineral Processing*, 74(1-4), pp.251–262.

Manono, M.S., Corin, K.C. & Wiese, J.G., 2012. An investigation into the effect of various ions and their ionic strength on the flotation performance of a platinum bearing ore from the Merensky reef. *Minerals Engineering*, 36, pp.231–236.

Manono, M.S., Corin, K.C. & Wiese, J.G., 2013. The effect of ionic strength of plant water on foam stability: A 2-phase flotation study. *Minerals Engineering*, 40, pp.42–47.

Mao, L., Luttrell, G.H., Adel, G.T. & Davis, R.M., 1998. Application of Extended DLVO Theory : Modeling of Flotation and Hydrophobicity of Dodecane Application of Extended DLVO Theory : Modeling of Flotation and Hydrophobicity of Dodecane.

Martinovic, J., Bradshaw, D.J. & Harris, P.J., 2005. Investigation of surface properties of gangue minerals in platinum bearing ores. *Proceedings of Platinum Adding Value*.

McFadzean, B., 2014. *Entrainment of chromite in flotation of UG2 ore using copper sulphate as activator*, University of Cape Town. (Unpublished).

McFadzean, B., Castelyn, D.G. & O'Connor, C.T., 2012. The effect of mixed thiol collectors on the flotation of galena. *Minerals Engineering*, 36-38, pp.211–218.

Mhlanga, S.S., O'Connor, C.T. & Mcfadzean, B., 2012. A study of the relative adsorption of guar onto pure minerals. *Minerals Engineering*, 36-38, pp.172–178.

Miller, J.D., Li, J., Davidtz, J.C. & Vos, F., 2005. A review of pyrrhotite flotation chemistry in the processing of PGM ores. *Minerals Engineering*, 18(8), pp.855–865.

Mineral Technologies International, I., 2010. Module 5: Froth Flotation - The Klimpel flotation model. Available at: http://mineraltech.com/MODSIM/ModsimTraining/Module5/Module5.html [Accessed August 27, 2015].

Montalti, M., 1994. *Interaction of ethyl xanthate with pyrite and pyrrhotite minerals*. PhD Thesis. University of South Australia.

Moolman, D.W., Aldrich, C. & Van Deventer, J.S.J., 1995. The interpretation of flotation froth surfaces by using digital image analysis and neural networks. *Chemical Engineering Science*, 50(22), pp.3501–3513.

Morris, G.E., Fornasiero, D. & Ralston, J., 2002. Polymer depressants at the talc–water interface: adsorption isotherm, microflotation and electrokinetic studies. *International Journal of Mineral Processing*, 67(1–4), pp.211–227. Available at: http://www.sciencedirect.com/science/article/pii/S0301751602000480.

Murray, B.S. & Ettelaie, R., 2004. Foam stability: Proteins and nanoparticles. *Current Opinion in Colloid and Interface Science*, 9(5), pp.314–320.

Muzenda, E., 2010. An investigation into the effect of water quality on flotation performance. *International Journal of Chemical, Materials Science and Engineering*, (9), pp.1–5.

Nagaraj, D. & Brinen, J., 1995. SIMS study of metal ion activation in gangue flotation. *Preprints-Society of Mining Engineers of AIME*.

Nagaraj, D.R. & Brinen, J.S., 1996. SIMS and XPS study of the adsorption of sulfide collectors on pyroxene: A case for inadvert metal in activation. *Colloids and Surfaces A: Physicochemical and Engineering Aspects*, 116(3), pp.241–249.

Nashwa, V.M., 2008. *The flotation of high talc-containing ore from the Great Dyke of Zimbabwe*. MSc Thesis. University of Pretoria.

Neethling, S.J. & Cilliers, J.J., 2002. The entrainment of gangue into a flotation froth. *International Journal of Mineral Processing*, 64(2), pp.123–134.

Nicol, M.J., 1984. An electrochemical study of the interaction of copper (II) ions with sulphide minerals. *Council of Mineral Technology*.

Parks, G.A., 1965. The isoelectric points of solid oxides, solid hydroxides, and aqueous hydroxo complex systems. *Chemical Reviews*, 65(2), pp.177–198.

Parsonage, P.G., 1984. Effects of slime and colloidal particles on the flotation of galena. , pp.111 – 139.

Parsons, I., 2012. *Feldspars and their Reactions*, Springer Science & Business Media.

Prestidge, C.A., Thiel, A.G., Ralston, J. & Smart, R.S.C., 1994. The interaction of ethyl xanthate with copper(II)-activated zinc sulphide: Kinetic effects. *Colloids and Surfaces A: Physicochemical and Engineering Aspects*, 85(1), pp.51–68.

Pugh, R.J., 2005. Experimental techniques for studying the structure of foams and froths. *Advances in Colloid and Interface Science*, 114-115, pp.239–251.

Pugh, R.J., Weissenborn, P. & Paulson, O., 1997. Flotation in inorganic electrolytes; the relationship between recover of hydrophobic particles, surface tension, bubble coalescence and gas solubility. *International Journal of Mineral Processing*, 51(1), pp.125–138.

Quinn, J.J., Kracht, W., Gomez, C.O., Gagnon, C. & Finch, J.A., 2007. Comparing the effect of salts and frother (MIBC) on gas dispersion and froth properties. *Minerals Engineering*, 20(14), pp.1296–1302.

Ralston, J. & Healy, T.W., 1980. Activation of Zinc Sulphide with CuII, CdII and PbII. II--Activation in Neutral and Weakly Alkaline Media. In *Int. J. Miner. Proc.* pp. 203–217.

Rao, S.R., 2003. *Surface chemistry of froth flotation*, Springer.

Ross, V.E., 1997. Particle-bubble attachment in flotation froths. *Minerals Engineering*, 10(7), pp.695–706.

Schouwstra, R.P., Kinloch, E.D. & Lee, C.A., 2000. A short geological review of the Bushveld Complex. *Platinum Metals Review*, 44(1), pp.33–39.

Shackleton, N.J., 2007. *Surface characterisation and flotation behavior of the platinum and palladium arsenide, telluride and sulphide mineral species*. PhD Thesis. University of Cape Town.

Shackleton, N.J., Malysiak, V. & O'Connor, C.T., 2007. Surface characteristics and flotation behaviour of platinum and palladium arsenides. *International Journal of Mineral Processing*, 85(1-3), pp.25–40.

Shackleton, N.J., Malysiak, V. & O'Connor, C.T., 2003. The use of amine complexes in managing inadvertent activation of pyroxene in a pentlandite-pyroxene flotation system. *Minerals Engineering*, 16(9), pp.849–856.

Smart, R.S.C., Amarantidis, J., Skinner, W., Prestidge, C.A., Lavanier, L. & Grano, S., 1998. Surface Analytical Studies of Oxidation and Collector Adsorption in Sulfide Mineral Flotation. *Scanning Microscopy*, 12(4), pp.553–583.

Somasundaran, P. & Moudgil, B.M., 1987. *Reagents in Mineral Technology*, CRC Press. Available at: https://books.google.com/books?hl=en&lr=&id=oZ6Y9eYjaEQC&pgis=1 [Accessed June 24, 2015].

Somasundaran, P. & Wang, D., 2006. *Solution chemistry: minerals and reagents* 1st ed. B. A. Wills, ed., Elsevier.

Subrahmanyam, T. V. & Forssberg, E., 1988. Froth Stability, Particle Entrainment and Drainage in Flotation - A Review. *International Mineral Processing*, 23, pp.33–53.

Trahar, W.J., Senior, G.D.D., Heyes, G.W.W. & Creed, M.D.D., 1997. The activation of sphalerite by lead—a flotation perspective. *International Journal of Mineral Processing*, 49(3), pp.121–148.

Tsatouhas, G., Grano, S.R. & Vera, M., 2006. Case studies on the performance and characterisation of the froth phase in industrial flotation circuits. *Minerals Engineering*, 19(6), pp.774–783.

Vermaak, M.K.J., 2005. *Fundamentals of the flotation behaviour of palladium bismuth tellurides.* PhD Thesis. University of Pretoria.

Verwey, E.J.W. & Overbeek, J.T.G., 1948. Theory of the stability of lyophobic colloids. , pp.22 – 46. Courier Corporation.

Wang, X., Forssberg, E. & Bolin, N.J., 1989. The aqueous and surface chemistry of activation in the flotation of sulphide minerals—A review. Part II: A surface precipitation model. *Mineral Procesing and Extractive Metallurgy Review*, 4(3-4), pp.167–199.

Weissenborn, P.K. & Pugh, R.J., 1996. Surface Tension of Aqueous Solutions of Electrolytes: Relationship with Ion Hydration, Oxygen Solubility, and Bubble Coalescence. *Journal of Colloid and Interface Science*, 184(2), pp.550–563.

Wesseldijk, Q., Reuter, M., Bradshaw, D. & Harris, P., 1999. The flotation behaviour of chromite with respect to the beneficiation of UG2 ore. *Minerals Engineering*, 12(10), pp.1177–1184.

Wiese, J., Becker, M., Bradshaw, D.J. & Harris, P.J., 2007. Interpreting the role of reagents in the flotation of platinum-bearing Merensky ores. *South African Institute of Mining and Metallurgy*, 107(1), p.29.

Wiese, J., Harris, P. & Bradshaw, D., 2005. Investigation of the role and interactions of a dithiophosphate collector in the flotation of sulphides from the Merensky reef. *Minerals Engineering*, 18(8), pp.791–800.

Wiese, J., Harris, P. & Bradshaw, D., 2011. The effect of the reagent suite on froth stability in laboratory scale batch flotation tests. *Minerals Engineering*, 24(9), pp.995–1003.

Wiese, J., Harris, P. & Bradshaw, D., 2006. The role of the reagent suite in optimising pentlandite recoveries from the Merensky reef. *Minerals Engineering*, 19(12), pp.1290–1300.

Wiese, J., Harris, P. & Bradshaw, D.J., 2007. The response of sulphide and gangue minerals in selected Merensky ores to increased depressant dosages. *Minerals Engineering*, 20(10), pp.986–995.

Woodburn, E.T., Austin, L.G. & Stockton, J.B., 1994. A froth based flotation kinetic model. *Chemical engineering research & design*, 72(2), pp.211–226. Available at: http://cat.inist.fr/?aModele=afficheN&cpsidt=4040340 [Accessed March 23, 2015].

Zanin, M., Wightman, E., Grano, S.R. & Franzidis, J.P., 2009. Quantifying contributions to froth stability in porphyry copper plants. *International Journal of Mineral Processing*, 91(1), pp.19–27.

Zeta-Meter, I., 1997. Zeta Potential: A complete course in 5 minutes. Available at: https://scholar-google-co-za.ezproxy.uct.ac.za/scholar?q=zeta+potential+a+complete+course+in+5+minutes&btnG=&hl=en&as_sdt=0%2C5 [Accessed June 21, 2015].

Zieminski, S.A. & Whittemore, R.C., 1971. Behavior of gas bubbles in aqueous electrolyte solutions. *Chemical Engineering Science*, 26(4), pp.509–520.

APPENDICES

Appendix A: Surface coverage calculations

The method of calculation of copper sulphate and xanthate surface coverage for pure minerals and the ore particles is shown in the calculations below. These calculations were based on the theoretical surface area required per atom uptake of copper or xanthate; taken to be 20.8 $Å^2$ (Gaudin et al.,1959) and 37 $Å^2$ (Bradshaw, 1997) for copper and xanthate respectively.

The surface area of each pure mineral at a particular particle size distribution was determined using the BET method. The surface areas obtained are summarised in Table 3.1 in the experimental procedure section of this dissertation. The sample calculations show the surface coverage determination of talc which has a BET surface area of 5.9503 m^2/g for particles less than 25 microns in size. This was the particle size class used for the zeta potential determinations.

A.1 Copper surface coverage

Molar Mass of Cu (g/mol) = 63.546

Cu stock solution concentration (mol/dm^3) = 5×10^{-3}

Cu stock solution concentration (g/dm^3) = $5 \times 10^{-3} \times (63.546)$

$= 0.3177$

Moles of Cu added in 1 cm^3 = $0.001 \times (5 \times 10^{-3})$

$= 5 \times 10^{-6}$

Atoms of Cu added in 1 cm^3 = $5 \times 10^{-6} \times (6.023 \times 10^{23})$

$= 3.0115 \times 10^{18}$

Talc BET surface area (m^2/g) = 5.9503

Talc surface area ($Å^2/g$) = 5.9503×10^{20}

Total mineral surface area $Å^2$ (0.075 g) = $5.9503 \times 10^{20} \times 0.075$

$= 4.4627 \times 10^{19}$

Theoretical Cu atom coverage $Å^2$ = 20.8

Cu pseudo monolayer coverage $Å^2 = 3.0115 \times 10^{18} \times 20.8$

$= 6.2639 \times 10^{19}$

Number of Cu monolayers = $6.2639 \times 10^{19} / 4.4627 \times 10^{19}$

= 1.4

A.2 Xanthate surface coverage

Molar Mass of Xanthate (g/mol) = 149.24

Xanthate stock solution concentration (mol/dm^3) = 5×10^{-3}

Xanthate stock solution concentration (g/dm^3) = $5 \times 10^{-3} \times (149.24)$

$= 0.7462$

Moles of Xanthate added in 1 $cm^3 = 0.001 \times (5 \times 10^{-3})$

$= 5 \times 10^{-6}$

Atoms of Xanthate added in 1 $cm^3 = 5 \times 10^{-6} \times (6.023 \times 10^{23})$

$= 3.0115 \times 10^{18}$

Talc BET surface area (m^2/g) = 5.9503

Talc surface area ($Å^2/g$) = 5.9503×10^{20}

Total mineral surface area $Å^2$ (0.075 g) = $5.9503 \times 10^{20} \times 0.075$

$= 4.4627 \times 10^{19}$

Theoretical Xanthate atom coverage $Å^2 = 37$

Xanthate pseudo monolayer coverage $Å^2 = 3.0115 \times 10^{18} \times 37$

$= 1.1143 \times 10^{20}$

Number of Cu monolayers = $1.1143 \times 10^{20} / 4.4627 \times 10^{19}$

= 2.5

Appendix B: Determination of froth stability parameters

1. The values of H_{max} and $t_{1/2}$ were obtained by fitting the experimental data to equations 2.4 and 2.5 and minimising the sum of least squares.

$$H(t) = H_{max}(1 - e^{-\frac{t}{\tau}}) \quad \text{.....2.4}$$

$$\frac{H_f}{H_{f\,max}} = \frac{1}{2} - \alpha ln\left(\frac{t}{t_{\frac{1}{2}}}\right) \quad \text{.....2.5}$$

2. The 'Solver' function in Microsoft Excel 2013 was used by selecting the 'Solver Add-In' from the 'Analysis ToolPak' from the Excel Options tab.
3. Initial estimates 'guesses' of H_{max} and τ were made for the dynamic test.
4. For the static test, initial estimates of $t_{1/2}$ and α were made.
5. The least squares method was used to determine the lines of best fit for the models.

$$Residual = \sum_{i=1}^{i=n} (Y_{observed,i} - Y_{calculated,i})^2$$

where $Y_{observed}$ was from the experimental data and $Y_{calculated}$ was from the model. n was the number of observations made.

6. Figure B1 shows how Solver was used to determine H_{max} and τ.

	A	B	C	D
1	τ (s)	47.2344	50.8877	48.7221
2	H_{max} (mm)	675.546	715.941	673.688
3				
4	**Time (s)**	**Run 1**	**Run 2**	**Run 3**
5	0	0	0	0
6	5	37.7579	64.0035	86.3671
7	10	906.324	1244.01	1935.59
8	15	449.304	539.353	1120.96
9	20	316.97	300.29	492.202
10	25	301.78	82.8667	158.781
30	125	178.356	71.3414	198.874
31	130	72.9922	7.29841	81.9214
32	135	17.7694	6.2783	20.1825
33	140	0.10365	52.2087	0.1433
34	145	10.115	132.337	11.1165
35	150	40.0811	236.594	44.6856
36	**Σ of squares**	**4845.2**	**5656.06**	**7072.43**

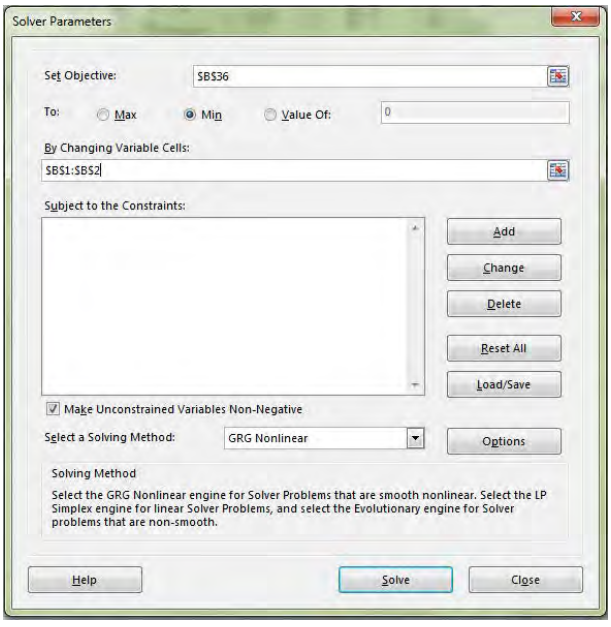

Figure B1: Determination of froth stability parameters using Solver

7. As shown in Figure B1, the residual value (sum of least squares) was set as the objective cell "**B36**" and this was minimised by changing H_{max} "**B2**" and τ "**B1**". For the dynamic test, $t_{1/2}$ and α were changed.
8. This was repeated for the other two measurements and the average values of H_{max} and $t_{1/2}$ were calculated as well as the standard error which was used to compute the error bars.

Appendix C: Determination of flotation rate constants

1. The values of R_{max} and k were also obtained by minimising the sum of least squares and fitting the experimental data to the Klimpel flotation model in equation 4.1.

$$R = R_{max}\left(1 - \frac{1}{kt}\left(1 - e^{-kt}\right)\right) \quad \text{.....4.1}$$

2. The method outlined in Appendix B steps 6 and 7 was followed and the initial guesses for R_{max} and k were made.
3. The residual value (sum of least squares) was set as the objective cell which was minimised by changing R_{max} and k.

Appendix D: EDTA copper calculations

The following calculations are for the EDTA extractable copper from a copper activated Merensky ore in the absence of xanthate in deionised water.

EDTA Molar Mass (g/mol) = 416.23

$CuSO_4.5H_2O$ Molar Mass (g/mol) = 249.685

Cu Molar Mass (g/mol) = 63.546

Pulp Density (%) solids = 30

Total Mass of ore (g) = 2028

$CuSO_4.5H_2O$ dosage (g/tonne of ore) = 80

Table D1: Calculation of the amount of solids in 200 ml of pulp

Beaker (g)	53.6
Beaker + Pulp (g)	309.9
Pulp Mass (g)	256.3
Average Solids (g)	76.89

Cu dosage = (Mr mass of Cu/ Mr mass of $CuSO_4.5H_2O$) x 90 g/tonne

= 22.9 g/tonne

Dosage of copper in ~ 2 kg of ore = (2028/1000) kg x (22.9 g/1000 kg)

= 0.04645 g

= 46.45 mg

Cu in 76.89 g of solids = (76.89/2028) g x 46.45 mg **= 1.761 mg**

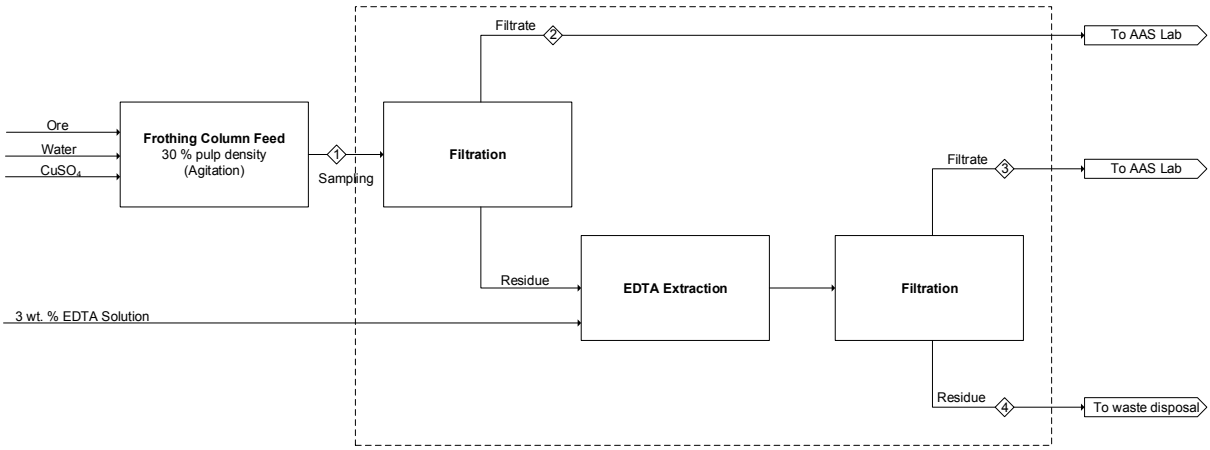

Figure D1: Block Flow Diagram of EDTA extraction procedure

As stated earlier, the amount of copper on the mineral surface was calculated using the following equation.

$$Cu_{total} = Cu(OH)_{2,surface} + Cu_{solution} + Cu_{surface} \ldots\ldots\ldots\ldots\ldots 4.2$$

According to Figure D1, stream 1 corresponds to the total copper added to the system (1.761 mg). Stream 2 is the copper in solution before EDTA extraction. Stream 3 is the EDTA-extractable copper which is in the form of copper hydroxide. Stream 4 is the surface copper which is chemically bonded to the mineral and could

not be extracted by the EDTA which was calculated from the mass balance since streams 1 – 3 were known.

The total volume in stream 2 was approximately 200 ml.

Stream 2 concentration from analytical lab (mg/l) = 0.02

Stream 2 copper (mg) = volume x concentration

= 0.2 L x 0.02 mg/l

= 0.004 mg

The total volume in stream 3 was approximately 250 ml.

Stream 3 concentration from analytical lab (mg/l) = 4.19

Stream 3 copper (mg) = volume x concentration

= 0.25 L x 4.19 mg/l

= 1.048 mg

Stream 4 copper (mg) = 1.761 – 0.004 – 1.048 **= 0.709**

Appendix E: Raw Data

E.1 Froth Stability Tests

Table E1: Merensky ore in DW – dynamic test

	Raw data (mm)		
Time (s)	1	2	3
0	200	200	200
5	274	275	275
10	314	317	324
15	360	360	367
20	406	404	404
25	450	441	438
30	486	472	471
35	514	522	503
40	543	539	536
45	563	560	556
50	589	581	578
55	605	612	599
60	624	638	615
65	643	651	634
70	659	680	647
75	680	700	664
80	701	721	683
85	707	734	700
90	722	744	717
95	735	760	730
100	749	778	745
105	760	796	759
110	776	804	768
115	785	815	785
120	796	817	785
125	796	817	791
130	796	817	791
135	796	817	791
140	796	817	791
145	796	817	791
150	796	817	791

Table E2: Merensky ore in DW – static test

	Raw data (mm)		
Time (s)	1	2	3
0	804	818	790
2	762	766	757
4	728	736	720
6	700	712	688
8	666	673	659
10	622	634	610
12	586	600	572
14	539	528	550
16	500	498	501
18	459	460	458
20	428	427	429
22	404	399	408
24	364	354	374
26	336	327	344
28	312	299	325
30	283	282	283

Table E3: UG2 ore in DW – dynamic test

	Raw data (mm)		
Time (s)	1	2	3
0	250	250	250
5	307	326	313
10	343	356	343
15	398	402	387
20	427	431	414
25	451	445	436
30	474	485	467
35	490	508	489
40	509	513	508
45	528	527	522
50	547	540	534
55	559	548	543
60	568	561	556
65	577	570	568
70	585	581	575
75	590	591	585
80	598	602	596
85	605	610	603
90	611	619	614
95	619	623	617
100	619	627	623
105	621	637	630
110	621	637	630
115	636	644	637
120	647	648	641
150	680	669	663
180	718	717	702
210	723	728	710
240	728	730	720
270	731	732	725
300	731	745	735

Table E4: UG2 ore in DW – static test

	Raw data (mm)		
Time (s)	1	2	3
0	730	728	705
2	701	700	671
4	665	670	643
6	638	641	610
8	604	613	573
10	567	594	538
12	520	565	502
14	492	542	467
16	422	500	428
18	383	475	389
20	347	444	352
22	306	340	330
24	278	305	298
26	260	270	270
28	250	260	264
30	250	250	250

Table E5: Merensky ore in SPW – dynamic test

	Raw data (mm)		
Time (s)	1	2	3
0	250	250	250
5	315	334	327
10	363	375	367
15	396	408	400
20	421	428	420
25	438	445	439
30	450	456	446
35	461	466	456
40	470	478	467
45	477	485	475
50	485	490	483
55	492	494	490
60	498	506	495
65	503	512	502
70	507	518	507
75	515	522	511
80	518	522	511
85	520	525	515
90	521	526	517
95	526	526	518
100	526	528	518
105	526	533	522
110	529	531	522
115	529	546	532
120	531	550	539
150	536	554	547
180	542	559	547
210	547	556	556
240	551	557	556
270	552	559	554
300	552	559	554

Table E6: Merensky ore in SPW – static test

	Raw data (mm)		
Time (s)	1	2	3
0	540	525	533
2	504	496	500
4	465	468	467
6	442	437	440
8	405	405	405
10	379	374	377
12	347	322	335
14	315	293	304
16	282	267	276
18	260	250	255
20	250	250	250
22	250	250	250
24	250	250	250
26	250	250	250
28	250	250	250
30	250	250	250

Table E7: UG2 ore in SPW – dynamic test

	Raw data (mm)		
Time (s)	1	2	3
0	250	250	250
5	294	298	302
10	337	343	351
15	374	383	391
20	399	409	409
25	420	429	423
30	436	442	436
35	448	456	446
40	459	467	455
45	469	478	465
50	478	487	470
55	486	492	477
60	493	498	477
65	500	498	485
70	507	504	492
75	513	509	496
80	518	515	500
85	518	519	500
90	522	525	508
95	527	525	508
100	527	530	510
105	534	530	521
110	534	536	521
115	534	538	528
120	534	540	534
150	548	561	542
180	556	563	560
210	578	565	570
240	578	570	570
270	583	570	574
300	583	570	574

Table E8: UG2 ore in SPW – static test

	Raw data (mm)		
Time (s)	1	2	3
0	538	520	538
2	487	482	512
4	468	449	473
6	423	416	437
8	392	394	408
10	365	366	381
12	342	346	360
14	327	328	341
16	318	315	325
18	313	309	316
20	307	305	310
22	307	305	308
24	307	302	308
26	307	302	308
28	307	302	308
30	307	302	308

E.2 Zeta Potential Tests

Zeta potential raw data for pure minerals with no reagent addition.

Table E9: Talc zeta potential raw data – no reagents

pH	Zeta Potential (mV)		
	Run 1	Run 2	Run 3
2	15.0	15.2	14.3
4	6.41	6.19	4.80
6	-23.9	-27.5	-29.4
8	-52.1	-57.2	-61.3
10	-55.1	-64.5	-68.7

Table E10: Pyrrhotite Zeta Potential raw data – no reagents

pH	Zeta Potential (mV)		
	Run 1	Run 2	Run 3
2	17.2	15.4	16.7
4	16.50	17.20	16.70
6	-2.22	-3.40	-3.70
8	-48.0	-53.0	-48.7
10	-47.8	-52.4	-52.9

Table E11: Plagioclase Zeta Potential raw data – no reagents

pH	Zeta Potential (mV)		
	Run 1	Run 2	Run 3
2	4.79	3.78	3.38
4	13.0	12.1	17.4
6	3.92	3.14	1.62
8	-54.2	-59.3	-64.0
10	-54.2	-55.7	-65.7

Table E12: Chromite Zeta Potential raw data – no reagents

pH	Zeta Potential (mV)		
	Run 1	Run 2	Run 3
2	19.9	18.0	18.7
4	14.6	15.0	14.7
6	-3.07	-5.56	-8.19
8	-39.5	-44.8	-45.9
10	-46.7	-48.5	-53.0

Zeta potential raw data for pure minerals with copper addition.

Table E13: Talc zeta potential raw data – copper addition

pH	Zeta Potential (mV)		
	Run 1	Run 2	Run 3
2	15.2	15.8	16.3
4	3.42	2.38	2.86
6	-3.58	-3.89	-4.20
8	-10.8	-10.6	-10.6
10	-37.8	-40.7	-44.2

Table E14: Pyrrhotite zeta potential raw data – copper addition

pH	Zeta Potential (mV)		
	Run 1	Run 2	Run 3
2	8.23	4.88	6.59
4	17.10	17.70	12.50
6	3.94	3.69	-1.71
8	-12.4	-11.3	-10.9
10	-23.2	-28.3	-16.9

Table E15: Plagioclase zeta potential raw data – copper addition

pH	Zeta Potential (mV)		
	Run 1	Run 2	Run 3
2	1.51	1.69	1.78
4	7.05	7.20	13.6
6	14.3	16.5	17.2
8	-13.9	-14.4	-13.4
10	-40.2	-43.0	-43.0

Table E16: Chromite zeta potential raw data – copper addition

pH	Zeta Potential (mV)		
	Run 1	Run 2	Run 3
2	13.0	12.7	12.1
4	11.9	11.2	12.1
6	3.46	4.09	4.37
8	-3.45	-3.43	-5.32
10	-34.6	-39.0	-42.7

E.3 Microflotation

Table E17: Talc microflotation raw data – synthetic plant water

Talc, No Reagents	**C1**	**C2**	**C3**	**C4**	**T**
Filter Paper (g)	0.3244	0.316	0.3182	0.3212	0.3149
Filter Paper + Mineral (g)	0.8754	0.8127	0.7059	0.5096	0.5916
Mineral (g)	0.551	0.4967	0.3877	0.1884	0.2767
Talc, Cu	**C1**	**C2**	**C3**	**C4**	**T**
Filter Paper (g)	0.3341	0.3256	0.3169	0.3325	0.3426
Filter Paper + Mineral (g)	0.9248	1.2022	1.1377	0.7219	0.5970
Mineral (g)	0.5907	0.8766	0.8208	0.3894	0.2544
Talc, X-	**C1**	**C2**	**C3**	**C4**	**T**
Filter Paper (g)	0.3170	0.3188	0.3198	0.3180	0.3201
Filter Paper + Mineral (g)	0.9964	0.8604	0.6182	0.4313	0.6718
Mineral (g)	0.6794	0.5416	0.2984	0.1133	0.3517
Talc, Cu + X-	**C1**	**C2**	**C3**	**C4**	**T**
Filter Paper (g)	0.3342	0.3453	0.3365	0.3326	0.3421
Filter Paper + Mineral (g)	0.9846	1.2709	1.1699	0.6475	0.5879
Mineral (g)	0.6504	0.9256	0.8334	0.3149	0.2458

Table E18: Pyrrhotite microflotation raw data – synthetic plant water

Pyrrhotite, No Reagents	**C1**	**C2**	**C3**	**C4**	**T**
Filter Paper (g)	0.3181	0.3147	0.3179	0.3182	0.3181
Filter Paper + Mineral (g)	0.4902	0.5012	0.5630	0.3860	2.4334
Mineral (g)	0.1721	0.1865	0.2451	0.0678	2.1153
Pyrrhotite, Cu	**C1**	**C2**	**C3**	**C4**	**T**
Filter Paper (g)	0.3176	0.3110	0.3206	0.3094	0.3188
Filter Paper + Mineral (g)	0.4451	0.5234	0.5058	0.4817	2.4958
Mineral (g)	0.1275	0.2124	0.1852	0.1723	2.1770
Pyrrhotite, X-	**C1**	**C2**	**C3**	**C4**	**T**
Filter Paper (g)	0.3182	0.3164	0.3191	0.3119	0.3127
Filter Paper + Mineral (g)	0.5839	0.5859	0.4893	0.4141	2.2955
Mineral (g)	0.2657	0.2695	0.1702	0.1022	1.9828
Pyrrhotite, Cu + X-	**C1**	**C2**	**C3**	**C4**	**T**
Filter Paper (g)	0.3192	0.3148	0.3128	0.3148	0.3176
Filter Paper + Mineral (g)	0.6277	0.6870	0.7297	0.4766	1.9467
Mineral (g)	0.3085	0.3722	0.4169	0.1618	1.6291

E.4 EDTA Extraction Tests

Table E19: Raw data for Merensky and UG2 ore copper analysis

Condition	Water	Ore	Solution Cu (mg/l)	EDTA Cu (mg/l)
Cu	DW	Merensky	0.02	4.19
Cu, Xanthate			0.13	3.89
Cu	SPW		0.28	3.86
Cu, Xanthate			0.09	2.94
Cu	DW	UG2	0.05	3.58
Cu, Xanthate			0.01	2.97
Cu	SPW		0.05	3.46
Cu, Xanthate			0.04	3.06

Table E20: Raw data for Merensky ore iron analysis

Condition	Water	Solution Fe (mg/l)	EDTA Fe (mg/l)
No Cu	DW	6.04	5.65
Cu		4.58	9.50
No Cu, Xanthate		1.49	14.1
Cu, Xanthate		3.00	6.10
No Cu	SPW	1.36	2.29
Cu		0.76	4.76
No Cu, Xanthate		0.12	4.14
Cu, Xanthate		2.88	3.40

Table E21: Raw data for talc copper analysis

Condition	AAS Cu (mg/l)	EDTA Cu (mg/l)
No Cu	0.14	0.15
Cu	0.30	0.52
No Cu, Xanthate	0.08	0.11
Cu, Xanthate	0.16	0.24